Aus dem Department für Augenheilkunde Tübingen

Universitäts-Augenklinik

Evaluation of brimonidine loaded DNA-nanoparticles

Inaugural-Dissertation
zur Erlangung des Doktorgrades
der Medizin

der Medizinischen Fakultät
der Eberhard Karls Universität
zu Tübingen

Vorgelegt von

Frößl, Katharina

2020

Dekan:	Professor Dr. I. B. Autenrieth
1. Berichterstatter:	Universitätsprofessor Dr. M. S. Spitzer
2. Berichterstatter:	Professor Dr. M. D. Fischer
Tag der Disputation:	10.11.2019

Meinen Eltern

Table of contents

Index of figures

Index of tables

Index of abbreviations

ANOVA	analysis of variance
apt	aptamer
aptU4T	NP with aptamer elongation
Å	angstrom (unit), equivalent to 10^{-10} m
BriTar	brimonidine tartrate
CO_2	carbon dioxide
cU4T	DNA strand that is complementary to U4T
cU4T-apt	cU4T that got elongated with an aptamer
DAPI	4`6-diamidine-2`phenylinodole dihydrochloride
DNA	deoxyribonucleic acid
dsT4T	double stranded U4T without lipid modification (T4T + cU4T)
dsU4T	double stranded U4T (U4T + cU4T)
EDTA	ethylenediaminetetraacetic acid
HPLC	high-performance liquid chromatography
IOP	intraocular pressure
MALDI-TOF	matrix-assisted laser desorption/ ionization with time of flight analysis
mAU	milli absorption units (unit)
$MgCl_2$	magnesium chloride
mmHg	millimeter of mercury (unit)
MWCO	molecular weight cut off
NaCl	sodium chloride
NP	nanoparticle/ Nanopartikel
OD	optical density (unit)
PCR	polymerase chain reation
PBS	phosphate buffered saline
PFA	paraformaldehyde
Poly (I:C)	polyinosinic:polycytididylic acid
RFU	relative fluorescence unit (unit)

RNA	ribonucleic acid
rpm	rounds per minute (unit)
SD	standard deviation
SDS	sodium dodecyl sulfate
SELEX	systematic evolution of ligands by exponential enrichment
ssU4T	single stranded U4T
SYBR Green	dye
T4T	DNA strand without lipid modification
TAE	buffer made of Tris-Acetate, EDTA, NaCl and $MgCl_2$
TBS	tris buffered saline
TBST	tris buffered saline supplemented with Triton X-100
TEAT	triethylammonium acetate buffer
TUNEL	terminal deoxynucleotidyl transferase dUTP nick end labeling
U4T	DNA nanoparticle with lipid modification made of 12 nucleotides
UV	ultraviolet

1. Introduction

1.1 General introduction to the eye

The organ of vision is situated in the *orbita* and composed of the eye ball, accessory visual structures, protecting parts such as muscles, blood vessels and nerves. The eye is vascularised by the *arteria* and *vena ophtalmica*. The *optical nerve*, which is the second cranial nerve, leads from the eye ball to the *area striata* of the brain. At the *chiasma opticum*, nasal fibres of the *retina* cross to the other side. The eye lid protects the eye ball and distributes the tear film that is manly produced by the *lacrimal gland*. The drainage of the tear film is enabled through the *canaliculi lacrimales* in the medial corner of the eye. Outer skeletal muscles enable the movement of the eye ball in each direction. The inner smooth muscles are responsible for *accommodation* and *pupillomotorics*.

The eyeball is surrounded by a tissue composed of three layers. The outer layer is called *tunica fibrosa* and can be divided into *sclera* and *cornea*. The *sclera* covers the biggest part of the eye ball and the outer muscles insert here. The *cornea* is situated where light falls into the eye. The middle layer, named *tunica vasculosa* or *uvea*, is divided into three parts: *choroidea, ciliary body* and *iris*. The *choroidea* contains vessels that supply oxygen and nutrients to the layers that are situated nearby. Towards the front of the eye, the *ciliary body* is located. This enables *accommodation* of the eye by moving the lens and produces the *aqueous humor*. The last part is the *iris*, which is coloured and regulates the width of the *pupil*. The most inner layer, the *tunica interna*, can be divided into the *retina* and *pigment epithelium*. The *retina* is composed of nine cell layers. The first layer, that is located at the outer part of the eye ball, is the layer containing the *sensory cells*, namely *rods* and *cones*. There are 120 million *rods* that are responsible for *scotopic vision* by weak illumination and 6 million *cones* for *photopic vision*. In the other layers, neurons of the visual pathway are located that enable synaptic contact beneath each other and enable the first processing of the incoming signals. On the *retina* there are several special landmarks. Firstly, the *blind spot* is the place in the back of the eye ball where the *optic nerve* leaves the eye. Here, no sensory cells are located and no visual perception is possible. In contrast, the most sensitive place, the *macula lutea area* and in particular its centre, the *fovea*, can be found at the intersection of the back of the

eye ball and the *orbita axis*. At this point only *cones* are situated, causing it to be the place with the highest visual acuity and sharpest view.

The inner structure of the eye ball can be divided into anterior and posterior chamber. They are separated by the *iris* and communicate over the *pupil*. The posterior chamber contains the *lens* and the *vitreous body*. Through the *ciliary body* the lens is able to change its shape, thereby enabling sharp vision. The *aqueous humor* is produced by the *ciliary body* and flows from the posterior chamber through the *pupil* into the anterior chamber. The anterior chamber reaches from the back of the *cornea* to the *iris*. In the angel between *iris* and *cornea* the *aqueous humor* is drained to the *Schlemm's canal* (Schlote et al., 2004).

1.2 Glaucoma

The most common blinding illnesses of the visual system are cataract, glaucoma and age-related macular degeneration (Pascolini and Mariotti, 2012). All can harm vision seriously and greatly reduce life quality. Cataract and age-related macular degeneration will be shortly discussed before introducing glaucoma.

Cataract is the most frequent cause of blindness worldwide and characterised by an increased opacity of the lens. Sharp vision is reduced and the perception of contrasts hindered. Cataract especially occurs in elderly, but also earlier and congenital forms exist. The disease is not treatable with topical drug application but only by surgery. After removal of the clouded lens, an artificial lens can be inserted and thus the cataract is treated efficiently (West, 2007) (Schlote et al., 2004).

Age-related macular degeneration leads to a progressive loss of central vision. Thereby, extracellular degradation products accumulate and cause dysfunction of the *retinal pigmented epithelial cells and the photoreceptors*. This leads to atrophy of *pigment epithelia and photoreceptors*, the so-called dry or non-exudative form or to *choroidal neovascularisation*, representing the wet or exudative form. Therapy generally aims only to slow down disease progression as causal treatment does not exist up to now. However, for dry age-related macular degeneration, there is no therapy. The wet form is most commonly treated by *anti-vascular endothelial growth factors* that are applied intravitreally supressing abnormal growth of blood vessels as well as laser coagulation or photodynamic therapy (Zajac-Pytrus et al., 2015) (Schlote et al., 2004).

Glaucoma is the second leading cause of blindness worldwide after cataract. In contrast to cataract, blindness caused by glaucoma is irreversible which makes it even more important to treat before permanent damage is done or if this is not possible anymore, to preserve the remaining vision. In general, glaucoma is treated by applying topical drugs with pressure lowering effects or by pressure lowering surgery when drops do not provide adequate pressure control. Surgery, however, is associated with certain risky and has a tendency for failure. Worldwide, 64.3 million people are affected by the disease, with a prevalence of up to 3.54% for people aged 40-80 years. In Europe, 6.77 million people (2.93%) are affected. In contrast, Asians and Africans are more likely to develop glaucoma and as such the prevalence in these regions is much higher than in

Europe. It is expected that in 2040 there will be 112 million people suffering from glaucoma, from which 7.85 million will be living in Europe (Tham et al., 2014).

Glaucoma is a group of diseases that leads to damage of the optic nerve and thereby results in loss of the visual field. It is often accompanied with an elevated *intraocular pressure* (IOP), although there is also a normal tension glaucoma variant. There are several types of glaucoma. First, one differentiates between primary and secondary glaucoma. The latter is the result of another (eye) disease or can be a side effect of medical treatment. Two subtypes of primary glaucoma are known, namely the primary open angle glaucoma and the primary angle closure glaucoma (Weinreb et al., 2014). This classification relates to the pathophysiology underlying the disease and becomes better understandable when having a closer look at the *aqueous humor* flow of the eye.

In a healthy eye the *aqueous humor* is produced by the *ciliary processes* and flows through the *pupil* from the posterior chamber to the anterior chamber. There, most of it is absorbed by the *trabecular meshwork*, *Schlemm's canal*, *collector channels* and *episcleral venous system*. Also part of the *aqueous humor* is evacuated from the eye via the *uveoscleral pathway*.

Primary open angle glaucoma is caused by obstruction of the *trabecular meshwork* and leads to a chronic and progressive increase in IOP, which is most often only noted by the patient when vision problems appear. On the other hand, blockage of the *uveoscleral pathway* and the *iridocorneal angle* result in primary closed angle glaucoma, which can lead to a sudden increase in IOP and painful glaucoma attacks. Both types lead to decreased *aqueous humor* drainage, hence to an increase in IOP which in turn leads to *retinal ganglion cell death*. *Retinal ganglion cells* and their axons constitute the third neuron and form the optic nerve. The death of *retinal ganglion cells* lead to reduced vision and a typical form of glaucomatous *optic disc cupping* (Weinreb et al., 2014). Criteria for diagnosis of primary open angle glaucoma are the typical optic nerve damage, corresponding visual field scotomas and temporary increased IOP. The IOP of a healthy eye generally ranges between 10 and 21 mmHg (BVA and DOG, 2006) (Schlote et al., 2004).

The loss of vision starts slowly and is often compensated by the other eye, if this is not affected too. Because of this and since the disease is painless most of the times the effects often remain unnoticed for a long time, especially for primary open angle glaucoma. Most patients describe their loss in vision as having a blurred vision or missing spots. One out of four patients does not notice a loss of vision at all (Crabb et al., 2013). Nevertheless, the loss of vision in glaucoma is progressive and if kept untreated often leads to blindness (Peters et al., 2013).

1.2.1 Glaucoma treatment

Disease treatment of glaucoma generally aims to lower the IOP, thereby minimizing the risk of (further) damage to vision and improving the quality of life of patients. This is the only proven protective factor against further visual field loss, optic nerve damage and thus the progression of glaucoma (Boland et al., 2013) (Leske et al., 2003). Patients receiving IOP lowering medication are less likely to show a progression of the disease compared to untreated patients and symptoms occur later (Maier et al., 2005) (Heijl et al., 2002). These studies further underline the fact that treatment is essential to prevent progression of the disease.

To control the IOP in people suffering from glaucoma, both pharmaceutical as well as surgical approaches exist, either aiming at decreasing production of *aqueous humor* or increasing the outflow through the *uveoscleral pathway*.

Glaucoma treatment with surgical interventions

Surgical interventions are considered as second line therapy and especially employed when topical medication does not have the desired IOP lowering effect, severe side effects appear or the patient is unable to adhere to the prescribed dropping scheme. Here, several approaches exist. Some of the most common types of glaucoma surgery are described in the following:

Laser trabeculoplasty results in an increased outflow of *aqueous humor*. *Laser ciliary body ablation* destroys parts of the *ciliary body* that normally produces the *aqueous humor*. In most cases, this intervention can only reduce the number of additional topical treatments. Aside from laser mediated treatment, also surgical interventions are an

option. For non-penetrating surgical intervention as *sclerectomy* and *viscocanalostomy*, drainage can be enabled via the *conjunctiva*, a naturally occurring membrane, which also restricts the outflow (Crawley et al., 2012). Penetrating surgery such as *trabeculectomy* or the installation of an *aqueous shunt* drain the *aqueous humor* from the eye to a bleb of conjunctival tissue (Weinreb et al., 2014). The surgery effect in general is time limited and decreases over time. 84% of patients without medical glaucoma treatment reach IOP values below 21 mmHg (Edmunds et al., 2001). However, clinical failure of *trabeculotomy* and *aqueous shunts* was experienced at around 10% per year (Minckler et al., 2008).

Topical glaucoma treatment

Despite surgical possibilities, generally eye drops are prescribed for treatment as they present a noninvasive, self-administrable therapy option for which the patient does not need any medical assistance.

Different classes of drugs are available for topical glaucoma treatment. Reduction of IOP can be achieved by either decreased production or increased outflow of *aqueous humor*. Decreased production of *aqueous humor* can be achieved by pharmacological modification of adrenoreceptors, carbonic anhydrase and adenosine triphosphatases that are located in the *aqueous humor* producing tissues. Increased outflow of *aqueous humor* results from modification of adrenorecptors and prostanoid receptors. These are situated on the *trabecular meshwork* and the *ciliary body* (Crawley et al., 2012).

There are five major classes of anti-glaucoma drugs that should be mentioned: Prostaglandins, β-blockers, carbonic anhydrase inhibitors, parasympathomimetics and α_2-selective agonists. In the following each class will be presented shortly together with IOP lowering effects and side effects (van der Valk et al., 2005) (van der Valk et al., 2009).

Prostaglandins are today's first line drugs for glaucoma treatment. Examples are bimatoprost, latanoprost and travoprost. Especially the fact that they are dosed only once a day makes them today's first-line medication. The IOP reduction is around 25-32% and achieved by increasing the outflow via the *trabecular* such as *uveoscleral*

pathway (Bahler et al., 2008). Possible side effects range from *conjunctival hyperemia*, increased growth of eye lashes, *anterior uveitis* to *upper lid ptosis* (Alm et al., 2008).

The class of β-blockers can be divided into non-selective (e.g. timolol) and selective β_1-blockers (e.g. betaxolol) that are dosed twice a day and reduce IOP by 17-28%. Both decrease the production of *aqueous humor* (Volotinen et al., 2011). Timolol bears some quite important side effects such as *bradycardia*, *nocturnal arterial hypotension* and *bronchospasm* (Pratt et al., 2015) (Kirwan et al., 2002) (Hayreh et al., 1999).

Carbonic anhydrase inhibitors can be applied as topic formulations (e.g. brinzolamide) two to three times a day and decrease the *aqueous humor* production. As side effects of brinzolamide discomfort, blurred vision and headache can be experienced (Sall, 2000). Next to topical carbonic anhydrase inhibitors, also systemic formulations exist (e.g. methacetolamide) which may lead to more severe side effects (Schuman, 2000).

Pilocarpine is a parasympathomimetic that is used since the 19th century. It leads to *miosis* and increases the outflow of *aqueous humor*. Possible side effects are accommodative blur and *atypical band keratopathy* (Wu et al., 2011)

Brimonidine is an example for an α_2-adrenergic agonists and decreases the IOP around 14-21% by both lowering the aqueous production and increasing the outflow through the *uveoscleral pathway* (Greenfield et al., 1997) (Toris et al., 1995). The dosing scheme is twice a day and current side effects are burning, stinging, blurred vision, dry mouth and fatigue (Derick et al., 1997).

When ranking the presented drugs regarding their ability to lower IOP (peak), the following order is presented: bimatoprost, latanoprost, travoprost, brimonidine, timolol, dorzolamid, betaxolol, brinzoloamid. Regarding this ranking and the absolute numbers of the IOP reduction ability (peak), brimonidine reveals better results as timolol. However, no statistically difference between brimonidine and timolol was found (van der Valk et al., 2009).

So far only single drug formulations have been presented. However, especially in recent years a wide range of fixed combinations have been launched. Here the achieved levels of IOP reduction compared to the single drugs vary between formulations (Sall et al.,

2003) (Webers et al., 2010). When two or more drugs are applied, side effects of all are possible. Nevertheless, the patient only needs to drop fixed combinations once, which will positively influence the compliance.

Brimonidine for glaucoma treatment

As brimonidine is a very well established drug and possesses several advantages over other options, a closer look will be taken at this drug. It achieves an IOP reduction comparable to most other anti-glaucoma drugs (van der Valk et al., 2005). For example, when compared to latanoprost applied once a day, brimonidine dosed twice daily is more effective in reaching a targeted IOP (85% vs 65%) (DuBiner et al., 2001). However, there are also reviews contradicting these findings and reporting that latanoprost has a significant higher ability to reduce IOP than brimonidine (Fung et al., 2007). Furthermore, in a direct comparison between brimonidine and timolol, both dropped twice a day, the prior drug revealed more side effects but resulted in less visual field loss (Krupin et al., 2011). Also, as adjunctive therapy to β-blockers or timolol/dorzolamide, latanoprost and brimonidine achieve comparable results. However, side effects are slightly more often reported in latonoprost-treated patients (Akman et al., 2004) (Simmons and Earl, 2002).

As outlined above, brimonidine reduces the IOP by both lowering the aqueous production and increasing the outflow through the *uveoscleral pathway* (Greenfield et al., 1997) (Toris et al., 1995). However, when applying the drug in long-term treatment, the IOP reduction is mainly due to the increased outflow. The decreasing effect on the production of *aqueous humor* drops after a certain time of treatment. This may be due to a new steady state regarding the by brimonidine evoked vasoconstriction or a loss of sensibility of α_2-adrenergic receptors (Toris et al., 1999). Side effects reported can be explained easily when bearing in mind that brimonidine is a sympathomimetic drug with affinity to the α_2-adrenoceptor. Effects on the central nervous system are sedation and *hypotonia,* influences on the peripheral function include *vasoconstriction*. Experienced side effects upon the use of topical brimonidine include stinging, burning, dry mouth, blurred vision and fatigue. These effects are more pronounced with higher concentrations of brimonidine (Derick et al., 1997). Finally, the drug is contraindicated for use in children and infants below the age of two years. Side effects are frequent at

that age. Brimonidine in children might cause sleepiness and lethargy, beside the already mentioned possible side effects. These side effects are caused by the fact that brimonidine is able to pass the blood-brain barrier and thus can cause effects on the central nervous system (Al-Shahwan et al., 2005) (Enyedi and Freedman, 2001). Next to the use in ophthalmology, brimonidine is also used as a gel to treat *rosacea*, a dermatological disease.

Next to the IOP lowering effect, brimonidine was shown to have a neuroprotective effect. This is independent of the IOP lowering ability and is significantly larger than the effects found for latanoprost (Hernandez et al., 2008) (Ahmed et al., 2001). Unfortunately, real proof for neuroprotection has only been shown in animal models and the effects in human still needs to be confirmed. Nevertheless, with current developments in delivery vehicles that allow an increased bioavailability at the *retina*, there is good hope that these effects might soon be measureable in primates.

Comparison of surgical and topical treatment

Surgical approaches are especially envisaged for patients without the desired IOP lowering effect for topical application, who suffer from side effects or are unable to adhere to the dropping scheme. In general, topical treatment and surgical approaches achieve comparable results in long term effects. However, surgery has a 3% higher chance leading to blindness after 10 years. Patients are mainly concerned about the long time outcome and not about the mode to achieve this, even if topical treatment often includes a lifelong need of medication (Bhargava et al., 2006). Next to non-invasivity this is one reason why topical formulations are first line therapy.

Difficulties in topical treatment of eye diseases

Despite the prevalent use of eye drops, this application form is burdened with several problems. Firstly, after application of the topical treatment the major part of the eye drop is cleared away from the *cornea* and never reaches the targeted tissue (Amrite et al., 2008). The bioavailability is only 1 to 5% for hydrophobic drugs and below 0.5% for hydrophilic substances. This is caused by the architecture of the *cornea*, the clearance by tear flow and eye movements (Zhang et al., 2004). Due to this poor bioavailability and effectiveness, it is necessary to administer eye drops at high concentrations and with a high frequency. The frequent need of application results in a

poor compliance, as patients increasingly disobey the doctor's advice at higher dosing regimens. Some authors mention the high frequency of drop application as one of the main reasons for poor compliance and concluded that monotherapy has a strongly beneficial effect. Hence, a lower dropping frequency and simpler dropping scheme are easier to handle for patients and improve the effect of the therapy. (Dietlein et al., 2016) (Hermann et al., 2011) (Tsai, 2009) (Tsai, 2006). Indeed, this is also the major reason why prostaglandins are currently the first line treatment option for glaucoma. Next to this, there are drug associated problems. The need of highly concentrated eye drops also causes side effects ranging from simple local reactions to more serious allergic reactions (Osborne et al., 2005) (Bowman et al., 2004). Finally, the handling and administration of eye drops is difficult due to motoric disabilities or reduced vision of many patients. Some even need to rely on other people to give them their medication (Tsai et al., 2007) (Winfield et al., 1990). For an ideal (topic) treatment, the frequency and concentration of topical treatment should be as low as possible and should require in the best only one drug. However, due to the inefficiency of eye drops, this ideal treatment is still far away.

1.3 Improving topical treatment

To enhance the efficacy of glaucoma treatment, different improvements of eye drops have been investigated. One way to improve the uptake of drug is to extend the time of contact to the *cornea*. Different application forms such as emulsions, suspensions or ointments are available. The latter often cause blurred vision and irritation. Also altered viscosity can improve the bioavailability. One example to achieve this is hyaluronic acid. It is a polysaccharide that expresses a three dimensional structure and is able to bind water. Next to its use as additive to drug containing solutions, there are also anti-glaucoma drug containing hyaluronan complexes improving the bioavailability (Battistini et al., 2017). Hyaluronic acid is also used in treatment of the dry eye disease. Although it is relatively well tolerated, solutions with increased viscosity cause blurred vision and as a consequence result in a decreased compliance (Baranowski et al., 2014). Furthermore, substances that increase the permeability of the *cornea* have been used in the past to increase the therapeutic effects. However, most of them are toxic, like benzalkonium chloride (de Jong et al., 1994), and in recent years there has been a tendency to remove them from formulations. Moreover, non-invasive sustained release devices, in-situ gelling systems and implants have been developed. They all release the drug over a prolonged period of time and acts as depot. The focus of side effects here is especially the foreign body sensation (Baranowski et al., 2014). Blurred vision, increased tearing and foreign body sensation reduces compliance and hence, the aim of a better therapy is not reached.

1.3.1 Nanoparticles in medicine

One novel and very promising approach to solve the before mentioned problems in topical treatment is the use of nanoparticles (NPs). NPs are defined as objects that are sized between 1 and 100 nm. They are employed in many aspects of daily life, such as in toothpaste or disinfectants. For the production of NPs, a vast amount of materials and assembly mechanisms are available, opening a large variety of possibilities for diseases treatment. Many materials come into consideration for the synthesis of NPs. Roughly they can be divided in two groups: inorganic and organic materials. Examples for inorganic materials are metal oxides, gold and silver (Austin et al., 2015). Organic

materials are carbon based compounds and include most polymers, proteins and DNA. Additionally, NPs can also be fabricated from a combination of materials. NPs of various shapes can be realized such as simple geometric forms or more complex ones like wires, tubes, monolayers or micelles (Ju-Nam and Lead, 2008). In medicine, NPs can be used for diagnosis, drug and gene delivery and tissue targeting. A main field of research and application is the diagnosis and treatment of cancer (Murthy, 2007) (Salata, 2004).

In ophthalmology NPs are applied to treat various diseases, e.g. diabetic macular oedema or glaucoma. Many NP carrier systems have been reported to be successful in animals' experiments. Diclofenac, a nonsteroidal anti-inflammatory drug, has been successfully assessed with solid lipid NPs and has shown higher intraocular concentrations than commercial drug after injection in the eyes of rabbits (Abrishami et al., 2016). Albumin carriers loaded with ganciclovir, an anti-viral drug, revealed to be safe NPs after intravitreal application in rats (Merodio et al., 2002). In humans, γ-cyclodextrin NPs loaded with dexamethasone have been successfully assessed for the therapy of diabetic macular oedema. Compared to triamcinolone that is injected into the eye, this new approach that is applied as topical treatment revealed comparable results (Johannesson et al., 2014). First promising approaches were done to employ these NP also to other diseases like macular oedema and vitritis (Shulman et al., 2015). For glaucoma different approaches to improve therapy by using NPs or nanotechnology exist. Brinzolamide was successfully established as a formulation with nanocrystals and its IOP lowering effect in rats proven (Tuomela et al., 2014). Brimonidine tartrate loaded in for example poly (ethacrylate, methylmetacrylate and chlorotrimethyl ammonioethyl methacrylate) NPs revealed IOP reduction in glaucomatous rabbit eyes superior to that of conventional eye drops (Bhagav et al., 2011).

1.3.2 DNA nanoparticle and their use in medicine

Especially inorganic materials bear the problem that they may accumulate in the body as they are not biodegradable and can cause toxic effects (Austin et al., 2015). Whereas organic materials, like DNA, is biodegradable and in the best made of substances known to the human body. Thus, DNA is a very attractive material due to its excellent

biocompatibility. The assembly procedure of DNA based NPs are relatively simple as only a heat gradient is needed to hybridize the NPs in the desired shape (Smith, 2006).

For manufacturing of NPs, various possibilities exist. DNA can be used in its pristine form or with modifications. Pristine DNA is able to load drug via intercalation. This is in the same time the easiest possibility to load drug into DNA as no further modification e.g. with lipids or aptamers is needed. Regarding the characteristics of brimonidine as an example, one can assume that this drug can be successfully loaded in DNA NPs (Figure 1).

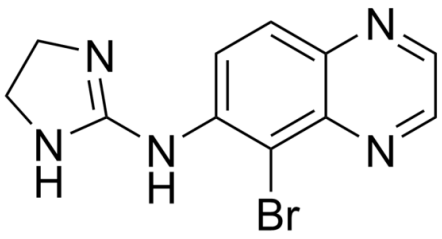

Figure 1: Chemical structure of brimonidine. Due to ring structures containing double bounds, brimonidine has a planar structure, which promotes effective loading into the DNA NPs. (https://commons.wikimedia.org/w/index.php?curid=3880893 (last accessed 16.5.2017, 8:08; public domain))

Brimonidine has a planar structure that is very well suitable for intercalation with DNA. This planar structure is due to the polycyclic nature of the molecule. In addition, its structure is also related to the structure of nucleobases. For these reasons, it is expected that brimonidine can easily interact with double stranded DNA, which leads to successful and effective loading into the investigated dsU4T NPs.

Next to this, NP can be made of modified DNA. For example, when modifying the DNA with a gold binding moiety, they can be linked to gold nanorods and loaded with an intercalating chemotherapeutic agent, for example doxorubicin. Upon irradiation, the structure is heated, which causes the DNA to denaturate and thereby the drug is released. These hybrid NPs have been shown to be effective in drug delivery to a targeted tumor (Xiao et al., 2012).

Also, the functionalization of DNA with alkyl chains is possible. Hereby amphiphilic molecules are created where part of the molecule is hydrophobic and part is hydrophilic. Due to microphase separation, these materials assemble into micellar structures in an

aqueous surrounding. Here, the hydrophobic part comprised of the lipid modification forms a soft core, whereas the hydrophilic DNA is sticking out of the micelle and forming the shell (Rösler et al., 2012) (Anaya et al., 2010). It was found, that DNA chains with twelve nucleotides whereof four are modified with an alkyl chain adhere best to the ocular surface among the tested entities. The NP were found to adhere to the cornea of rats for at least four hours (de Vries et al., 2018) (Herrmann, A., De Vries, J. W., Spitzer, M. S., & Schnichels, S. O. inventors; 2015, Means and methods for ocular drug delivery, International publication number: WO 2015/041520 Al, 26.3.2015). For the drug loading into those DNA NPs various possibilities exist (Figure 2).

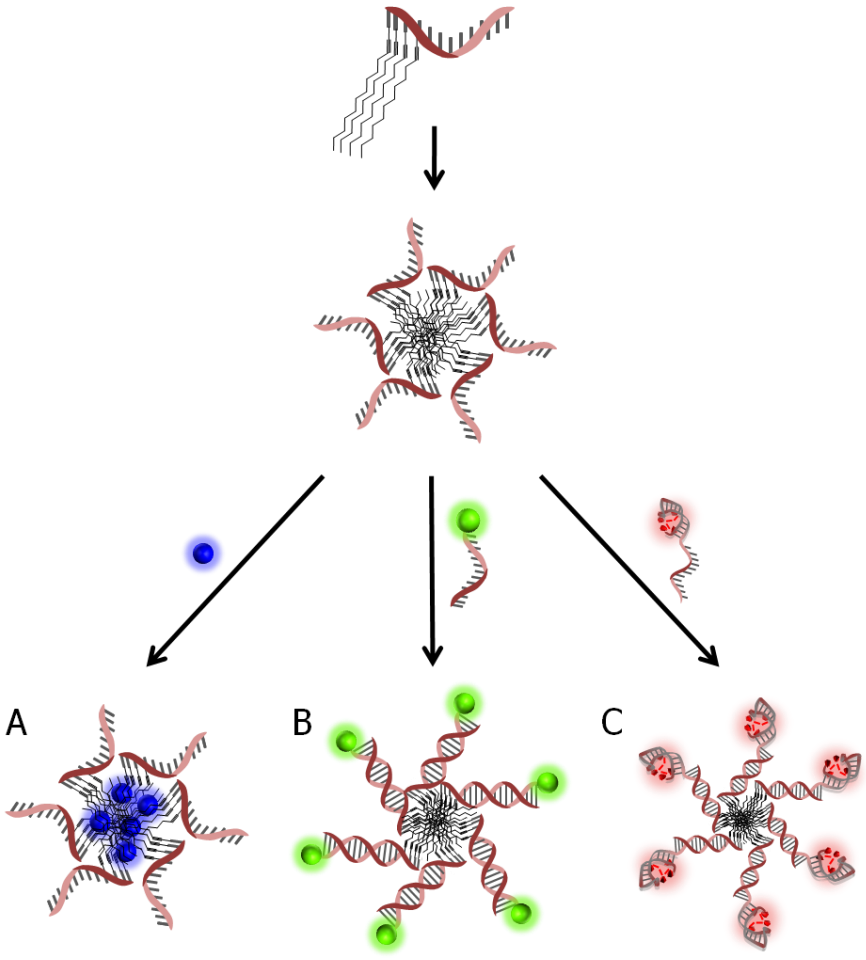

Figure 2: Formation of NPs from lipid modified DNA in aqueous environment. Several loading possibilities are given in a second step. Drugs can be loaded into the hydrophobic soft core (A), by covalent attachment to the complementary strand (B) or by elongating the complementary strand with an aptamer that binds specifically to the drug of interest (C) Figure (modified from original): (de Vries, 2015)(The figure is used with kind permission of Dr. Jan Willem de Vries), Patent: (Herrmann, A., De Vries, J. W., Spitzer, M. S., & Schnichels, S. O. inventors; 2015, Means and methods for ocular drug delivery, International publication number: WO 2015/041520 Al, 26.3.2015).

Firstly, it is possible to load drugs that are poorly water soluble into the hydrophobic core of the NPs. With this kind of medication, incorporation in the hydrophobic core of the NPs is favourable due to the minimized interactions with water. However, this method is limited to hydrophobic drugs and cannot be employed for the large number of hydrophilic drugs, such as antibiotics. Additionally, the release properties of the drug cannot be influenced.

An alternative loading method is based on the covalent attachment of the drug to the complementary sequence to the NP. However, the required chemical alteration of the drug to bind it covalently to the NP might influence the pharmaceutical activity and tolerance drastically. In addition, controlled cleavage of the bond between carrier and the drug is troublesome.

For controlled drug loading and release, the NP can be functionalized with an aptamer by elongating the complementary DNA sequence. Aptamers are small pieces of DNA or RNA that are able to bind a drug specifically. One possibility to select those aptamers is the systematic evolution of ligands by exponential enrichment (SELEX). Here, a library of oligonucleotides is exposed to the immobilised target drug. After washing, the bound sequences are amplified using PCR. With the gained sequences, the procedure is repeated with more and more stringent washing conditions until only the strongest binding sequences are selected (Ellington and Szostak, 1990). Binding between the aptamer and the drug is based on non-covalent interaction such as hydrogen binding and van der Waals forces. Hence, no chemical modification of the drug is needed. This method does not only allow for facile loading, but also the release profile can be adjusted by altering the affinity. As aptamers can be developed for any target molecule, this NP can be modified to bind any desired drug.

Previously, those DNA NPs were conjugated with two antibiotics: kanamycin and neomycin B. The loading of the antibiotics was achieved with the second here presented loading possibilities by elongation of the DNA strand at the 3’ end of the complementary strand. For those loaded NPs, a prolonged adherence could be shown towards rat cornea for at least 30 minutes as well as human cornea epithelium. The residence time of the antibiotic was estimated to be ten times longer than without the use of NP. No toxic effects were found in cell culture. The antibiotic activity of the drug

loaded NPs was tested on porcine cornea epithelium and bacteria growth was inhibited effectively (de Vries et al., 2018) (Herrmann, A., De Vries, J. W., Spitzer, M. S., & Schnichels, S. O. inventors; 2015, Means and methods for ocular drug delivery, International publication number: WO 2015/041520 Al, 26.3.2015).

In this thesis, DNA NPs were functionalized with brimonidine with the aim for an improved glaucoma treatment.

1.4 Thesis overview and motivation

One way to improve the therapeutic problems outlined before (chapter 1.2.1) is to enhance the drug delivery of topically applied ocular medication. In previous investigations the DNA NPs described before (chapter 1.3.2) showed a high affinity to the corneal tissue and for this reason would make an ideal candidate as vehicle for ocular drug delivery. In this thesis the use of lipid modified DNA NPs for the application of brimonidine will be investigated. Brimonidine is not used as first choice for glaucoma treatment by many physicians anymore as it needs to be administered repeatedly per day. In the same time it exhibits several advantages compared to other drugs. When loaded in NPs the drug is released over a prolonged period of time. Thus, the NPs serve as sort of depot. Because of the resulting higher availability and the longer exposure time, the dropping frequency and drug concentration could be decreased. This in turn results in less local and systemic side effects and an improved patient compliance. This is why, the use of lipid-DNA NPs as ocular drug delivery platform offers the opportunity to greatly enhance the treatment of glaucoma.

In this thesis initially the loading of brimonidine into DNA NPs will be established. For this the loading of the drug via two methods will be investigated. First the compound will be incorporated in the core through hydrophobic interaction. Secondly, also the functionalization through the use of aptamers will be explored. As an integral part of both loading methods, also the release of brimonidine from the NPs is studied. In a next step the adherence time of NP to the cornea will be tested in-vitro and in-vivo. Afterwards a safety evaluation of the newly developed NPs is performed. To this extent the toxicity of the NPs will be screened in cell culture experiments on primary corneal epithelial and in an in-vivo assay on rat eyes. Finally, the stability of the NPs under different conditions is elucidated. These facts will be the groundwork for further studies to enable the formulation of DNA NP containing eye drops for human use.

2. Materials and methods

Materials were purchased by commercial suppliers and used as received if not otherwise noted.

2.1. Material

2.1.1 Material

- 15 ml falcon tube, Falcon, Corning Inc., USA
- 96 well black plate, Falcon, BD Biosciences, USA
- Eppendorf tubes (different sizes, plastic or glass), Eppendorf AG, Germany

2.1.2 Chemicals and solutions

- brimonidine, Sigma Aldrich, USA
- brimonidine tartrate, Sigma-Aldrich, USA
- Caspase-Glo 3/7 buffer and Substrate, Promega, USA
- CellTiter 96® Aqueous One Solution Cell Proliferation Assay, Promega, USA
- CnT-Prime epithelial cell culture Medium, CELLnTEC, Switzerland
- crystal violet solution, Sigma Aldrich, USA
- DAPI (4`6-diamidine-2`phenylinodole dihydrochloride), Sigma Aldrich, USA
- dimethyl sulfoxide, Merck, Germany
- DNAse, Sigma Aldrich, USA
- Dulbecco's Modified Eagle Medium F-12 Nutrient Mixture (Harn), Thermo Fisher Science, USA
- fetal bovine serum, Thermo Fisher Science, USA
- FluorSave, Calbiochem Germany
- hydrochloric acid, Merck, Germany
- liquid nitrogen, WestfalenGas, Germany
- PBS (phosphate buffered saline), Thermo Scientific, USA
- penicillin/ streptomycin, Sigma Aldrich, USA
- PFA (paraformaldehyde), Merck, Germany

- Poly (I:C), Sigma Aldrich, USA
- SDS (sodium dodecyl sulfate) Roth, Germany
- sodium chloride, Sigma Aldrich, Germany
- SYBR Green, Thermo Fisher Scientific, Germany
- Tissue-Tek O.C.T., Sakura Finetek, Netherlands
- TRIS (Tris-(hydroxymethyl)-aminomethan)-base, Sigma Aldrich, Germany
- TUNEL In-Situ Cell Death Detection Kit, Roche, Germany
- Tween 20, Serva, Germany

2.1.3 DNA

- Aptamer sequences, Neoventures Biotechnology Inc., Canada
- DNA compounds, biomers, Germany
- synthesized by a chemist in the group

2.1.4 Animals and eyes

- Adult female Lister Hooded or Brown Norway rats, Charles River, Germany
- Pig eyes, abattoir, Gärtringen, Germany

2.1.5 Machines and software

- Cryostat: Leica CM 1900, Germany
- DNAMAN, Version 5.2.9, Lynnon LLC., San Ramon, USA
- Fluorescent microscope: Axioplane2 imaging®, Zeiss, Germany with Openlab software, Improvision, Germany
- Fluorophotometer: Fluorotron ^{TM} Master, Ocumetrics, Langley, USA
- Incubator: Heraeus bad 6220, Thermo scientific, USA
- JMP 13.0.0, SAS, USA
- Luminometer, BioTek, Synergy HT, Germany
- Magnetic stirrer: IKA COMBIMAG RCT, Germany

- Microplate Reader, BioTek, Synergy HT, Germany
- Rotary evaporator: Vacuum Concentrator BA-VC-300 H, Saur, Germany
- Shaker: Thermomixer comfort, Eppendorf, Germany
- Shimadzu VP series HPLC, Shimadzu, Japan with a PDA (photo diode array) detector and equipped with a Jupiter C4 4.6x250mm, 90 Å column
- Spectrophotometer: Ultrospec 1000, Pharmacia Biotech, Sweden
- Glass slides, Superfrost plus, R. Langenbrinck, Germany
- Rubber rings, Hornbach, Germany
- Semi-permeable membrane with a molecular weight cut-off (MWCO) of 1000 Da, Spectrum Laboratories, USA

2.2 Nanoparticles

The here used NPs are composed of lipid-modified DNA strands. These DNA strands were synthesized from nucleotides and lipid-modified nucleotides, namely dodec-1-ynyluracil, which is the nucleobase uracil that was elongated with twelve C atoms. Synthesis was followed by purification with reverse phase chromatography and purity verification using MALDI-TOF mass spectrometry.

The NP is called U4T-12 and its sequence is UUUUGCGGATTC (5' → 3'). The name is composed by the number of modified nucleotides (four), the location of the modification (T for 5' end) and total length of the strand (twelve nucleotides). U represents the modified nucleotides. 33% of the nucleotides are modified, which was found to be the best ratio between modified and non-modified nucleotides. Through the modification, the DNA strand has a hydrophobic as well as a hydrophilic part. This is why the strand self-assemble to spherical structures, so called micelles, in aqueous environment (de Vries et al., 2018). These micelles are here named nanoparticle, which will also be the further used term.

2.2.1 Preparation of nanoparticles

To prepare NP with a final concentration of DNA compounds of 100 µM or 500 µM, lipid DNA stocks were diluted with buffer to obtain a final composition of 50 mM NaCl and 0.2 x TAE buffer (8 mM Tris-Acetate, 0.2 mM EDTA, 4 mM NaCl, 2.4 mM $MgCl_2$, pH 8.0) in ultrapure water. This solution was thermocycled at 85°C for 30 min, followed by a decrease of temperature of -1 °C every two minutes until a level of 21 °C was reached. The sequences of used DNA entities are given (Table 1). From these basic entities, different NPs were prepared (Table 2).

Table 1: Sequence details of the DNA entities U4T, cU4T and T4T. U represents the lipid modified nucleotide which is the hydrophobic entity (Anaya et al., 2010)

name	sequence (5' → 3')
U4T	UUUUGCGGATTC
cU4T	GAATCCGCAAAA
T4T	TTTTGCGGATTC

Table 2: Details of used NP and DNA controls without aptamer modification. The abbreviation, as well as the full description and the used entities are given.

name	details	used entities
ssU4T	single stranded NP	U4T
dsU4T	double stranded NP	U4T + cU4T
dsT4T	double stranded DNA controls without lipid modification and thus not forming NPs	T4T + cU4T

Aside from hydrophobic loading in the NPs, also aptameric binding was performed for brimonidine. To this extent, a DNA aptamer was developed using the SELEX method. For SELEX, a library of oligonucleotides is exposed to the immobilized target drug. After washing, the sequences with the highest binding affinity to the target are amplified using PCR. With the gained sequences, the procedure is repeated with more and more stringent washing conditions until only the strongest binding sequences are selected (Ellington and Szostak, 1990). The resulting aptamer sequence of this process was named Bra3, is 40 nucleotides long and exhibits a stem-loop structure (Figure 3). Several shortened DNA sequences were deduced from Bra3 by logic design and tested for their binding affinity to brimonidine (Chapter 2.2.5). The shortened aptamers were called Bra3.1 and Bra3.2 and their sequence details (Table 3) and secondary structures (Figure 4) are given below. Compared to Bra3, they are truncated at the 5'-end or both ends to investigate in the important regions for brimonidine binding such as the possibility to shorten the aptamer and thus save costs. For binding to the NPs, the aptameric sequence was elongated on the 3'-end with the cU4T sequence. All figures of secondary structures were made with DNAMAN. DNAMAN was used for prediction of the approximated secondary structure of the aptamers, as the exact determination via crystolography would have taken around one year.

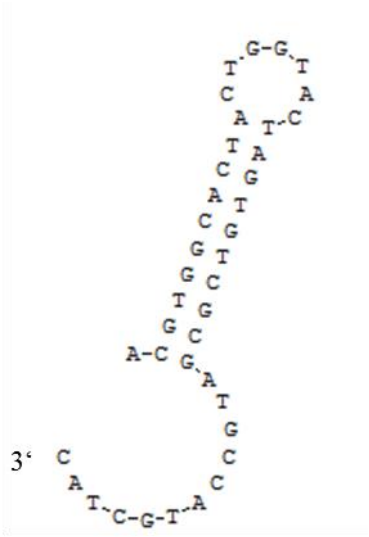

Figure 3: Secondary structure of the brimonidine binding aptamer Bra3.

Table 3: Nucleotide sequences of the three investigated aptamers. Bra3.1 and 3.2 represent shortened versions of Bra3. The different colours represent parts of the secondary structure of Bra3: green – double stranded part, yellow – small closed loop, blue – big open loop.

name	sequence (5' → 3')
Bra3	ACGTGGCACTACTTGGTACTAGTGTCGCGATGCCATGCTAC
Bra3.1	GTGGCACTACTTGGTACTAGTGTCGCGATGCCA
Bra3.2	ACTTGGTACTAGTGTCGCGATGCCATGCTAC

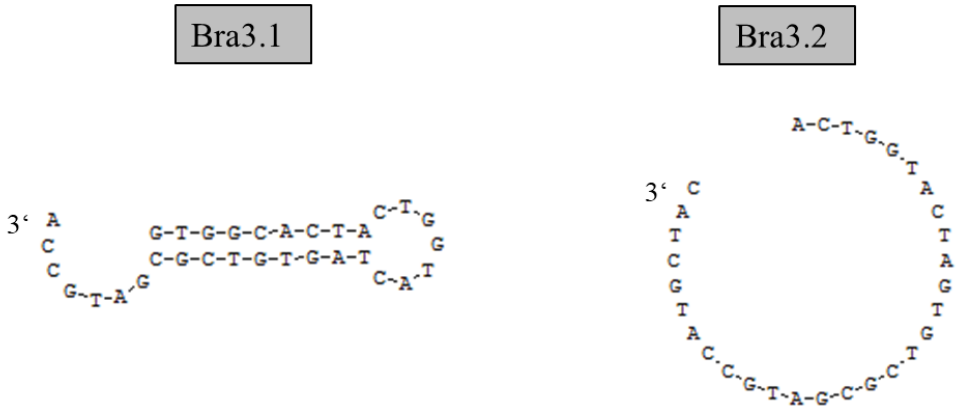

Figure 4: Secondary structure of the aptamers Bra 3.1 and Bra 3.2 as shortened versions of Bra3.

For visualization of the NPs under the fluorescence microscope (chapter 3.3.2 and 3.4.2) or the fluorophotometer (chapter 3.3.1), the NPs were labeled with the dye Atto488. The dye was bound either to cU4T or the 5' end of the cU4T-Bra3.1 DNA aptamer.

2.2.2 Preparation of brimonidine

Brimonidine is a hydrophobic agent and thus poorly water soluble. In current drugs brimonidine is formulated as its water soluble salt, brimonidine tartrate. For loading into the NPs, pristine brimonidine was used.

Therefore, dry brimonidine was dissolved in pure dimethyl sulfoxide to obtain a stock solution of 25 mM. Therefrom defined amounts were aliquoted in 0.5 ml Eppendorf tubes for small scale and in 2 ml glass vials for larger scale. Both quantities were then placed in a rotary evaporator to remove the solvent and obtain a drug pellet.

2.2.3 Loading of brimonidine in nanoparticles

NPs and brimonidine were prepared as described before (chapter 2.2.1 and 2.2.2). The NP containing solution was then added on the brimonidine pellet and incubated (Figure 5). Incubation was performed on a shaker with 750 rpm at 21 °C with protection from light.

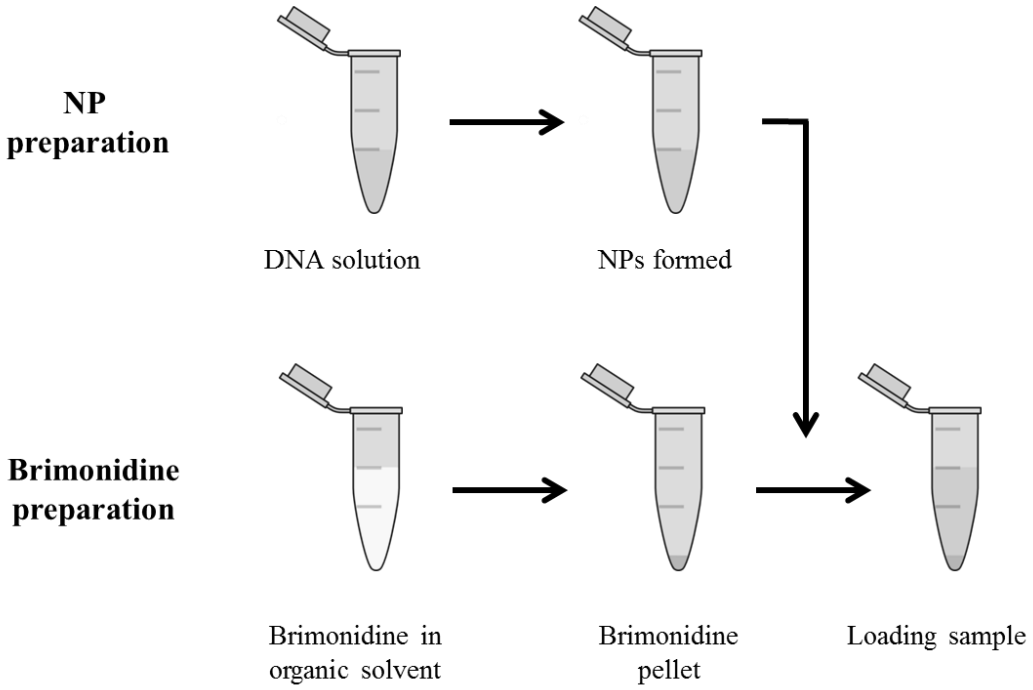

Figure 5: Schematic representation of loading of brimonidine into NP solution. NPs are prepared by combining in water solved DNA entities which are then thermocycled to enable the formation of NPs. Brimonidine in organic solvent is dried down to achieve a pellet. The NP solution is then added to the pellet and the two of them incubated over time. (Figure composed from Cliparts: http://www.clker.com (last accessed 15.5.17 8:00; public domain))

For loading investigation, samples were taken from the supernatant of the loading sample (n=3-5) every 12 hours for 96 hours (chapter 3.1.1) or 48 hours (chapter 3.2.2). The loaded amount of brimonidine was determined by measuring the absorption of these diluted samples. Dilution was necessary due to technical conditions; the absorption maximum would have been exceeded otherwise. Absorption was measured with a spectrophotometer at 260 nm, which is the absorption maximum of brimonidine. To set the spectrophotometer to 0, the same buffer as for DNA samples preparation was used.

Hydrophobic loading of brimonidine in nanoparticles

To establish hydrophobic loading of brimonidine in NPs, different concentrations of DNA (100 and 500 µM) and brimonidine (1000 and 5000 µM) were investigated. As DNA entities single and double stranded NPs were used. Unloaded NPs samples, as well as buffer served as controls. Incubation was performed overnight or samples taken every 12 hours for 96 hours to determine the loading over time.

Brimonidine loading in aptamer functionalized nanoparticles

For the loading experiment into aptamer functionalized NPs, DNA concentrations for those NPs were taken to be 500 µM, whereas brimonidine concentration was 4.5 mM. The amount of loaded brimonidine was determined as described in the paragraphs above using absorption measurements.

Loading of samples for further experiments

For release experiments (Chapter 3.1.2 and 3.2.3) loading time of brimonidine was 48 hours. After this time, the supernatant was taken off and corresponding samples were combined (e.g. supernatant from loading sample dsU4T 1-3 were combined). Before continuing the following experiments, the concentration was determined by absorption measurement. For some experiments, these samples were subsequently co-formulated with brimonidine tartrate to adjust samples to 5 mM of brimonidine in total. To obtain this, solid brimonidine tartrate was diluted in ultrapure water to get a stock solution of 25 mM. Incubation time was fixed to 48 hours for loading.

Statistical analysis

For data presentation, the average (n=3-5) - after deducing the reference values - as well as the standard deviation (+/-) were depicted. Statistical analysis was conducted using JMP 13. The data was evaluated with the ANOVA test followed by the Tukey-Kramer post-hoc test. Significance was defined as $p < 0.05$. The p-values were annotated in the diagrams: ***/###/+++ - $p < 0.001$; **/##/++ - $p < 0.01$; */#/+ - $p < 0.05$; * compared to the depending buffer control, # compared to the depending sample with the same brimonidine feed concentration but different NP concentration, + compared to the depending sample with the same NP concentration but different brimonidine feed concentration.

2.2.4 Release of brimonidine from loaded samples

For release experiments a two compartment device was constructed that allowed the measurement of released brimonidine from loaded NPs. The two compartments were separated from each other by a semi-permeable membrane with a molecular weight cut-off (MWCO) of 1000 Da. This membrane is permeable for brimonidine and non-permeable for DNA. The smaller compartment was filled with 90 µl of sample solution and covered with the membrane and closed. This compartment was then placed in a 15 ml falcon tube (represented in the figure as Eppendorf tube), filled with 1.5 ml of 0.2x TAE buffer. This set up was then placed on a shaker and agitated at 750 rpm at 21°C. The NPs also liberate brimonidine without shaking. To achieve consistent release conditions and to increase the speed of the brimonidine liberation, the samples were stirred. The released amount of brimonidine was determined by absorption measurement of the solution in the falcon tube. Measurements were done at 260 nm. A schematic representation of this set up is given (Figure 6).

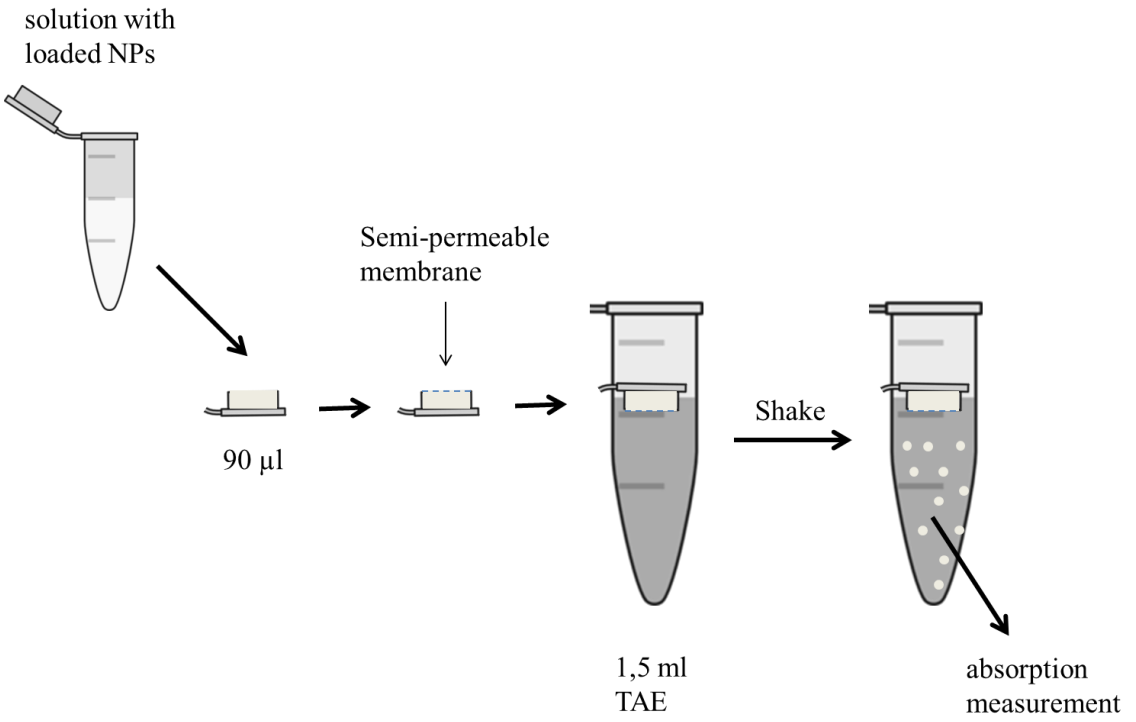

Figure 6: Schematic representation of the release experiment. After decanting the solution with loaded NPs into the device, this is covered with the semi-permeable membrane. The covered device is placed in 1.5 ml of TAE buffer and incubated on a shaker. The release of brimonidine is measured in the buffer solution over time. (Figure composed from Cliparts: http://www.clker.com (last accessed 15.5.17 8:11; public domain)).

Measurements were done every 15 minutes for 1.5 hours, followed by every 30 minutes for 2.5 hours, or overnight. To evaluate the released amount of brimonidine, the OD of buffer was measured at time point 0 and deduced from the following measurements.

To analyze the effect of different concentrations of brimonidine in the release compartment, two different approaches were chosen. For the first set, the supernatant from the loading samples was taken for the release experiment without any modification. The results from this approach are thus named “non-adjusted”. For the other set, called “adjusted”, the concentration of the supernatant from loading samples was determined and then adjusted to be the same everywhere by dilution with 0.2x TAE buffer.

To analyse the results, the mean (n=3) and the standard deviation (+/-) of samples for absolute values as well as relative values were compared for different set ups. For relative values the absorption measured after overnight shaking were set as 100%.

2.2.5 Binding verification between brimonidine and aptamers

To verify the binding between brimonidine and the designed aptamer sequences, a fluorescence based binding assay with SYBR Green was employed. SYBR Green binds unspecific to double stranded DNA. In its bound conformation it emits green light (529 nm) when excited with blue light (495 nm). SYBR Green also binds to single stranded DNA, but to a less strong extend than to double stranded DNA. Unbound and bound to single stranded DNA, SYBR Green shows little fluorescence. As soon as a target molecule, e.g. brimonidine, binds to the double stranded DNA, the aptameric structure and the SYBR Green fluorescence is altered. Hence, SYBR Green is removed or incorporated and the fluorescent signal decreases or increases, respectively. Consequently, SYBR Green can be used to determine the interaction between aptamer and the analyte (Sarpong and Datta, 2012) (McKeague et al., 2014).

DNA samples were prepared to achieve a final concentration of 100 nM in the wells. SYBR Green was diluted in ultrapure water to a final concentration of 1x. After combining DNA samples, SYBR Green, 0.26x TAE and 65 mM NaCl the mixture was plated out in a 96 well black plate and the fluorescence was measured as a reference. After addition of defined amounts of brimonidine (final concentration of 1 µM; 0.5 µM; 0.25 µM and 0.125 µM), fluorescence intensity was determined after incubation of 40 minutes. To analyze the results, fluorescence (t = 40 min) were deduced from references and the averages (n=3, controls n=4) for different concentrations depicted and compared. The standard deviations (+/-) are given. For statistical analysis, a linear regression line was drawn. Its formula and coefficient of determination are given in the graphs.

2.3 Evaluation of adherence time of brimonidine nanoparticles

2.3.1 In-vitro determination of adherence time of brimonidine nanoparticles on pig eyes

To evaluate the adherence-time of functionalized DNA NP to the pig cornea, the NPs were labelled with Atto488 that is bound to the 5' end of the cU4T-Bra3.1 DNA aptamer. Like this NPs can be visualized with a fluorescence microscope or a fluorophotometer.

Pig eyes were obtained from a local abattoir. Before using them for the experiment, they were cleaned by carefully cutting the muscles and surrounding connective tissues. After washing the eyes in PBS, they were allowed to adjust to room temperature. The eye was placed on a bulbus holder and a pre-scan was done with a fluorophotometer. 50 µl of NP solution (20 µM) were incubated five minutes with the help of rubber rings to maintain the solution on the cornea. The fluorescence signal at the cornea was determined immediately after the incubation time. This was repeated after 5, 15 and 30 minutes; one, two and four hours. In between the measurements, the eyes were kept in PBS buffer to simulate blinking. dsU4T NPs as well as cUT-Bra3.1 NPs were compared to the fluorophore Atto488. The fluorescent signal was integrated and depicted relatively to the instant signal in a graph.

2.3.2 In-vivo determination of adherence time of brimonidine nanoparticles on rat eyes

The same method to visualize NP by labelling them with a fluorophore as for the in-vitro experiment was used. The NPs were diluted in 0.2x TAE, NaCl 20 mM and $MgCl_2$ 4 mM to obtain a DNA concentration of 20 µM.

Two adult female Lister Hooded rats per time point were administered one drop of the prepared NP or control solution and sacrificed after 15, 30 or 60 minutes. The rats were treated according to the German animal protection law (AK1/15 to S. Schnichels). For eye drop application, the solution was filled in dropping devices as they are used for application of eye drops in humans. The volume of the drop was approximately 30 µl. The conscious rats were shortly fixed with a towel for administration of the eye drops and neither hindered from blinking during the drop application nor afterwards. Animals

were sacrificed after 15, 30 or 60 minutes post application with carbon dioxide inhalation.

The enucleated eyes were frozen in Tissue-Tek O.C.T. using liquid nitrogen. The eyes were cut into slides of 12 µm on a cryostat and transferred onto glass slides. Until further use the slides were stored at -28°C.

For visualisation of all corneal cells, a DAPI staining was done. DAPI (4`6-diamidine-2`phenylinodole dihydrochloride) binds to double stranded DNA and stains all cells with a cell body. For the staining, several solutions needed to be prepared. 4% paraformaldehyde was prepared by dissolving 40 g paraformaldehyde in PBS (phosphate buffered saline) and stirred at 50°C over night. If not used directly, it was stored in small portions at -28°C. TBS 10x was obtained by dissolving 60.75 g tris base and 87.66 g sodium chloride in 900 ml of ultrapure water. This solution was then titrated to pH 7.6 by addition of hydrochloric acid (25%) and filled up to one liter with ultrapure water. For the experiment, this stock solution was diluted ten times with ultrapure water.

For the DAPI staining slides were embedded in ice cold methanol for 10 minutes. After washing with TBS, 0.2 µg/ml DAPI was incubated on the slides for 1 minute. Following multiple washing steps with TBS and ultrapure water, the slides were after short drying embedded with FluorSave.

The eyes with fluorescently labeled and thus detectable nanoparticles were evaluated manually under the fluorescence microscope. The ratio between eyes with detectable NPs and the total number of examined eyes was determined.

2.4 Safety evaluation of DNA-nanoparticles using in-vitro and in-vivo assays

2.4.1 Safety evaluation of DNA-nanoparticles using an in-vitro cell culture assay

Primary cornea epithelium cells from pig eyes (local abattoir) were cultivated in a 1:1 mixture of CnT-Prime epithelial cell culture Medium and Dulbecco's Modified Eagle Medium F-12 Nutrient Mixture (Harn) supplemented with 10% fetal bovine serum and 1% penicillin and 1% streptomycin. The cells were seeded at 30.000 cells/ well in a 96-well plate having a surface of 0.32 cm^2. 48 hours after seeding, samples were added to achieve a final concentration of 500 µM for each tested sample. The tested entities were with brimonidine loaded NPs made of double stranded DNA as well as NPs functionalized with U4T-Bra3.1. Additionally, brimonidine tartrate alone was tested. Staurosporine and Poly (I:C) served as controls. After four hours of incubation (37°C, 5% CO_2, 95% humidity) cells were washed three times and once more incubated for 24 hours. Thereafter, the toxicity was evaluated with the following assays.

Evaluation of apoptosis induction using the Caspase-Glo 3/7 Assay

To determine the activity of caspase 3/7 which is among other part of the apoptosis pathway, Caspase-Glo 3/7 buffer and substrate was combined and 100 µl were directly supplemented to the culture well. After one hour of incubation at room temperature, the luminescence was measured with a luminometer. The average (n=5) as well as the standard deviation were depicted for analysis of the results.

Evaluation of cell viability (MTS Viability Assay)

Per well, 20 µl of CellTiter 96® Aqueous One Solution Cell Proliferation Assay was added directly to the culture wells. After 90 minutes of incubation at room temperature, absorption was measured at 490 and 690 nm with a Microplate Reader. For results analysis, the difference between the two wavelength were deduced from each other and the average as well as the standard deviation depicted (n=5).

Evaluation of cell amount using the crystal violet staining

Following the MTS Viability Assay, solution was removed from the wells and cells were fixed with 100 µl of 4% PFA for 15 min. After washing, 100 µl of crystal violet solution was added to each well and incubated on the cells for 30 minutes at room temperature. Following three steps of washing, 100 µl of 1% SDS was added.

Absorption was determined after one hour of incubation at a wave length of 595 nm. The average (n=5) as well as the standard deviation were depicted for analysis of the results.

Statistical analysis

For data presentation, the average (n=5) as well as the standard deviation (+/-) were depicted. Statistical analysis was conducted using JMP 13. The data was evaluated with the ANOVA test followed by the Tukey-Kramer post-hoc test. Significance was defined as $p < 0.05$.The p-values were annotated in the diagrams: *** - $p < 0.001$; ** - $p < 0.01$; * - $p < 0.05$ compared to the depending brimonidine control.

2.4.2 In-vivo safety evaluation of DNA-nanoparticle using an in-vivo rat eye assay

Beside the in-vitro model, toxicity was evaluated with an in-vivo model. Living rats were administered eye drops containing different formulations. Adult female Brown Norway rats were purchased from Charles River. Animals were treated according to the German animal protection law (AK1/15 to Schnichels). For this experiment with brimonidine loaded dsU4T and loaded U4T + cU4T-Bra3.1 as well as brimonidine tartrate were tested on their apoptic effects. Thereby a NP concentration of 500 µM was used. Buffer solution served as control. Rats were given one single drop. For each tested NP or buffer, two rats were given eye drops. The conscious rats were neither hindered from blinking during the drop application nor afterwards and euthanized 24 hours after the application with carbon dioxide inhalation. The eyes were enucleated, frozen and cut as described in chapter 2.3.2.

For visualization of the toxic effects on rat eyes, the slides were stained with two different assays: TUNEL In-Situ Cell Death Detection Kit and DAPI staining. TUNEL is the abbreviation for terminal deoxynucleotidyl transferase dUTP nick end labeling. It stains double strand breaks as they occur in apoptosis and thus marks cells suffering from toxic effects. DAPI (4`6-diamidine-2`phenylinodole dihydrochloride) binds to double stranded DNA and stains all cells with a cell body. Solutions were prepared as described in chapter 2.3.2. For TBST, TBS 1x was supplemented with 0.1% Tween 20.

After defrosting the slides from the freezer, cells were fixed with 4% paraformaldehyde for 20 minutes at room temperature. After this, the slides were washed for 30 minutes with TBS 1x. Thereafter, cells were permeabilized for two minutes with 1g/l sodium citrate and 10% of Triton x-100 in ultrapure water. The slides were then stained using a TUNEL In-Situ Cell Death Detection Kit following the manufacturer's instruction. 50 µl of enzyme solution were combined directly after unfreezing them with 500 µl of label solution and applied to the slides. One slide was treated with DNAse for ten minutes as positive control; one slide was supplemented with label-solution only as negative control. All slides were incubated for one hour in the incubator (37°C, 5% CO_2, 95% humidity). After three times of five minutes washing in TBST 1x, slides were incubated - expect the DAPI negative control - for five minutes with 1 µg/ml of DAPI in PBS. Finally, the slides were washed two times five minutes in TBST followed by one washing step of five minutes in ultrapure water. The slides were after short drying embedded with FluorSave. Images were taken with a fluorescent microscope. Per condition, four eyes were obtained. From each eye, four slides were stained and from each slide five pictures taken. From these pictures, the total amount of epithelium cells and the apoptosis positive cells were counted and correlated to each other.

Statistical analysis

For data presentation, the mean (n=4) as well as the standard deviation (+/-) were depicted. Statistical analysis was conducted using JMP 13. The data was evaluated with the ANOVA test followed by the Tukey-Kramer post-hoc test. Significance was defined as $p < 0.05$.

2.5 Stability evaluation of U4T with HPLC

For analysis of NP stability, samples were stored under different conditions: at room temperature with cycled light (day and night light cycle), at room temperature in the dark and at 4 °C, also protected from light. Stored U4T had a concentration of 100 µM. Over one year in four weeks interval, three aliquots of each condition were taken and stored at -80°C until HPLC (high-performance liquid chromatography) analysis. HPLC is a widely used chromatography technic to separate components of a mixture due to polarity. The separation takes place on the stationary phase (HPLC column) with the help of a mobile phase (eluent). After the separation, the single components are detected with different detectors, e.g. UV or fluorescence. The results are depicted as elugram. An elugram is made of peaks, each peak representing a separated component. The area under a peak is proportional to the amount of the substance. The area can be related to the calibration line for the wanted substance and the amount can be calculated therefrom. A small peak or more exactly a smaller area under the peak is equal to a smaller amount of substance. HPLC is used here to detect deterioration of U4T. When deterioration occurs, degradation products accumulate and the peak representing U4T changes its appearance. Additionally, a second (or more peaks) representing the degradation products of U4T increase.

Analysis was done with HPLC using reversed phase chromatography. A Shimadzu VP series HPLC with a PDA (photo diode array) detector and equipped with a Jupiter C4 4.6x250mm, 90 Å column, was used. A linear gradient 0-100% of buffer B in 25 min was applied. Buffer A: 100 mM TEAT (triethylammonium acetate buffer) pH 8 in water, 5% acetonitrile; Buffer B: TEAT 100 mM in 95% isopropanol. For DNA monitoring the wavelength of 254 nm was used. For each run, 20 µl were injected in the column. The elugram is given from 21 to 27 minutes for comparison of the used samples.

3. Results

3.1 Establishing hydrophobic loading of brimonidine in nanoparticles

Brimonidine loaded DNA based NPs may be an elegant way to improve topical treatment of glaucoma. As a first step in establishing those NPs, drug loading has to be set up. For this several strategies can be employed. As introduced before, hydrophobic interactions, covalent binding or elongation with aptamers can be used for the functionalization of the NPs. The following paragraphs will deal with the loading and the release of brimonidine using hydrophobic interactions.

3.1.1 Loading of brimonidine in nanoparticles with hydrophobic interaction

To establish hydrophobic loading, two parameters were investigated. First, a comparison of loading efficiency in two different NPs was made between single stranded DNA NPs (ssU4T) and double stranded DNA NPs (dsU4T). The vehicles comprised of ssU4T are formed from a single entity, whereas the dsU4T NPs consist of ssU4T NPs that are fully hybridized with the complementary sequence. The second investigated parameter was the ratio of NPs concentration to the amount of brimonidine, which was optimized to load the largest quantity of drug into the NPs. To this end, two concentrations of NPs were used and the starting concentration of brimonidine was varied (feed concentration).

To investigate the loading behaviour of the two NPs, ssU4T and dsU4T were prepared at concentrations of 100 and 500 µM. Dried brimonidine pellets were prepared to obtain a concentration of 1000 and 5000 µM. The loading behaviour of the two NPs was then tested by combining the NP solution with the brimonidine pellets and measuring the absorption after incubation of the samples overnight. As control the buffer solution without any NP was included.

The more brimonidine is dissolved in a solution, the higher the absorption. In a NP solution brimonidine can be dissolved in the buffer and loaded in the NPs. Thus, the total brimonidine concentration in a NP solution is higher than in buffer resulting in a higher absorption.

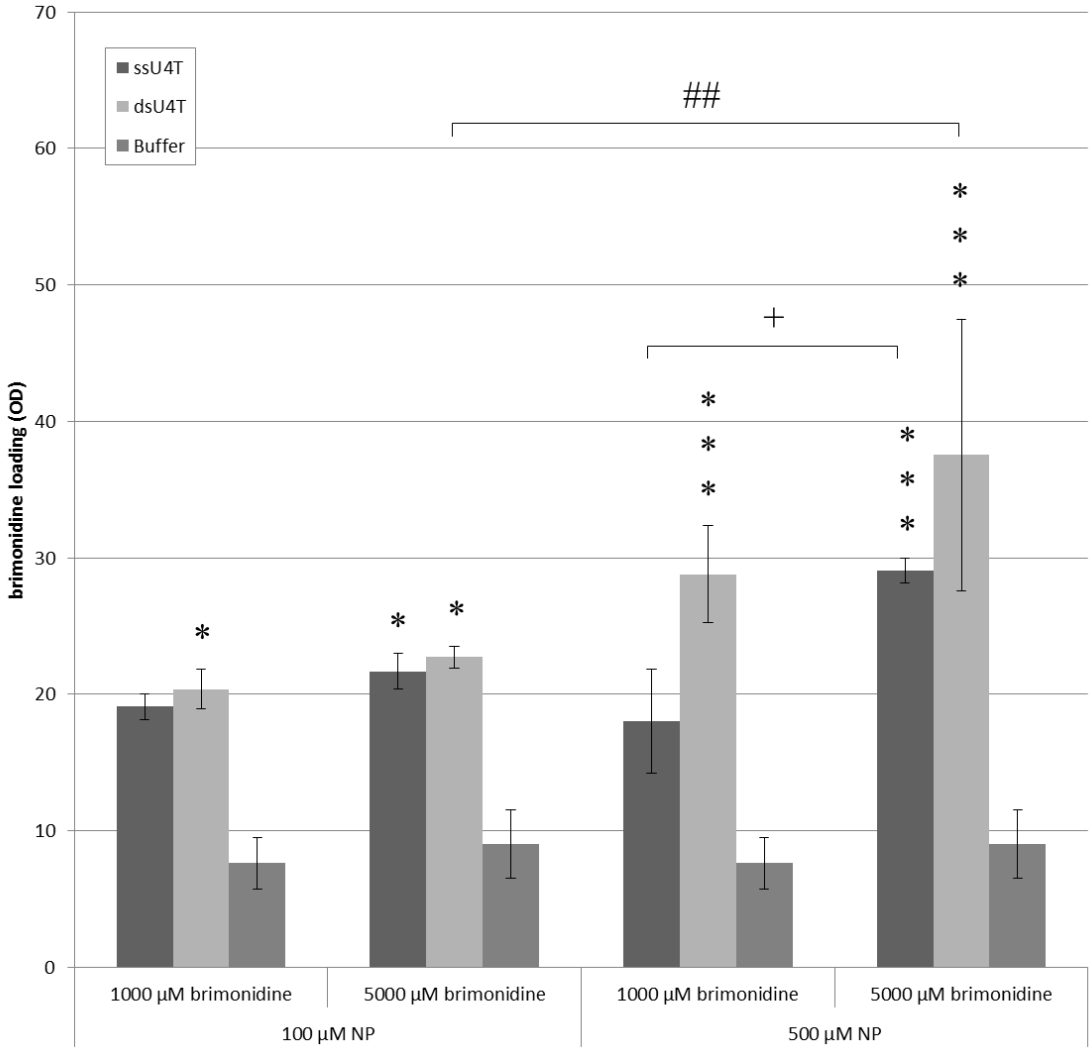

Figure 7: Analysis of solved brimonidine containing NPs in dependency of DNA concentration and brimonidine feed concentration. The used NP as well as the brimonidine feed concentrations are given. Samples were loaded overnight. Higher feed concentrations of brimonidine and higher concentration of NP are advantageous to load higher amounts of brimonidine. Remark: Buffer controls that are presented for the 100 µM as well as the 500 µM NP group are the same. Statistics: n=3, mean and standard deviation are given, * - p < 0.001; **/## - p< 0.01; */+ - p<0.05; */**/*** compared to the depending buffer control, for # and + depending samples are marked in the graph.**

For a NP concentration of 100 µM a higher loading of brimonidine was observed with increasing feed concentration (ssU4T: 1000 µM: 19.08 OD vs. 5000 µM: 21.67 OD; dsU4T: 1000 µM: 20.37 OD vs 5000 µM: 22.72 OD) (Figure 7). The control with only buffer (1000 µM: 7.61 OD, 5000 µM: 9.02 OD) showed a saturated solvation behaviour. For 1000 µM of feed concentration, dsU4T loaded significantly more brimonidine than buffer ($p = 0.023$). The loading for 5000 µM was significantly higher than buffer for both ssU4T ($p = 0.024$) and dsU4T ($p = 0.012$).

The loading of 500 µM NPs increased with the feed concentration (ssU4T: 1000 µM: 18.05 OD vs. 5000 µM: 29.05 OD; dsU4T 1000 µM: 28.80 OD vs. 5000 µM 37.53 OD). For 1000 µM of feed concentration, ssU4T did not loaded significantly more brimonidine than buffer ($p = 0.106$). All other samples loaded significantly more brimonidine than buffer (for all $p \leq 0.001$).

The experiment revealed that the loading of brimonidine increased with increasing feed concentration. Significant differences were observed between the 500 µM of ssU4T samples (1000 µM of brimonidine: 18.05 vs. 5000 µM: 29.05, $p < 0.05$). Furthermore, loading was more efficient for higher concentrations of NPs. This fact was significant for the dsU4T samples loaded with 5000 µM of brimonidine (100 µM of NP: 22.72 vs. 500 µM: 37.53, $p < 0.01$).

It can be concluded, that higher concentrations of NP as well as of brimonidine feed concentration and the use of dsU4T was advantageous for loading higher amounts of brimonidine into the NPs.

In the next step, the loading through hydrophobic interaction was investigated over time. dsU4T NPs were selected as the best carrier. It was used at 500 µM and loaded with 5000 µM of brimonidine. The absorption of these samples was measured every 12 hours for 96 hours. Buffer only served as control.

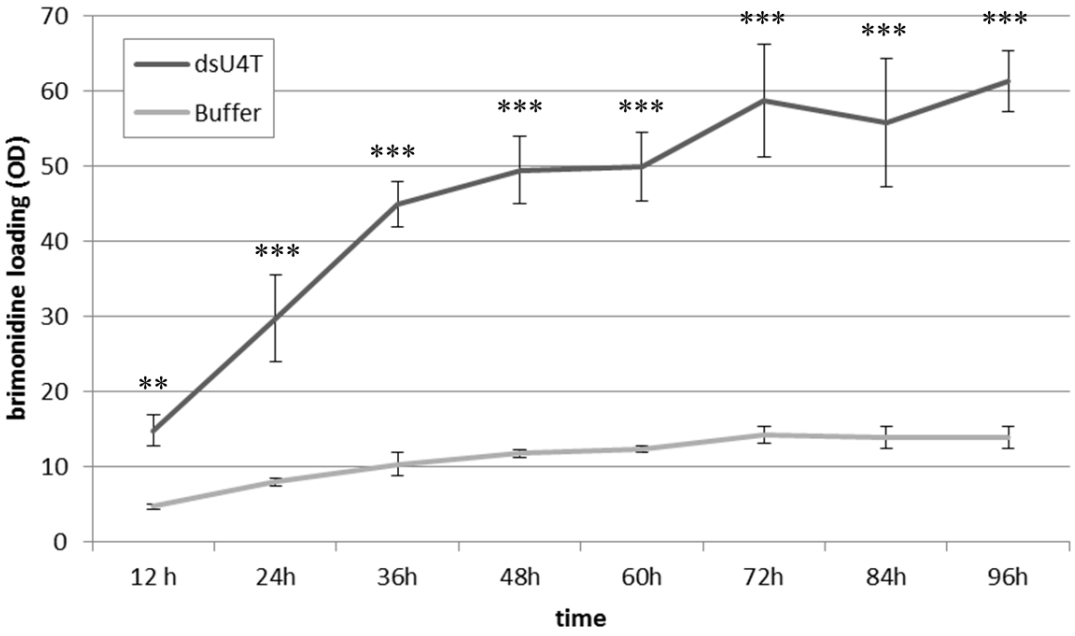

Figure 8: Analysis of solved brimonidine in solution containing dsU4T NPs over time. Buffer samples served as control. Brimonidine feed concentration was fixed to 5000 µM, the NP concentration was 500 µM. The absorption was measured after the given time points. dsU4T loaded significantly more brimonidine than buffer. Loading increased over time and reached a plateau after 48 hours. Statistics: n=4, mean and standard deviation are given, * - p< 0.001; ** p<0.01 compared to the buffer control.**

The amount of loaded drug increased over a period of 48 hours and reached a plateau hereafter (Figure 9). As expected, the dsU4T showed significantly more loading than buffer control (t = 96 hours: dsU4T: 61.25 OD, buffer: 13.82 OD, $p < 0.001$). For these samples the speed of loading also slowed down after 48 hours and a plateau was reached similarly as found for the NPs.

After determining the optimal loading conditions, in all following experiments the NPs were formulated at 500 µM and incubated with brimonidine for 48 hours unless otherwise noted.

3.1.2 Release of brimonidine from hydrophobic loaded nanoparticles

After proving the successful loading of brimonidine in DNA NPs, in the next step the release of the drug from the NPs was investigated. The release was quantified and studied over time.

To measure the release, devices were constructed that contain two compartments which are separated by a semi-permeable membrane (Figure 9). The pore size of this membrane was chosen so that the NPs cannot diffuse through, but the smaller molecule brimonidine is able to travel between the two compartments. The NPs were loaded in the top compartment of the device, whereas the bottom compartment contained a large excess of buffer. Due to the applied concentration gradient, the brimonidine diffused through the membrane into the buffer. To determine the release from the NPs, the amount of drug in the bottom compartment was followed over time by absorption measurement.

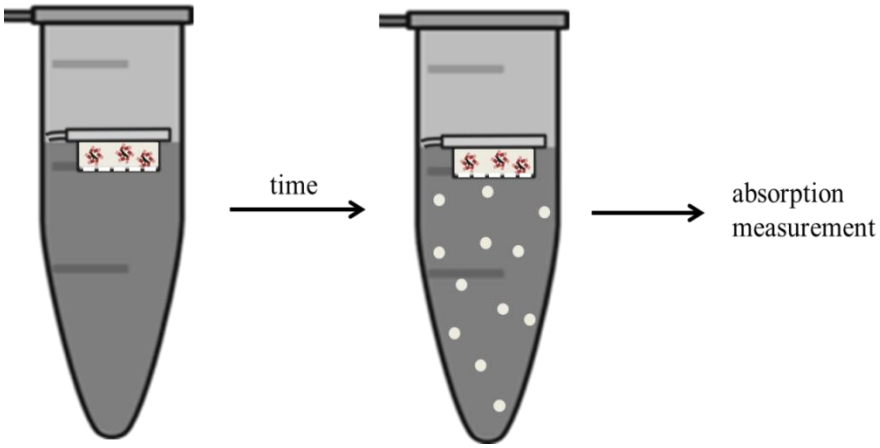

Figure 9: Schematic representation of the release experiment. On the left hand, solution containing brimonidine loaded NPs is filled in the devices and this device then placed in a larger excess of buffer. Over time, brimonidine passed the semi-permeable membrane, whereas the NPs did not. Light grey dots represent brimonidine in solution. (Figure composed from Cliparts: http://www.clker.com (last accessed 15.5.17 8:11; public domain)).

For the release of brimonidine two formulations were analysed. First, the drug liberation from the NPs as obtained directly after performing brimonidine loading. However, to reach the current clinical concentrations of brimonidine, the loaded NPs had to be supplemented with water soluble brimonidine-tartrate (second formulation). In contrast to pristine brimonidine, this compound is water soluble due to the charged nature of the tartrate. For this reason high concentrations in an aqueous environment can be obtained.

Release of brimonidine from loaded nanoparticles over time

First the proper design of the release device was confirmed. After placing NP solution without brimonidine loaded in the release device the absorption was measured in the bottom compartment over time and no NPs were detected.

In a first experiment the release properties of loaded NPs at a concentration of 500 µM were studied. The diffusion of brimonidine from loaded ssU4T, dsU4T and buffer (control) was tested. Additionally, another control was included, dsT4T. This is a pristine DNA strand that is double stranded with the same sequence as U4T, however, has no lipid modified nucleotides and thus cannot form NPs. It serves as comparison to the dsU4T NPs and functions to see the influence of brimonidine loading into the hydrophobic core of the NP and via interactions in the double stranded oligonucleotide. The same concentration of DNA as for ssU4T and dsU4T was used for dsT4T. For the loading brimonidine feed concentrations of 1000 and 5000 µM were used. Before starting the experiment, samples were loaded by combining the NP solution with the brimonidine pellet, as described in section 2.2.3 (Figure 5).

Afterwards, the release of brimonidine from the NPs loaded with different feed concentrations over time was determined.

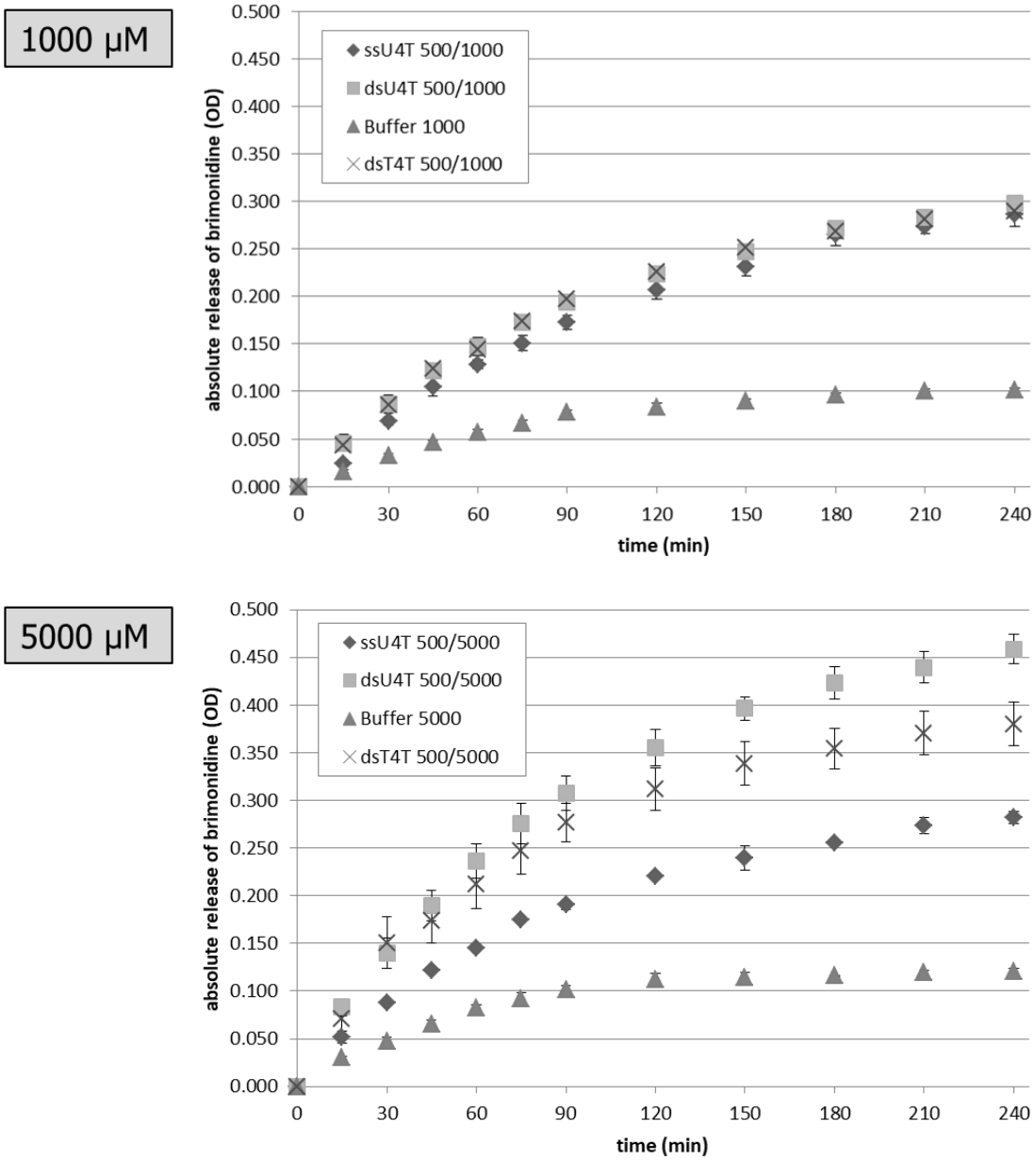

Figure 10: Comparison of brimonidine release from samples loaded with different brimonidine feed concentrations. Brimonidine feed concentration were 1000µM and 5000 µM. Both sets were prepared with 500 µM of DNA and loading was performed for 48 hours. dsT4T and especially dsU4T released more upon a higher loading concentration of brimonidine. Statistics: Mean and standard deviation are given.

It is visible that a higher feeding concentration did not influence the release of brimonidine from ssU4T (1000 µM brimonidine feed concentration: 0.286 vs. 5000 µM: 0.282) (Figure 10). The release from buffer is 1.2x higher when loaded with the higher feed concentration (1000 µM: 0.101 vs. 5000 µM: 0.121). The same applies to dsT4T which released 1.3x more (1000 µM: 0.290 vs. 5000 µM: 0.380). In contrast,

dsU4T released 1.5x more when loaded with more brimonidine (1000 µM: 0.298 vs. 5000 µM: 0.459) as a result from the higher loading observed at higher feed concentrations. Hence, for dsU4T it is advantageous to use a higher feeding concentration in regard to the released amount. For the rest of the samples the influence was small. As such, it can be concluded that better loading and consequently a bigger amount of released brimonidine is achieved by employing a higher feeding concentration. Further experiments will be performed using 5000 µM of brimonidine feed concentration.

The released amount is dependent on the loaded amount of brimonidine. This is also due to the fact that the speed of diffusion is dependent on the concentration gradient, a faster release can thus be observed upon higher loading. To determine the release rate independent of the difference in loaded amount, the samples were diluted to obtain the same brimonidine concentration and thus the same concentration gradient in each sample. For that purpose, first the loaded brimonidine amount of the samples was determined using absorption measurement. The samples were then diluted with TAE buffer in order to achieve the same amount of brimonidine in each solution. To this end ssU4T was diluted 1:4, dsU4T 1:6, buffer 1:0.33 and dsT4T 1:5.45. These diluted samples with the same amount of brimonidine were named “adjusted samples” subsequently. Undiluted samples, as directly obtained from the loading samples and with different brimonidine concentrations were called “non-adjusted”.

For several reasons, the results will be directly presented as relative release (Figure 11). Although absolute values give good insight in the quantity of released brimonidine, relative presentation makes comparison between samples easier. Also, relative values give a better understanding about the slope and speed of drug release. A slower release is an advantage here with regard to longer adhering NPs to the cornea and thus sort of a depot effect. In the meantime, a slower release could also implement a disadvantage if the adherence time is not long enough for the drug to be released. As NPs are expected to well adhere to the corneal surface, a slower release is considered favourable.

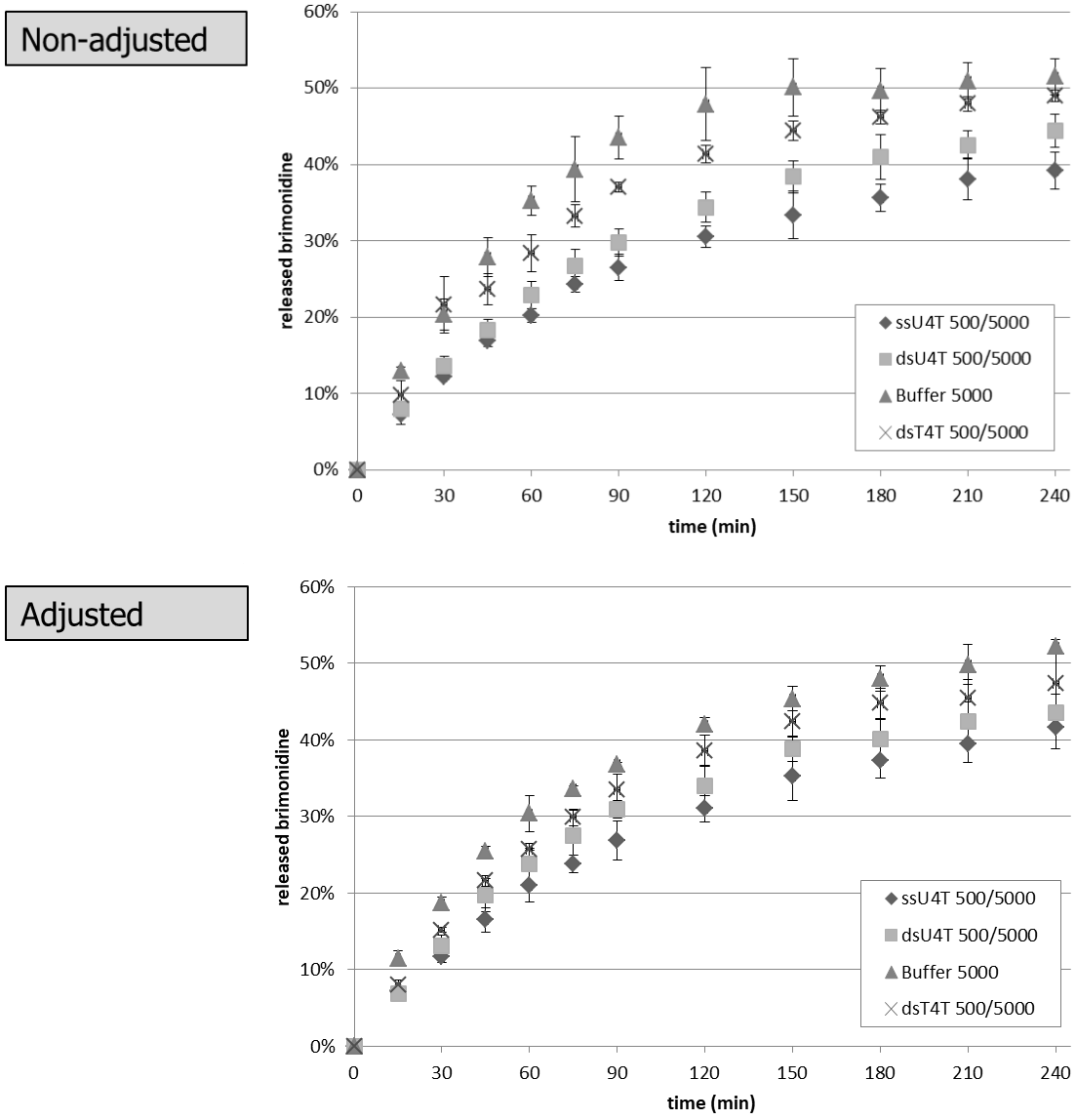

Figure 11: Relative release of brimonidine over time with non-adjusted and adjusted amounts of brimonidine in the release devices. The measurement 28 hours after initiation was set as 100%. Brimonidine feeding concentration was kept at 5000 µM, DNA concentration at 500 µM and loading time overnight. Buffer released brimonidine fastest, ssU4T and dsU4T the slowest. Differences between non-adjusted and adjusted sets are negligible. Statistics: Mean and standard deviation are given.

For both relative values of non-adjusted and adjusted experiments (Figure 11), it is visible, that buffer reached faster values that were over all higher than the other samples (e.g. non-adjusted (t = 240 minutes): ssU4T: 39.1% vs. buffer 51.5%, relation: buffer was 1.32x higher than ssU4T, slope is steeper for buffer). This indicated that diffusion of brimonidine from the buffer sample is fastest. dsT4T released the drug slower than buffer samples for both sets (non-adjusted: 0.95x less vs. adjusted: 0.91x less than

buffer, both: flatter slope). dsU4T (non-adjusted: 44.4% vs. adjusted: 43.5%, both flat slope) and ssU4T (non-adjusted 39.1% vs. adjusted: 41.6%, both flat slope) released slowest. Both achieved lower values than buffer (non-adjusted 51.5%, adjusted: 52.1%) and dsT4T (non-adjusted 49.0%, adjusted 47.3%). This indicated that the ssU4T and dsU4T NPs have stronger binding with brimonidine and can be considered as best performing samples.

When comparing non-adjusted (Figure 11 "Non-adjusted") and adjusted (Figure 11 "Adjusted") values, all samples reached analogue amounts regarding the percentage of released brimonidine (relation non-adjusted to adjusted (t = 240 minutes): ssU4T: 0.94x, dsU4T 1.02x, dsT4T: 1.04x, buffer: 0.99x). For all samples the influence of adjusting the amount of brimonidine seems to be negligible as the achieved relative values and thus the slope are comparable at the same time points for non-adjusted and adjusted sets.

Release from brimonidine-tartrate co-formulated and brimonidine loaded nanoparticles over time

To be able to compare commercially available brimonidine eye drops and the here developed formulation containing NPs in future in-vivo experiments, it is necessary to adjust the amount of brimonidine in solution to match the commercial one. To this end, the commercial active ingredient, brimonidine tartrate, needs to be added to the NP solution. This is due to the limited loading capacity of the NPs which does not reach the commercial concentration level. To prove that the release properties are unaffected when using a co-formulation with brimonidine-tartrate, the liberation of brimonidine from NPs was investigated after co-formulation.

For this purpose the amount of brimonidine in loaded NPs was determined by absorption measurement and brimonidine-tartrate added to adjust the total amount of brimonidine in solution to 5 mM ("non-adjusted set"). For this release experiment, a second set of samples was chosen to investigate the effects of having the same amounts of brimonidine loaded in NPs in the release samples ("adjusted set"). For this adjusted set, dsU4T samples with 1085 µM of loaded brimonidine were diluted 1:4.6 and buffer

sample 1:1.64 in order to achieve a brimonidine concentration of 235 µM for both samples. As the concentration of loaded brimonidine was then the same for both samples, the same amount of brimonidine tartrate (36.9 µl of a 25 mM brimonidine tartrate stock solution) was added to them to achieve a total amount of brimonidine in solution of 5 mM. A schematic representation of these samples can be seen below (Figure 12). The release rates of both sets were measured and compared.

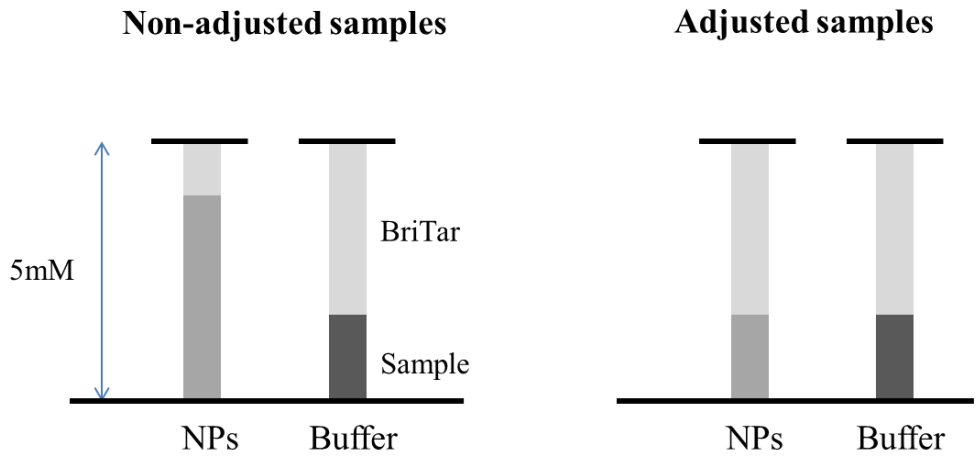

Figure 12: Schematic representation of the two sets of samples with brimonidine tartrate co-formulation. The height of the bars represents the concentration. For non-adjusted samples, brimonidine tartrate (BriTar) was added to reach 5mM of final brimonidine concentration in solution. For adjusted samples, the samples were diluted in order to achieve the same concentration of brimonidine. Then, the same amount of brimonidine tartrate was added. Legend: grey – brimonidine loaded in NPs, dark grey – brimonidine in buffer control, light grey – brimonidine tartrate added to reach 5 mM final concentration.

As dsU4T was found to be the NP with the best loading and releasing properties, it will be the only tested NP. The loaded buffer samples served as control. Only relative representation for the results will be shown as this is a more comprehensive way to compare the two sets. The overnight released amount is set as 100%.

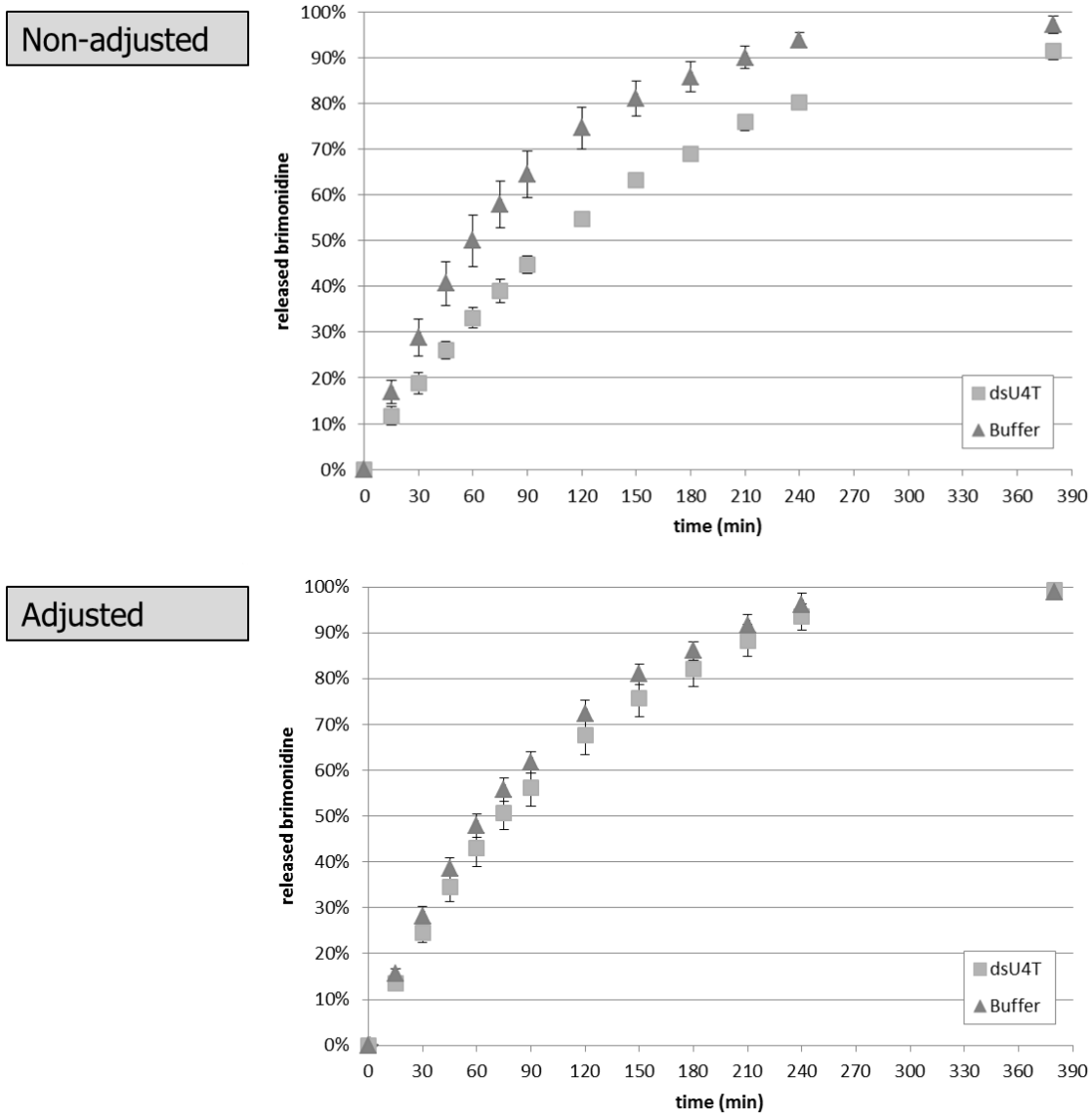

Figure 13: Relative release from brimonidine loaded dsU4T and buffer with additional co-formulation of brimonidine tartrate over time. The amount of brimonidine in the release devices was non-adjusted or adjusted to each other. For both sets, loading conditions were 500µM of DNA, 5000µM of brimonidine and 44 hours of loading. The released amount over night was set as 100%. Non-adjusted and adjusted sets reached comparable relative values after 390 minutes. dsU4T released brimonidine faster for the adjusted set. Statistics: Mean values and standard deviation are given.

In both experiments the buffer showed less retaining behaviour of release than dsU4T (steeper slope) (Figure 13). When comparing the adjusted samples, it can be seen, that both samples resembled each other more in release behaviour than they do for non-adjusted samples (released brimonidine after 240 min: adjusted: dsU4T: 93.5%, buffer 96.2%; non-adjusted: dsU4T: 80.1%, buffer: 93.9%). For adjusted samples both buffer

and dsU4T released almost 100% of the complete brimonidine amount in 380 minutes. When using, as done for the adjusted set, higher amounts of brimonidine tartrate (16% more brimonidine tartrate, adjusted: adjusted 0.923 µmol, non- adjusted: 0.795 µmol) and less of loaded NP (62.2% less loaded NPs, adjusted: 0.062 µmol, non-adjusted: 0.164 µmol), the release was faster and the retaining effect of NP decreased. This is expected, as less NPs were present in solution.

3.2 Brimonidine loading in aptamer functionalized DNA nanoparticles

The next step in establishing the use of NPs in eye drops was the evaluation of using aptamers for binding of the drug of interest. To establish the aptameric loading of brimonidine in the NPs, an aptamer binding this drug was first developed using the SELEX (systematic evolution of ligands by exponential enrichment) method. Thereby, the aptamer was chosen from a library of oligonucleotides by selecting the sequence with the highest binding affinity to brimonidine. Afterwards, two DNA sequences were deduced from this by logic design and tested for their binding affinity to brimonidine.

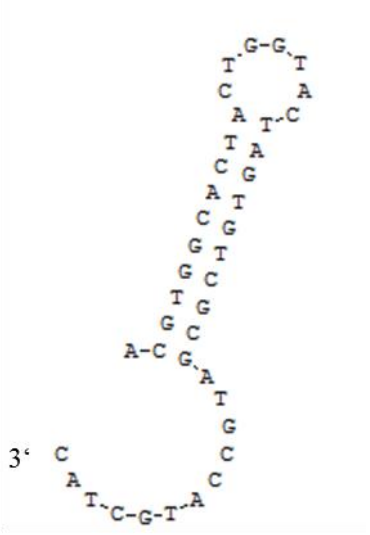

Figure 14: Secondary structure of the brimonidine binding aptamer Bra3. The 3'-end is marked.

The full length sequence of the brimonidine binding aptamer, called Bra3, contains 40 nucleotides and exhibits a stem-loop structure (Figure 14). Additionally, the 3'-end contains 12 nucleotides that do not seem to exhibit any secondary structure. In order to investigate the structural properties needed for binding of brimonidine, two shortened sequences were designed from the Bra3 aptamer. These were either truncated at the 5'-end or at both. The shortened versions, called Bra3.1 and Bra3.2, were also investigated for their binding properties towards brimonidine. The sequence details of Bra3 as well as the shortened aptamers are given below (**Table 4**). Their secondary structures are also shown (Figure 15).

Table 4: Nucleotide sequences of the three investigated aptamers. Bra3.1 and 3.2 represent shortened versions of Bra3. The different colours represent parts of the secondary structure of Bra3: green – double stranded part, yellow – small closed loop, blue – nucleotides at the 3' end without any special structure.

name	sequence (5' → 3')
Bra3	ACGTGGCACTACTTGGTACTAGTGTCGCGATGCCATGCTAC
Bra3.1	GTGGCACTACTTGGTACTAGTGTCGCGATGCCA
Bra3.2	ACTTGGTACTAGTGTCGCGATGCCATGCTAC

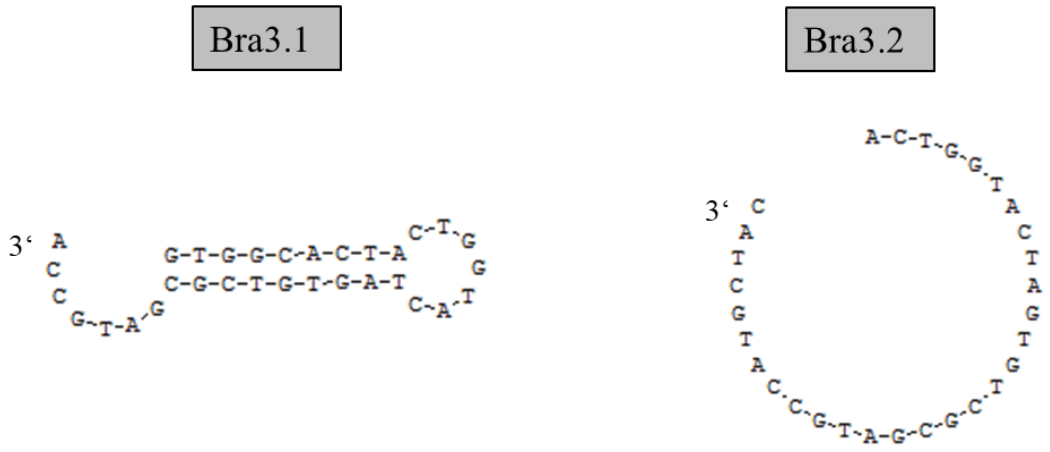

Figure 15: Secondary structures of the aptamers Bra3.1 and Bra3.2 as shortened versions of Bra3. The 3'-end of the aptamers are marked.

For validation of brimonidine binding of the three aptamers, first their affinity to the drug was determined. The best sequences were then selected and the loading of brimonidine into NPs with aptamers established. Finally, also the release from these NPs was investigated.

3.2.1 Validation of aptamer binding towards brimonidine

To evaluate the affinity of brimonidine to the designed aptamer sequences, a fluorescence based binding assay was employed. SYBR Green binds non-specifically to double stranded DNA. In its bound conformation it emits green light (529 nm) when exited with blue light (495 nm). Unbound and bound to single stranded DNA SYBR Green shows little fluorescence. As soon as a target molecule, e.g. brimonidine, binds to the double stranded DNA, the aptameric structure and the SYBR Green fluorescence is

altered. Hence, SYBR Green is removed or incorporated and the fluorescent signal decreases or increases, respectively. Consequently, SYBR Green can be used to determine the interaction between aptamer and analyte (Sarpong and Datta, 2012, McKeague et al., 2014). To analyse this effect, the fluorescence intensity was measured before and after addition of different amounts of brimonidine to the aptamer solution.

As a first step it needed to be shown that the full length and the shortened aptamers bind to brimonidine. The DNA aptamers at 100 nM were incubated with SYBR Green and brimonidine and the fluorescence measured. The results are presented as changes in RFU (relative fluorescence unit, in %) whereas the samples without drug addition is used as reference (Figure 16).

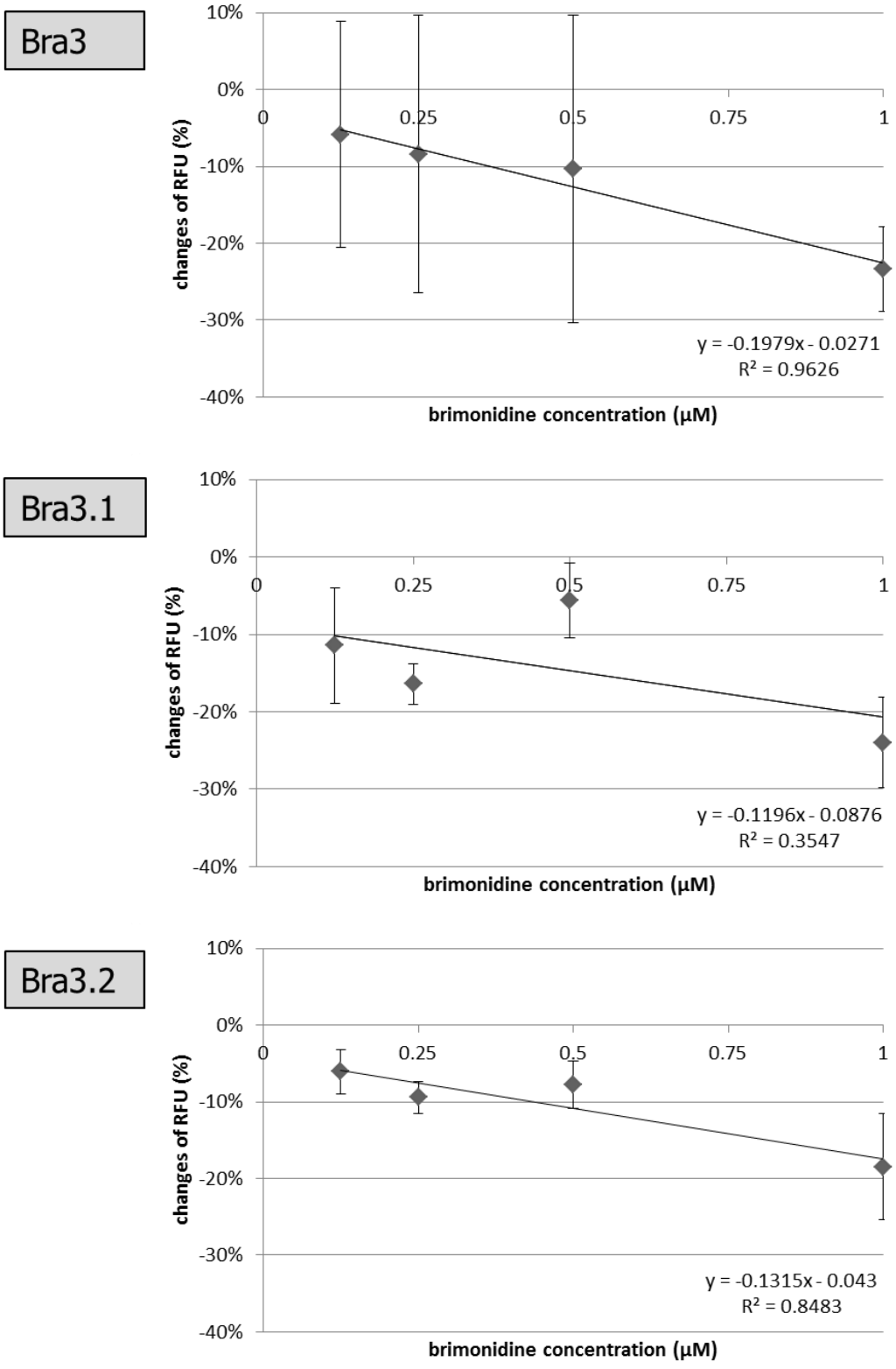

Figure 16: Changes of fluorescence (RFU, in %) in dependency of applied brimonidine concentration (0.125, 0.25, 0.5 and 1 µM) for different aptamers: Bra3, Bra3.1 and Bra3.2. Measurement (n=3) was performed 40 min after application of brimonidine. A general dependency between the applied brimonidine and changes of the measured fluorescence could be seen. Mean values, standard deviation, a linear regression line, its formula as well as the coefficient of determination are given.

There is in general a dependency visible between brimonidine concentration and measured fluorescence (Figure 16). Higher brimonidine concentration result in lower relative RFU values (linear regression lines: Bra3: y= -0.1979x – 0.0271, R^2= 0.9626, Bra3.1: y= -0.1196x – 0.0876, R^2= 0.3547, Bra3.2: y= -0.1315x – 0.043, R^2= 0.8483). Although standard deviations are rather high, the binding behaviour between brimonidine and the aptamers could be shown.

In a next step the aptamers were elongated with the complementary sequence of U4T to enable the binding to U4T and thus the formation of functionalized NPs. Each aptamer (apt) was tested and compared with cU4T-apt only, U4T + cU4T-apt and T4T + cU4T-apt (Figure 17).

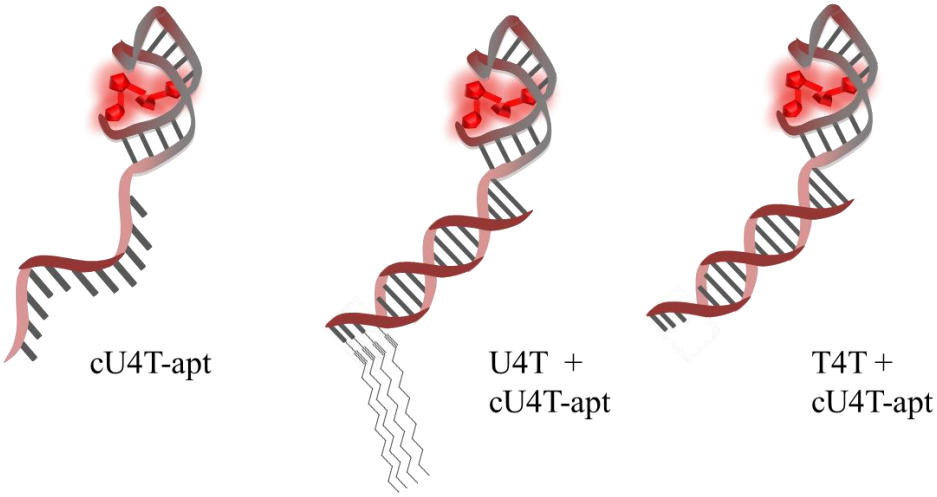

Figure 17: Scheme of the tested species: cU4T-apt, U4T + cU4T-apt and T4T + cU4T-apt. Each species containing an aptamer (apt) is elongated with the complementary strand of U4T to enable the formation of NPs.

cU4T-apt, U4T + cU4T-apt and T4T + cU4T-apt were tested for all aptamers. As representative example Bra3.1 is shown (Figure 18). For the comparison of the different aptamers, U4T + cU4T-apt is given for all aptamers (Figure 19).

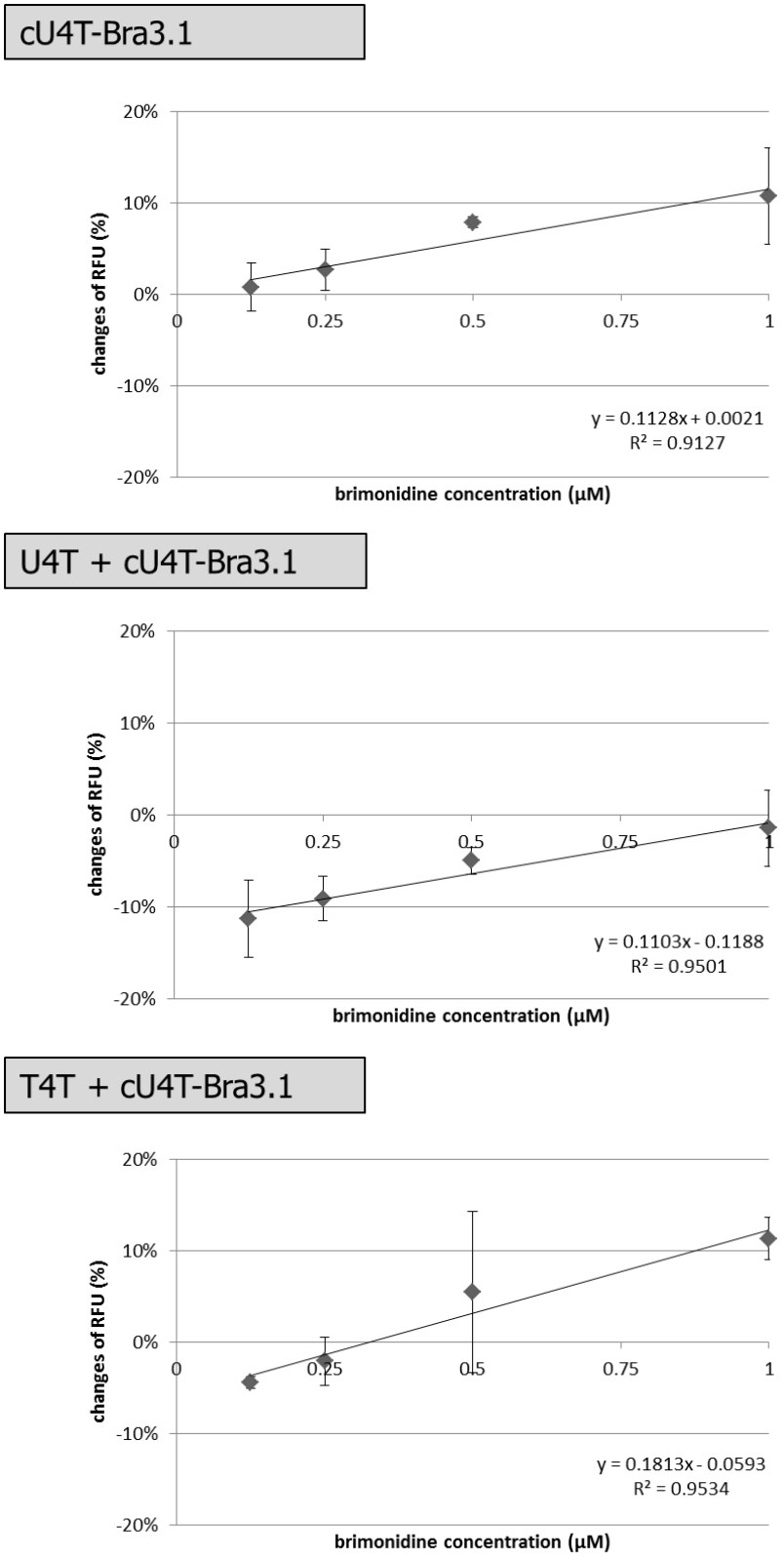

Figure 18: Aptamer Bra3.1. Changes of RFU (%) in dependency of the applied brimonidine concentration (0.125, 0.25, 0.5 and 1 µM) for the species cU4T-Bra3.1, U4T + cU4T-Bra3.1 and T4T + cU4T-Bra3.1. With increasing concentrations of brimonidine, the measured fluorescence increased. n=3, mean values, standard deviation, a linear regression line and its formula as well as the coefficient of determination are given.

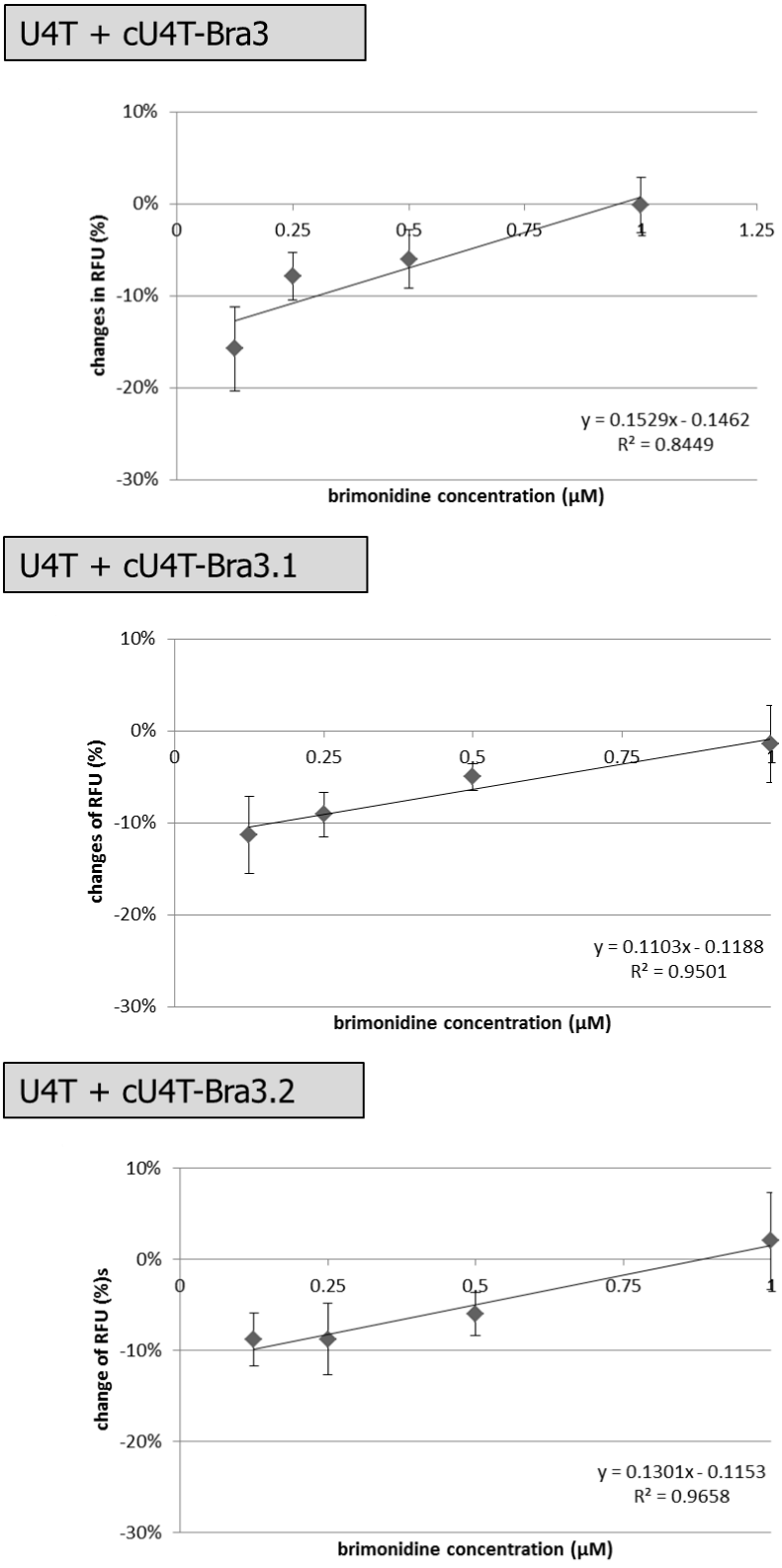

Figure 19: Comparison of three tested aptamers. Changes of RFU (%) in dependency of the applied brimonidine concentration (0.125, 0.25, 0.5 and 1µM) for the species U4T + cU4T-Bra3, U4T + cU4T-Bra3.1 and U4T + cU4T-Bra3.2. With increasing concentrations of brimonidine, the fluorescence increased. n=3, mean values, standard deviation, a linear regression line and its formula as well as the coefficient of determination are given.

When comparing cU4T-apt only, U4T + cU4T-apt and T4T + cU4T-apt for all tested species, it can be observed that for all samples there were clear properties. There was a tendency towards an increased fluorescence for increased brimonidine concentration. For Bra3.1 this tendency was clearest (cU4T-Bra3.1: y= 0.1128x + 0.0021, R^2= 0.9127, U4T + cU4T-Bra3.1: y= 0.1103x – 0.1188, R^2= 0.9501, T4T + cU4T-Bra3.1: y= 0.1813x – 0.0593, R^2= 0.9534) (Figure 19). For the aptamer Bra3 this increase in fluorescence with increasing brimonidine concentration could be experienced too. The Bra3.2 aptamer did not show binding behaviour for the samples of cU4T-Bra3.2 only (data not shown).

It could be seen in a first set of experiments that the aptamers Bra3, Bra3.1 and Bra3.2 showed a concentration binding behaviour between aptamer and brimonidine. In more detailed experiments functionalized NPs with Bra3 and Bra3.1 also revealed a binding behaviour of brimonidine.

3.2.2 Loading of brimonidine in nanoparticle with bound aptamers

In a next step the loading of brimonidine into aptamer functionalized NPs was investigated. Three aptamers were tested and compared with each other regarding their ability to load brimonidine and their loading behaviour over time.

In a first experiment NPs functionalized with the aptamers Bra3, Bra3.1 and 3.2 were tested. dsU4T served as comparison as it revealed to be the best performing hydrophobic NP (section 3.1.1). After combining dried brimonidine and NP solution, the absorption of the resulting solution was measured with a spectrophotometer every 12 hours for 48 hours to determine the loading over time.

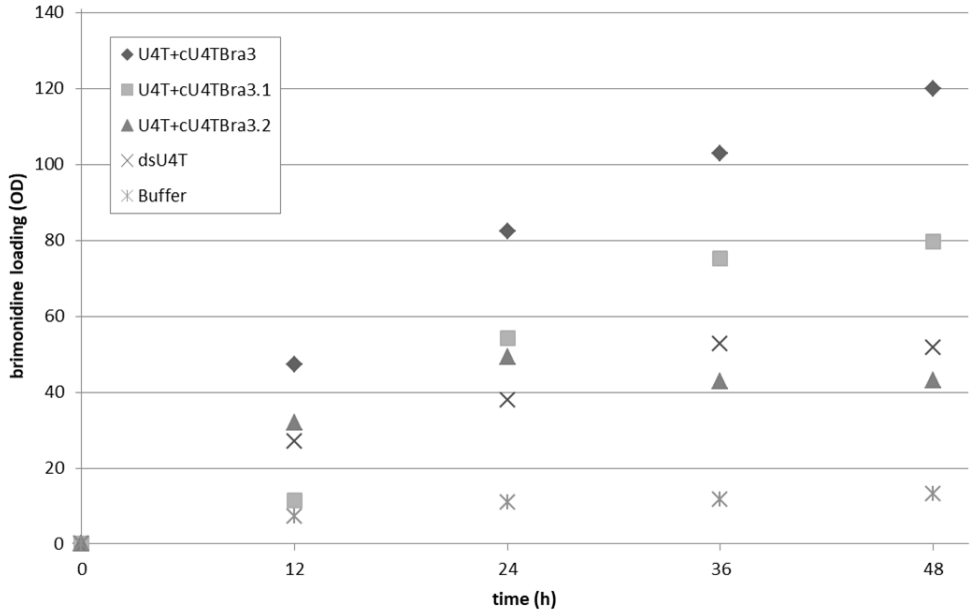

Figure 20: Loading of brimonidine in different with aptamer functionalized NPs, as well as a dsU4T and a buffer control over a time period of 48 hours. Except the aptamer Bra3.2 all samples reveal logarithmic loading behaviour.

Table 5: Mean and standard deviation of loading of brimonidine in different with aptamer functionalized NPs, as well as a dsU4T and a buffer control over a time period of 48 hours. Values are given in OD.

Sample	12 hours	24 hours	36 hours	48 hours
U4T + cU4T-Bra3	47.27±37.14	82.47±33.65	102.87±16.58	119.80±24.06
U4T + cU4T-Bra3.1	11.60±6.26	54.12±2.32	75.20±10.4	79.60±10.42
U4T + cU4T-Bra3.2	32.00±20.79	49.20±6.61	42.80±15.94	43.07±10.51
dsU4T	26.93±8.13	37.87±11.68	52.67±6.13	51.87±7.71
Buffer	7.37±0.51	10.98±0.30	11.8±0.05	13.17±0.20

Loading of brimonidine in functionalized NPs showed logarithmic behaviour for the aptamers Bra3, 3.1 and dsU4T (Figure 20) (Table 5). With ongoing time, OD and hence the loading of brimonidine increased (*U4T + cU4T-Bra3*: 12 h: 47.27 OD, 24 h: 82.47 OD, 36 h: 102.87 OD, 48 h: 119.8 OD; *U4T + cU4T-Bra3.1*: 12 h:11.6 OD, 24 h: 54.13 OD, 36 h: 75.2 OD, 48 h: 79.2 OD; *dsU4T*: 12 h: 26.93 OD, 24 h: 37.87 OD, 36 h: 52.87 OD, 48 h: 51.87 OD), on the other hand the speed of loading decreased. In this case the NPs functionalized with aptamer Bra3.2 was an exception as the loading even decreased slightly after 24 hours (12 h: 32 OD, 24 h: 49.2 OD, 36 h: 42.8 OD, 48 h: 43.07 OD). Additionally, after completion of the experiment, NPs with Bra3.2 exhibited

a gel-like behaviour, which hindered sample handling and measurements. Bra3 is loading the highest drug amount (119.8 OD), followed by Bra3.1 (79.6 OD) and dsU4T (51.87 OD). Loading for all samples is multiple times higher than for the buffer control (13.17 OD, *U4T + cU4T-Bra3*: 9.1 x, *U4T + cU4T-Bra3.1*: 6,04 x, *U4T + cU4T-Bra3.2*: 3.27 x, *dsU4T*: 3.94 x). Furthermore, it seems that the loading is reaching a plateau phase after 36 hours, this can be especially seen for Bra3.1 and dsU4T. For the hydrophobic NP loading experiment, this plateau was reached after 48 hours.

These experiments proofed that NPs functionalized with Bra3 and Bra3.1 aptamers showed good drug loading properties. In contrast, the Bra3.2 aptamer showed poor binding and loading behaviour and resulted in inconsistent gel formation.

Furthermore, the relation between synthesis costs of the aptamers and their loading ability was drawn (Table 6). A higher loading per € is advantageous.

Table 6: Relation between the loaded amount in the different NPs and their production costs.

aptamer	Loaded amount of brimonidine after 48 hours (in µM)	Production costs (per 10 µmol of NP) (€)	Loading per € (µM/€)
U4T-Bra3	6246	2750	2.27
U4T-Bra3.1	4150	2118	1.96
U4T-Bra3.2	2245	1938	1.16
dsU4T	2704	322	8.40

Regarding not only the absolute production costs (in €) but the relative loading per € of production cost (in µM/€), dsU4T loads more brimonidine than the aptamers per € (dsU4T: 8.40 µM/€ vs. aptamers 1.16 - 2.27 µM/€), thus dsU4T is cheaper than the aptamers. Beyond the aptamers, U4T-Bra3 is the aptamer with the lowest (2.27 µM/€) and U4T-Bra3.2 the one with the highest costs regarding the loading per € (1.16 µM/€). Additionally, the loading abilities of U4T-Bra3 and U4T-Bra3.1 were multiple times higher than U4T-Bra3.2 (U4T-Bra3: 2.78 x, U4T-Bra3.1: 1.85 x). This and its gel formation behaviour are the reasons why U4T-Bra3.2 was left out of consideration from here on.

3.2.3 Release of brimonidine from aptamer nanoparticles

To prove and quantify the ability of functionalized NPs to release the loaded drug, the release over time was determined in a similar fashion as described for hydrophobic NPs (chapter 2.2.4 and 3.1.2). To this end, the release of the loaded U4T + c4T-Bra3, U4T + cU4T-Bra3.1, dsU4T NPs and the loaded buffer control were investigated. The dsU4T NPs loaded with brimonidine using hydrophobic interactions served as a comparison as they revealed good release in the hydrophobic NP experiments (chapter 3.1.2). Non-adjusted and adjusted amounts of brimonidine were studied in the same set up as for previous release experiments (chapter 3.1.2) (Figure 21).

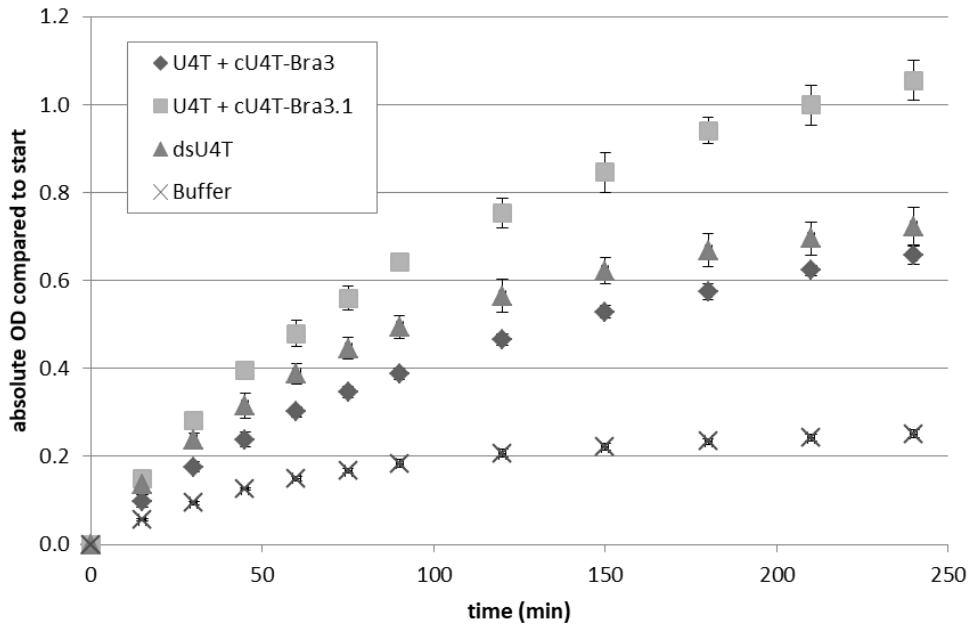

Figure 21: Absolute release of brimonidine from NPs (non-adjusted) over time. The compared entities are the functionalized NPs with Bra3 and Bra3.1 aptamers, as well as hydrophobically loaded dsU4T. Buffer served as control. Bra3.1 showed highest, dsU4T and Bra3 comparable absolute release. Statistics: n=3, mean values and standard deviation are given.

The dsU4T NPs released a comparable or even slightly higher amount of brimonidine than the Bra3 functionalized NPs (t = 240 min: dsU4T: 0.723 OD vs. U4T + cU4T-Bra3: 0.657 OD). In contrast, the release from NPs containing U4T + cU4T-Bra3.1 aptamers (U4T + cU4T-Bra3.1: 1.055 OD) was approximately 1.5 times higher than the release of U4T + cU4T-Bra3 and dsU4T. The relative release of sets with adjusted and non-adjusted amounts of brimonidine in the release devices is shown below (Figure 22).

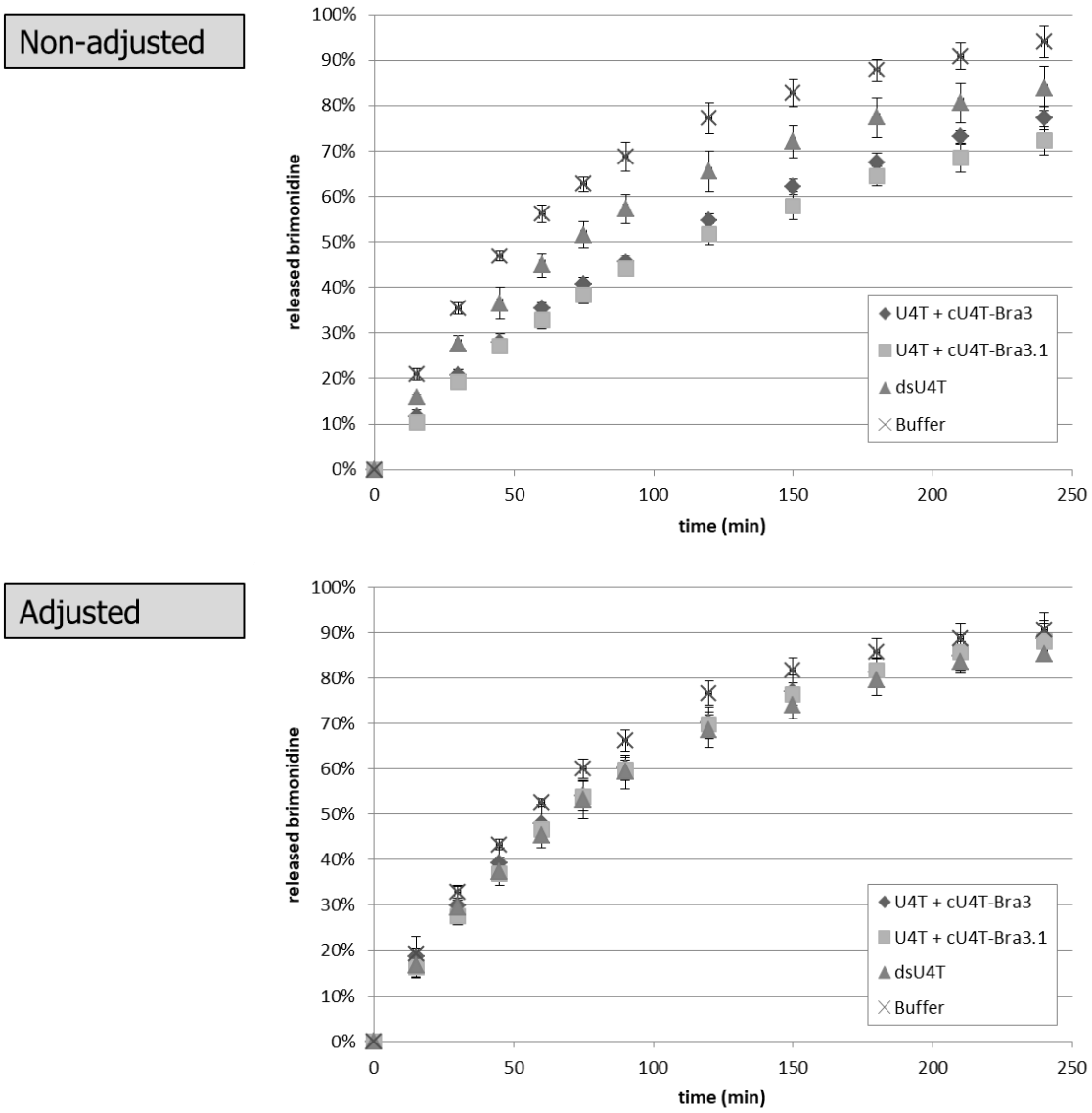

Figure 22: Relative release of brimonidine over time from with DNA aptamer functionalized NPs as well as dsU4T and a buffer control. Non-adjusted and adjusted set up are presented. The released amount over night was set as 100%. NPs with and without aptameric modification released brimonidine slower than buffer. Statistics: n=3, mean values and standard deviation are given.

For non-adjusted samples the buffer control released brimonidine fastest (t = 240 min: 94.0%) (Figure 22 "Non-adjusted"), followed by dsU4T (83.7%). Both aptamer functionalized NPs released the drug at the same speed (U4T + cU4T-Bra3: 77.2%, U4T + cU4T-Bra3.1: 72.2%, similar slope) but slower than buffer and dsU4T. This is an advantage when employing longer adhering NPs which can serve as drug depot. For adjusted amounts all DNA samples (U4T + cU4T-Bra3: 88.7%, U4T + cU4T-Bra3.1:

88.1%, dsU4T: 85.3%, similar slope) show similar behaviour, with the buffer sample releasing brimonidine slightly faster (90.6%, steeper slope) (Figure 24).

It could be proven, that there is an advantage of using DNA functionalized NPs for the release of brimonidine. Both aptamers showed beneficial effects in retaining the drug that will be of use when applying the NPs as eye drops. Given the higher absolute release and the slower release rate of the U4T-Bra3.1 NPs, their comparable loading, but lower cost of fabrication, this NP was selected for further experiments and will be used for further adherence and safety evaluation.

3.3 Evaluation of adherence time of brimonidine nanoparticles

Normal eye drops are cleared rapidly from the ocular surface by blinking and tearing that occurs directly after administration (Zhang et al., 2004). One advantage of the lipid NPs is their prolonged adherence time to the cornea (de Vries et al., 2018). They serve as depot, thereby resulting in a higher bioavailability of the drug. To proof the prolonged adherence, the adherence was evaluated with fluorescently labelled NP in-vitro on pig eyes as well as in-vivo towards rat cornea.

Previously, de Vries et al. found DNA nanoparticles with lipid modification to adhere up to four hours to rat cornea, NP with aptameric modification and loaded with kanamycin and neomycin up to one hour. Based on this paper, the incubation time was chosen (de Vries et al., 2018).

3.3.1 In-vitro evaluation of adherence time of brimonidine nanoparticles on pig eyes

For the in-vitro quantification on pig eyes, the fluorescently labelled NPs were administered to enucleated pig eyes and placed in buffer to simulate blinking. The fluorescence of NP adhering on the cornea was determined with a fluorophotometer (Ocumetrics, Langley, USA) instantly, after 5, 15, 30 minutes, one, two and four hours.

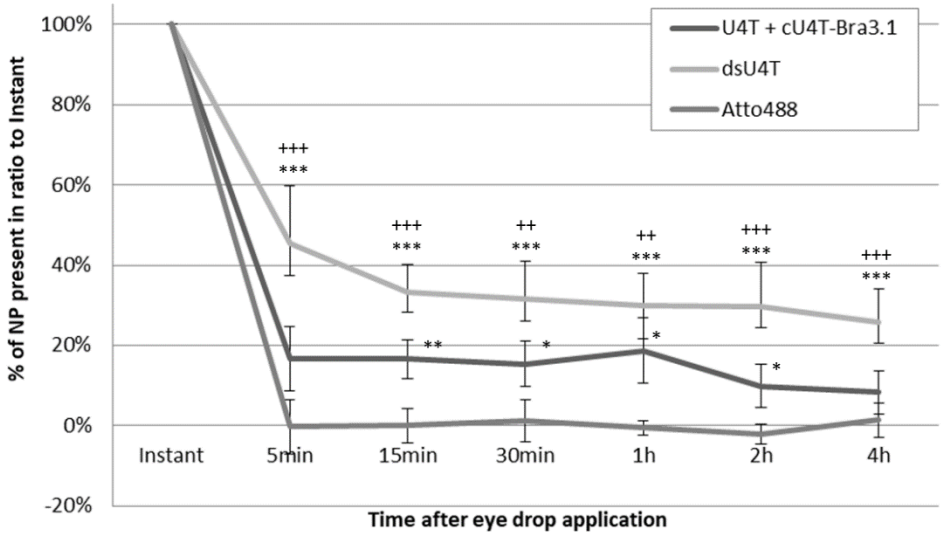

Figure 23: Ex-vivo evaluation of NP adherence to pig eyes up to four hours. U4T + cU4T-Bra3.1 and dsU4T NPs were tested. The fluorophore Atto488 served as control. Statistics: * compared to Atto488, + comparison between the two entities of NPs. */+++ p<0.001, **/++ p<0.01, */+ p< 0.05.**

The control (pristine Atto488) was cleared away rapidly from the corneal surface and no longer detectable five minutes after application (0%). In contrast to this, NPs could be detected up to four hours (4 h: dsU4T: 26%, aptamer: 8%). Thereby, U4T + cU4T-Bra3.1 revealed a less adhering potential towards the cornea. After four hours, the amount of U4T + cU4T-Bra3.1 that was still detectable was 1/3 of the dsU4T samples. Both dsU4T and U4T + cU4T-Bra3.1 samples showed a slightly decreasing level of NPs between 15 minutes (dsU4T: 33%, U4T + cU4T-Bra3.1: 17%) and four hours after application.

3.3.2 In-vivo evaluation of adherence time of brimonidine nanoparticle on rat eyes

After proofing the prolonged residence time of NPs in-vitro, the adherence time was also evaluated in an in-vivo model. The Atto488 fluorescently labelled U4T + cU4T-Bra3.1 NPs were applied to living rats. The animals were euthanized at the designated time points and the adherence determined 15, 30 and 60 minutes after application.

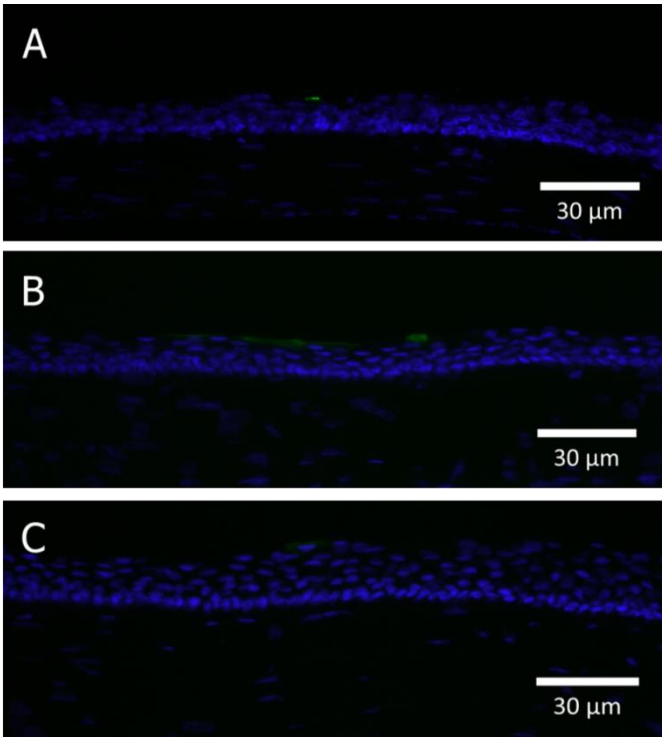

Figure 24: Representative micrographs of adherence evaluation of U4T-Bra3.1 NPs (green) to rat cornea (blue) at different time points: (A) 15 min), (B) 30 min, (C) 60 min.

Table 7: Evaluation of adherence time of U4T-Bra3.1 NP to rat cornea. Per time point four eyes were investigated. The ratio of positive eyes (with NP) to all eyes is given for the investigated time points.

Time points	Positive eyes of all investigated eyes
15 minutes	4/4
30 minutes	2/4
60 minutes	1/4

The NPs adhered well to rat cornea (Figure 24, Table 7). 15 minutes after application of the eye drop, all investigated eyes showed the presences of NPs (4/4 eyes). However, after 60 minutes, only on one eye NPs were found (1/4 eyes). As expected, the amount of eyes in which NPs were found decreased over time.

3.4 Safety evaluation of DNA nanoparticles using in-vitro and in-vivo assays

Before using DNA NPs in the treatment of ocular diseases, toxicity must be excluded to prevent side effects that may harm the patient. For this reasons, biosafety was examined using in-vitro cell culture methods and in-vivo application on rat eyes.

3.4.1 Safety evaluation of DNA nanoparticles using an in-vitro cell culture assay

To evaluate the biocompatibility of DNA NPs, in-vitro cultivated primary cornea epithelium cells from pig eyes were supplemented with different DNA formulations. Following an incubation time of four hours, cell amount, viability as well as apoptosis rate were evaluated. The results were then compared to the corresponding commercial brimonidine tartrate concentration, to evaluate the biosafety compared to the approved drug. Staurosporine and Polyinosinic-polycytidylic acid (Poly I:C) served as controls. Staurosporine is a commonly used inductor of apoptosis (Kruman et al., 1998). Poly (I:C) is a synthetic dsRNA and leads to an activation of inflammation response, among others through the activation of toll-like receptors (Field et al., 1967) (Matsumoto and Seya, 2008).

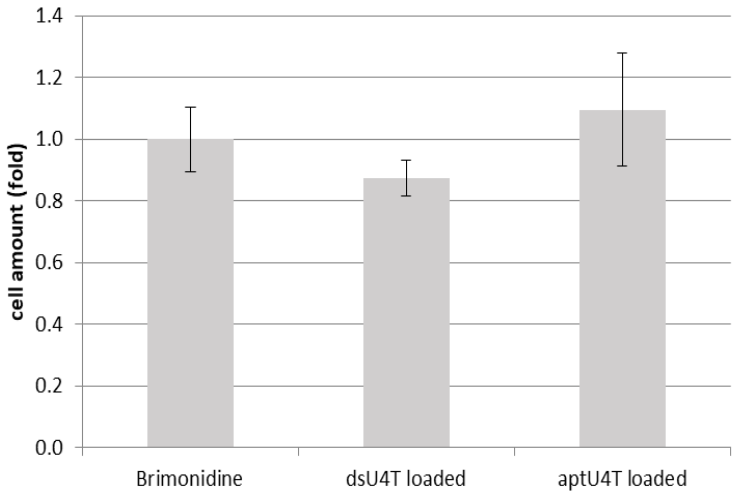

Figure 25: Cell amount of cultivated primary cornea epithelium cells after supplementation of different agents. The results are presented in fold. The brimonidine sample was set to 1. Samples with concentrations of 500 µM are given. Supplementation of loaded dsU4T and U4T + cU4T-Bra3.1 samples did not led to a significantly difference regarding the cell amount. Statistics: Mean values and standard deviation are given. Abbreviation: aptU4T - U4T + cU4T-Bra3.1.

The cell amount (Figure 25) was not significantly influenced by the applied NP (loaded dsU4T: 0.87x, p=0.34; unloaded U4T + cU4T-Bra3.1: 1.09x, p=0.29).

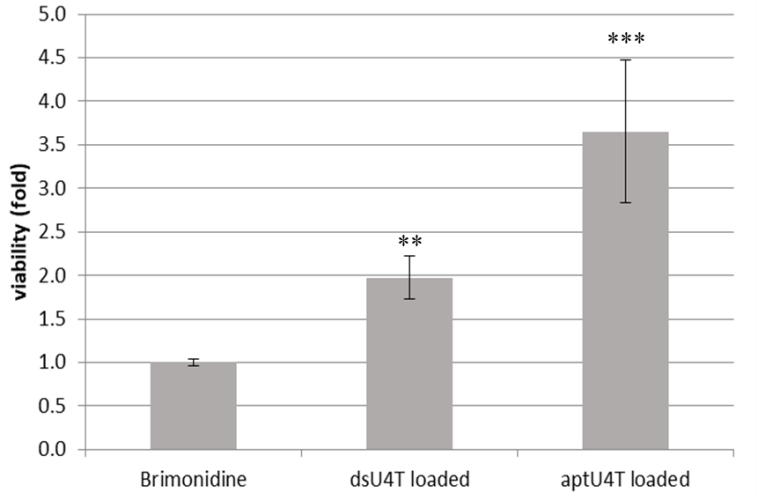

Figure 26: Viability of cultivated primary cornea epithelium cells after supplementation of different agents. The results are presented in fold. Samples with concentrations of 500 µM are given. The brimonidine sample was set to 1. Supplementation led for both samples to an increased viability. The viability of U4T + cU4T-Bra3.1 is higher than for dsU4T. Statistics: Mean values and standard deviation are given. p < 0.001 is shown with ***, p<0.01 with ** - each compared to the depending brimonidine control. Abbreviation: aptU4T - U4T + cU4T-Bra3.1.

Regarding the viability of epithelium cells (Figure 26), both NP samples revealed significantly higher results than brimonidine. U4T + cU4T-Bra3.1 treated samples (in the graphs given as "aptU4T") (3.65x, p<0.001) showed higher viability than dsU4T samples (1.97x, p<0.01).

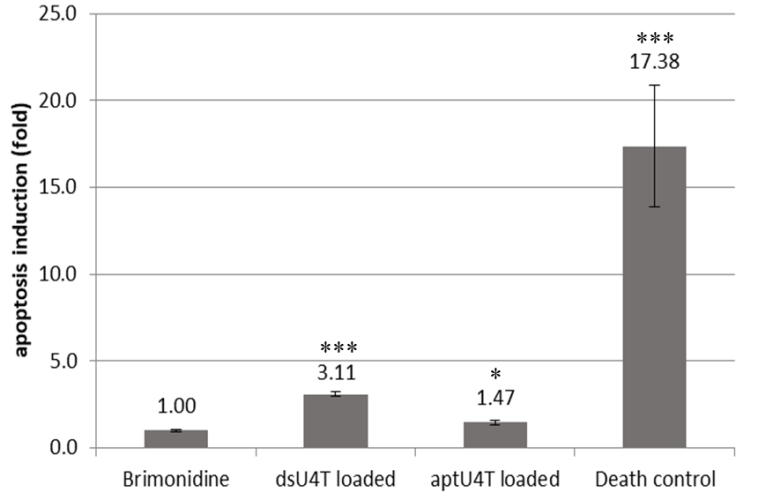

Figure 27: Apoptosis (caspase 3/7 activity) of cultivated primary cornea epithelium cells after supplementation of different agents. The results are presented in fold. The brimonidine sample was set to 1. Samples with concentrations of 500 µM are given as well as the death control. Both samples led to increased apoptosis induction. The death control showed much higher levels of apoptosis induction than the NP samples. Statistics: Mean values and standard deviation are given. p < 0.001 is shown with ***, p<0.05 with * - each compared to the depending brimonidine control. Abbreviation: aptU4T - U4T + cU4T-Bra3.1.

The level of caspase 3/7 activity (apoptosis induction) (Figure 27) was significantly elevated both for samples. dsU4T containing samples (3.11x, $p<0.001$) reached higher levels than aptamer modified NPs (1.47x, $p<0.05$). Here, it needs to be taken into account that none of the samples reached the level of apoptosis induction of the death control (staurosporine, 17.38x).

In general, it can be stated, that the cell amount was not influenced significantly. Cell viability is higher for the NP than for brimonidine supplemented samples. Apoptosis induction was increased for NP samples, but in a much smaller way than for the death control. U4T+ cU4T-Bra3.1 had a less negative impact on primary epithelium cells than dsU4T.

3.4.2 Safety evaluation of DNA nanoparticles using an in-vivo rat eye assay

Despite the good indication that cell culture studies give, they do not represent a complex living organism. Therefore, biocompatibility was also evaluated in-vivo. To this extend, eye drops were administered to living rats using different with brimonidine loaded formulations. The rats were not hindered from blinking during the application or afterwards and euthanized 24 hours thereafter. Apoptotic effects on corneal cells were determined using the terminal deoxynucleotidyl transferase dUTP nick end labeling In-Situ Cell Death Detection assay (TUNEL) (Figure 28). TUNEL positive cells as well as the total number of epithelium cells were counted manually (Figure 29).

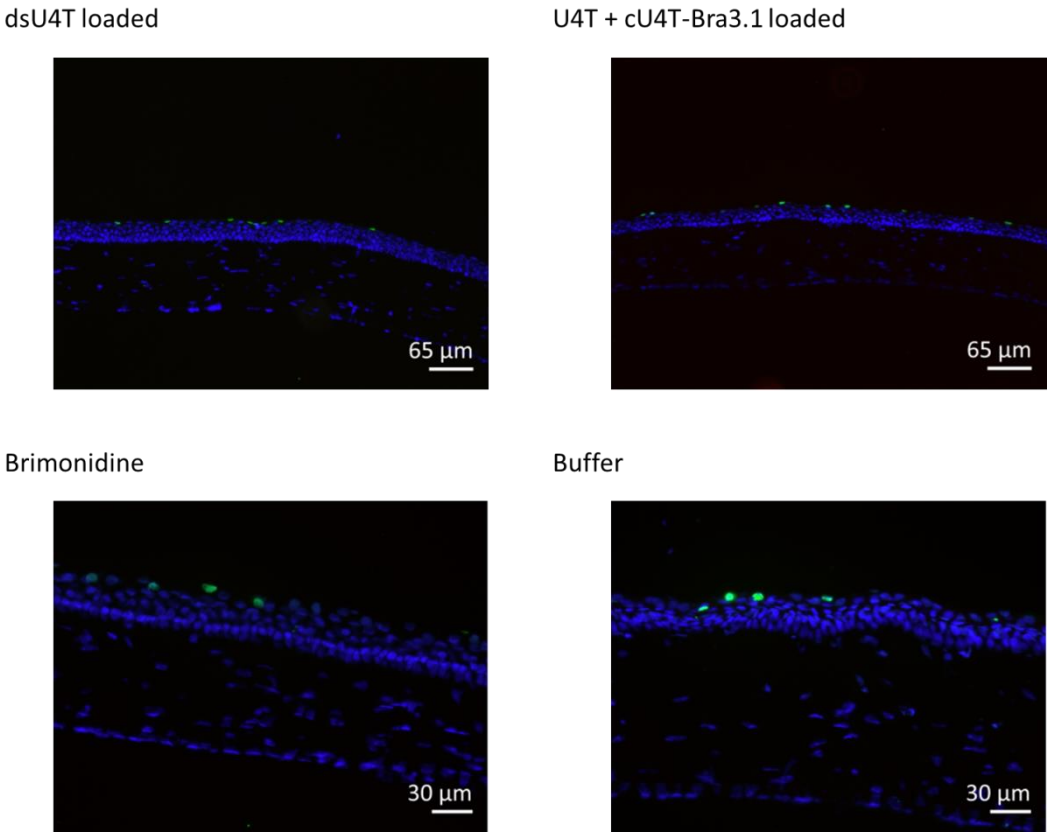

Figure 28: Representative micrographs of each investigated condition for safety evaluation of DNA-nanoparticles on rat eyes. Eye drops were administered as single drop to living rats. After euthanizing them, the eyes were cut und stained with DAPI (blue) and TUNEL (positive cells in green).

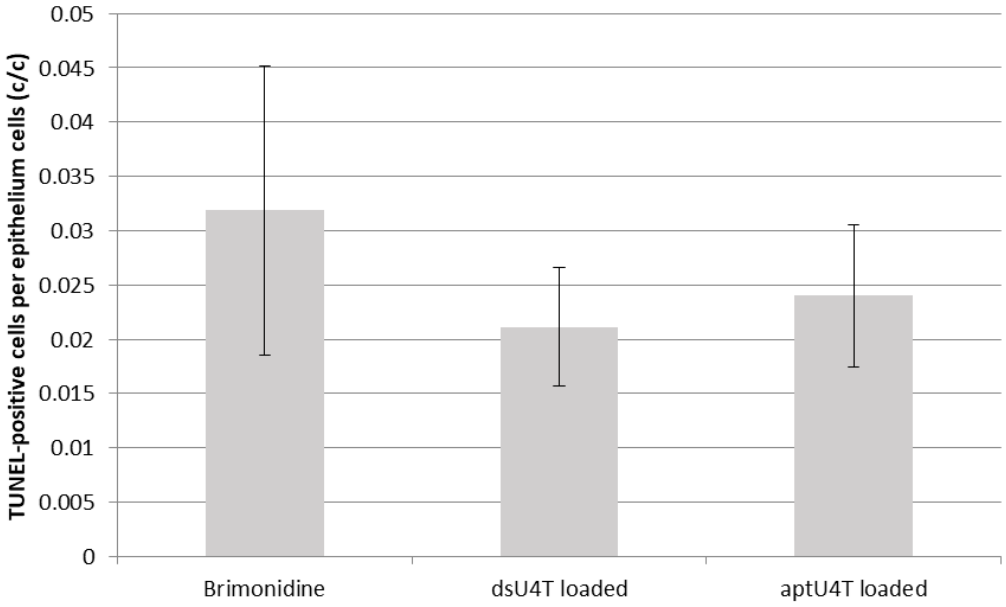

Figure 29: Mean values of the counted TUNEL-positive cells per epithelium cells in the in-vivo safety evaluation on rat eyes. After cutting and staining the eyes with TUNEL, TUNEL positive cells as well as epithelium cells were counted manually and the ratio depicted. Brimonidine treated eyes showed the highest number of TUNEL-positive cells. dsU4T and U4T + cU4T-Bra3.1 (given as "aptU4T") caused less TUNEL positive cells than brimonidine. Statistics: Mean values and standard deviation are given. Abbreviation: aptU4T = U4T + cU4T-Bra3.1.

Several observations can be made when comparing the average of apoptotic cells for different eye drops (Figure 29). Brimonidine revealed the highest number of TUNEL-positive cells per epithelium cells (c/c) (0.032 c/c). All samples caused less TUNEL positive cells than brimonidine. Comparing the different NP entities, dsU4T (0.021 c/c, p=0.35) revealed lower amounts of TUNEL positive cells than U4T + cU4T-Bra3.1 (0.024 c/c, p=0.67).

3.5 Stability evaluation of U4T under different storage conditions over time

The stability of carriers that are used for drug delivery is an important parameter. The used vehicle must be stable over time. Also, it needs to be clarified which conditions storage for storage are favourable.

For this reason, single stranded U4T was stored at 4 °C in the dark, at room temperature in the dark and at room temperature with light cycle (but protected from direct sunlight). NPs were used in the concentration of 100 µM. Of each sample, three aliquots were taken every month. These were then analysed with HPLC.

Generally it can be said, that the peak eluting around 23 minutes retention time ("peak 1") represented the U4T. Expected degradation products such as free nucleobases would elute after a shorter retention time. At later elution volume a smaller peak at 25 minutes ("peak 2") can be seen. This second smaller peak, eluting at 25 minutes increased proportionally with a decrease of U4T peak intensity. This effect was most pronounced for samples stored at roomtempertaure without protection from light.

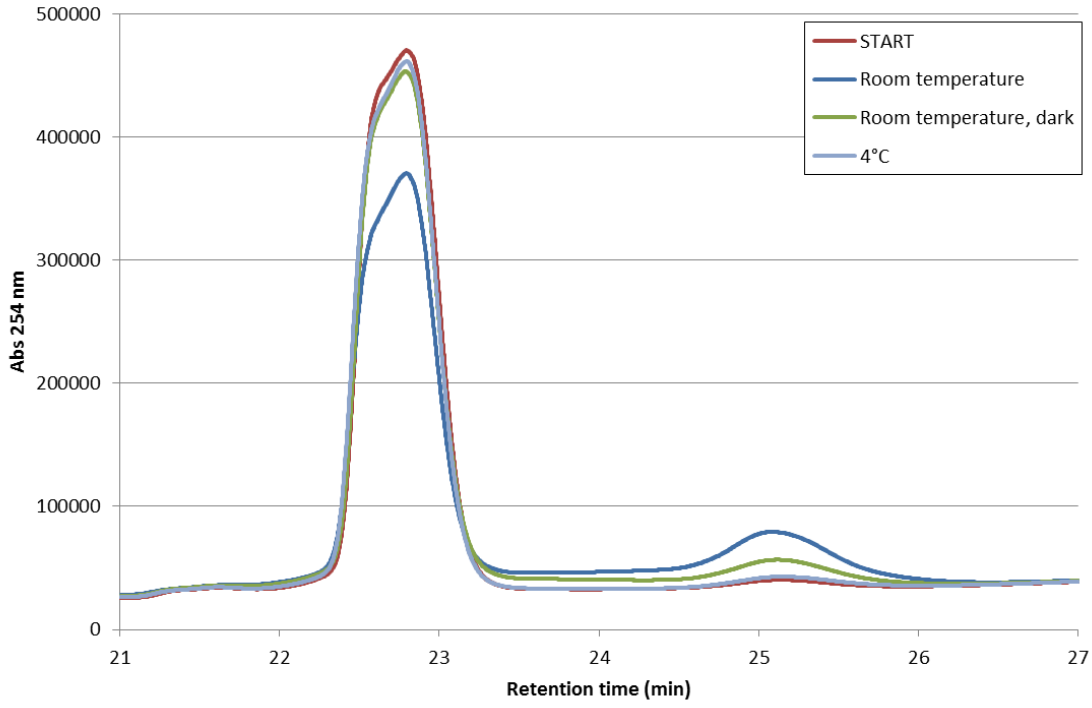

Figure 30: Comparison of HPLC analysis of U4T samples stored at different conditions for 12 months.

The U4T NPs stored at 4 °C in the dark showed the least degradation (Figure 30). For sample stored at roomtemperature with protection from light the degradation was minimal, whereas the degradation was much more pronounced for samples without protection from light, indicating the decay was due to light.

Samples were most stable at 4 °C (maximum: *peak 1*: 0 month: 470.1 mAU, 12 months: 461.4 mAU; *peak 2*: 0 month: 40.3 mAU, 12 months: 42.9 mAU), followed by samples stored at room temperature and protected from light (*peak 1*: 0 month: 470.1 mAU, 12 months: 453.3 mAU; *peak 2*: 0 month: 40.3 mAU, 12 months: 56.6 mAU) and most instable at room temperature without light protection/ cycled light (*peak 1*: 0 month: 470.1 mAU, 12 months: 370.4 mAU; *peak 2*: 0 month: 40.3 mAU, 12 months: 79.2 mAU) (Figure 30). After one year, samples with protection from light still gave comparable signals to the starting reference (*4°C*: 98.1% of the starting reference, *room temperature with protection from light*: 96.4%, *room temperature without protection from light:* 78.8%). From this it can be concluded that the NPs can be stored at temperatures between 4 °C and room temperature under the protection of light.

4. Discussion

For several good reasons topical treatment is the first line therapy of glaucoma. Nevertheless, the efficiency of this approach is compromised by some difficulties. These are especially pronounced as treatment is intensive, both in drug concentration as well as the application frequency, leading to poor compliance and bad treatment efficacy. This is why the ideal topical treatment would consist of a monotherapy with low doses of medicament. This would increase compliance and reduce side effects (Tsai, 2009) (Hermann et al., 2011).

Several methods for improvement of eye drop efficiency have been investigated in the past. These include increasing the uptake through longer contact times, improved drug permeability or by employing non-invasive sustained release devices (Baranowski et al., 2014). However, these approaches generally cause side effects which in turn lead to reduced therapy efficacy.

Nanoparticles (NP) are widely used in medicine (Murthy, 2007) (Zhang et al., 2011). Some experimental approaches already exist for the treatment of glaucoma in rats and rabbits (Tuomela et al., 2014) (Bhagav et al., 2011). In the here presented work lipid chain modified DNA NPs are used that have previously been described (de Vries et al., 2018) (Anaya et al., 2010) and patented (Herrmann, A., De Vries, J. W., Spitzer, M. S., & Schnichels, S. O. inventors; 2015, Means and methods for ocular drug delivery, International publication number: WO 2015/041520 Al, 26.3.2015). These NP could be one way to both decrease the concentration and thus side effects and reduce the frequency of administration, with the aim to improve glaucoma treatment.

In this thesis, NPs with lipid chain modifications were successfully loaded with the glaucoma medicament brimonidine in two different ways and their adherence time to rat cornea, safety and stability investigated.

4.1 Nanoparticles employing hydrophobic interaction

The NPs consisting of DNA strands with lipid modifications can be used as drug carriers and loaded in different ways (Figure 2). As outlined in the introduction, one mechanism for loading is to employ hydrophobic interaction between the core of the NP and the medication. In this chapter, the drug loading ability was assessed for NPs made of both single stranded (ssU4T) and double stranded DNA (dsU4T) and their release properties were compared.

4.1.1 Loading of brimonidine in nanoparticles employing hydrophobic interaction

First, the loading capacity of single and double stranded DNA NPs was investigated. It could be shown that ssU4T was able to bring 3.22 x more brimonidine into solution than the buffer control, confirming the hydrophobic loading of the drug into the NPs. Also, the dsU4T NPs have shown to be even more effective in solubilisation than its single stranded counterpart (1.29 x), indicating that there is interaction between brimonidine and the double stranded structure. Loading of brimonidine was found to be more effective with higher feed concentrations of brimonidine and NPs.

From the obtained loading results and the characteristics of brimonidine (Figure 1), it can be concluded that brimonidine is not only loaded into the hydrophobic core of NP, consisting of lipid chains, but that the drug also intercalates in the double stranded DNA. However, it is difficult to quantify the contribution of the different types of loading as double stranded NPs also have a different structure and as such the hydrophobic core is different from the single stranded NPs.

Furthermore, a plateau of loaded drug was reached for buffer and dsU4T after 48 hours.

It can be concluded, that the use of higher concentrations of NP as well as higher feeding concentrations of brimonidine resulted in higher solubilisation of brimonidine. The use of dsU4T can be considered beneficial over ssU4T and the optimal loading is considered as 48 hours.

4.1.2 Release of brimonidine from hydrophobic loaded nanoparticles

For the release experiment, a control was added to investigate the influence of the lipid modification of the DNA polymers on the ability to release the loaded drug. Here, a pristine double stranded DNA sequence was used (dsT4T), which does not bear any modification. This is why it also does not form NPs.

Regarding the absolute amounts of released brimonidine it was obvious, that ssU4T did not release more brimonidine when loaded with a higher feed concentration. This did not apply for double stranded entities, which released more brimonidine when the feed concentration was increased. Comparing double stranded NPs with the pristine double stranded DNA control, it became clear that with the help of the hydrophobic core, more brimonidine can be loaded and released. These results support the conclusion that the use of ds DNA NPs is advantageous.

A slower release of brimonidine from the NPs implements the need of a long adhering period of the NP to the corneal surface. Otherwise, less brimonidine is released referable to the slower release. Here, excellent adherence of the NPs was shown for one hour and an increased adherence for up to four hours (Chapter 3.3.1 and 3.3.2). The pristine molecules which served as controls did not adhere for longer than five minutes (Figure 23, Figure 24, Table 7). Literature research found adherence of 30 minutes to one hour (de Vries et al., 2018) (Chaiyasan et al., 2013). In regard to this, the here found adherence can be seen as a long period of time for the release. Thus, a slower release of brimonidine from the NPs is considered as an advantage as the longer adhering NPs will thereby increase the bioavailability.

Thereby, the longer adhering NPs serve as a drug depot and are able to release the drug over prolonged periods of time. It could be shown, that the buffer control released brimonidine fastest and resulted in the highest diffusion. This indicated no interaction of the drug with the buffer. In addition, the dsT4T control released the drug slightly slower than buffer, indicating only weak interactions between the pristine double stranded DNA and brimonidine. Even if ssU4T achieved slightly better results regarding the retaining release than dsU4T, though the differences were small. It can be concluded that also for the release properties there is a distinct advantage in the use of the investigated DNA NPs.

To understand which part of the NP is the one that bears the bigger influence on retaining behaviour, one needs to visualize the different NP structures (Figure 31). ssU4T expresses a lipid core, but no double stranded DNA; dsU4T has a lipid core and double stranded DNA; dsT4T no lipid core, but double stranded DNA. Ranking the entities from best to less retaining NP, the following order can be seen: ssU4T, dsU4T and dsT4T; indicating that interaction between ssU4T and dsU4T to brimonidine is more pronounced than to dsT4T. This leads to the conclusion that the core has a higher influence on the retaining behaviour than double stranded DNA.

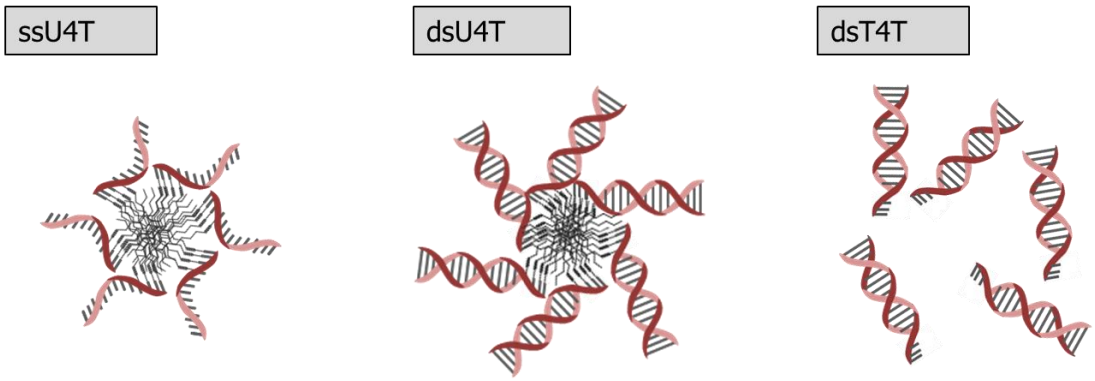

Figure 31: Structure of ssU4T, dsU4T and dsT4T in aqueous surrounding.

The influence of adjusting the amount of brimonidine into the samples revealed similar results for all samples expect buffer. It released up to the same amount regarding the relative endpoint but in an apparently less retaining behaviour. For the non-adjusted samples, a plateau is reached after 120 minutes. To adjust samples and the containing amount of brimonidine to each other, the triple amount of loaded buffer sample was taken for the adjusted set up. This is why, a more increased amount of totally released brimonidine can be set free and up to 250 minutes, no plateau is reached leading to a relative presentation of values that seems to be more retaining. This is the only sample that revealed an effect of adjusting the amount of brimonidine. The effect on DNA containing samples is negligible. Regarding both absolute and relative release, it can be said that dsU4T 500 µM with 5000 µM brimonidine feed concentration is the best performing NP.

Analysis of brimonidine tartrate coformulated dsU4T and buffer samples revealed a an influence of the coformulation on the release behaviour. As expected, the absolute release was much higher. In agreement with earlier release measurements, dsU4T showed higher drug retention compared to buffer. The release was faster for adjusted samples of dsU4T and the retaining effect decreased when using higher amounts of brimonidine tartrate and less of loaded NP. Strikingly, almost 100% of the total amount of brimonidine is released within the first 380 min and around 95% in the first 240 min. At this time point, samples without addition of brimonidine tartrate only released 40-50%. This indicates that the coformulation did have influence on the release properties and presumably weakened the interaction of the loaded brimonidine with the NPs. When using increased relatively higher amounts of brimonidine tartrate and less loaded NP, release is faster and the retaining effect of NP decreased. This fact needs to be kept in mind for further studies in which coformulation is needed for direct comparison.

4.1.3 Findings in the context of current research results

In literature, brimonidine was shown to be successfully loaded and released from nanosponges made of modified δ-valerolactone. The NPs were used to improve the ability of brimonidine to cross the optic nerve sheets. It was found that the use of these NPs restrained the diffusion, enabling a depot effect. Compared to pristine brimonidine, the release was slower and more prolonged. With this approach the authors hope to be able to decrease the drug concentration (Grove et al., 2014). These two facts were also seen with the here established DNA NPs. As the release is delayed due to interactions with the DNA NPs, the bioavailability of the brimonidine is improved and the necessary drug concentration can be decreased.

Regarding the release from brimonidine loaded NPs, comparable results have been published. In one investigation, three lipid NPs containing docetaxel were studied and shown to almost immediately release 45% of the loaded drug. One of the tested carriers released up to 85% of the loaded drug in a period of eight hours. The other two docetaxel NPs showed no further release after the initially burst. Here, 100% was defined as all detectable drug – loaded in NPs and released - in mouse plasma and was determined by chromatography (Feng et al., 2011). There are several striking differences from the here used measuring methods and experimental setup. As such, the results are not directly comparable. However, the release of 40-50% after four hours found for our NPs is similar to what was measured in the paper. It could even be said that our NPs are performing slightly better, with regard to the sustained release without initial burst and to their improved depot effect.

4.2 Brimonidine loading in aptamer functionalized DNA nanoparticles

To load brimonidine in NPs, several strategies can be employed. This gives more alternatives and results in higher chances to succeed in employing the envisaged NPs as potent drug delivery vehicles. Possibilities to load NP are hydrophobic interaction, covalent binding or the use of aptamers (Figure 5).

Aptamers in general represent a very elegant method to recognise structures and more specifically load drug into NPs. This strategy is not limited to small drug molecules and is employed in a vast number of applications. For example, they can be used as potent drug delivery systems in oncological treatment. Thereby, the aptamer serves as molecule that recognises pathological cells and delivers the drug that is linked to the aptamer (Jiang et al., 2015). In another approach, the specific interaction of the aptamer with the target is used for the loading of drugs in NPs. Like this, almost any drug can be loaded into the NP, and it can be in addition to loading with hydrophobic interaction into the hydrophobic core and with intercalation into the double stranded part of the NPs. The use of aptamers is thus a very elegant possibility to load even more drug into the NPs.

4.2.1 Validation of aptamer binding towards brimonidine

All three aptamers – the original and the two shortened ones - were tested on their binding behaviour towards brimonidine with a fluorescence based binding assay with SYBR Green.

All aptamer sequences showed good binding behaviour of brimonidine (Figure 16). Furthermore, binding experiments were also done with elongated aptamers. For that purpose, cU4T was linked to the 3' end of the aptamer enabling the hybridizing onto the NPs.

All samples with elongated aptamers showed an increasing fluorescence with increasing brimonidine concentrations (Figure 18 and Figure 19). This effect was most pronounced in the samples of Bra3.1 and Bra3 aptamers. The brimonidine dependant increase was in contrast to what was observed for the pristine aptamers, where the signal decreased with increasing target concentration. Although it is difficult to explain such differences, both

have been observed in literature (Sarpong and Datta, 2012) (Zipper et al., 2004). To obtain a better understanding about these irregularities, further experiments would be needed. However, this is outside the scope of this thesis.

When looking at the results of brimonidine binding to the aptamers and comparing this with the secondary structure of the aptamers, insight in the important parts for binding can be obtained. The two aptamers with good binding characteristics, Bra3 and Bra3.1, exhibit a stem-loop structure flanked by a single stranded sequence. When comparing the structure of the good binders with Bra3.2, it becomes evident that the stem-loop structure plays an important role in binding. Bra3.2 does not express the stem-loop structure as Bra3 and Bra3.1 (Figure 32).

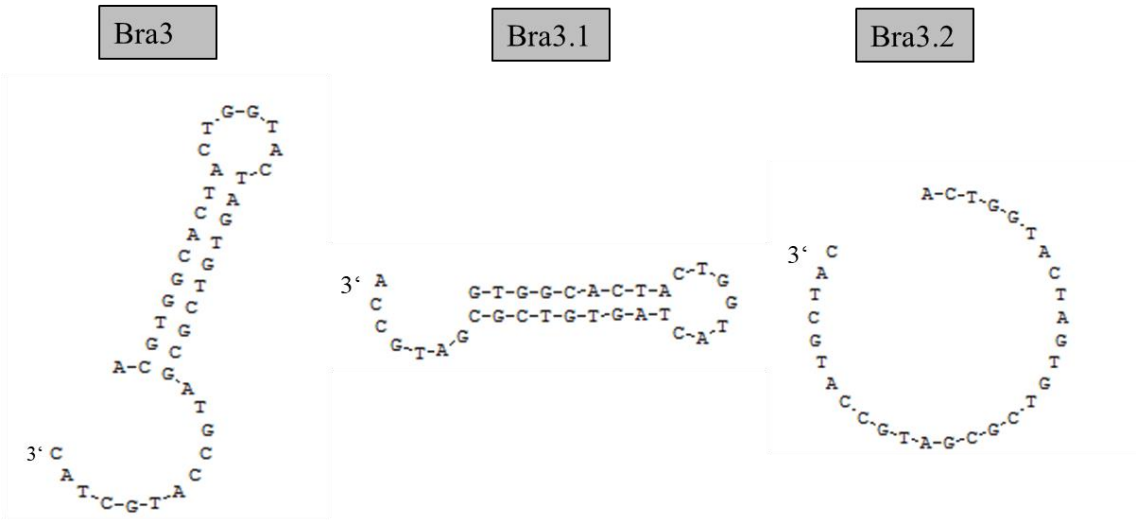

Figure 32: Secondary structure of aptamers. The unshortened aptamer Bra3 is depictured, such as the shortened versions, Bra3.1 and Bra3.2.

Both pristine as well as elongated aptamers showed a concentration dependant change in relative RFU and thus it can be concluded that no impairment of the elongation can be seen. For all the samples successful binding of brimonidine to the aptamer functionalized NPs was proven. Bra3 and Bra3.1 are considered the best binding aptamers.

4.2.2 Loading of brimonidine in nanoparticles with bound aptamers

Bra3 loaded most drug compared to the other samples, followed by Bra3.1 (66% of Bra3) and dsU4T (36% of Bra3) (Figure 20). Loading for these samples showed a logarithmic behaviour. The buffer control resulted in much lower solubilisation (11% of Bra3), whereas the aptamer Bra3.2 did not show logarithmic loading and the values were around the same height than dsU4T. Strikingly, when finishing the experiment, the supernatant of the Bra3.2 sample was like a gel. This hindered proper handling of the sample and could be the reason why the loading and measurements were unreliable. Regarding the structure of the used aptamers (Figure 32), it strikes that Bra3.2 is the only one with a less complex secondary structure and thus other binding options. All other aptamers express a stem-loop structure. This could be the reason why Bra3.2 formed more easily a gel than the other aptamers.

Results for dsU4T are comparable with the earlier obtained loading (chapter 3.1.1). In the initial experiments a plateau is reached after 48 hours at an optical density (OD) of around 50. Here, dsU4T samples showed a similar behaviour, but the plateau was reached after 36 hours, also around OD 50. This could be due to higher room temperature for the aptamer experiment. Temperature differences reached around 10 °C. For these reasons and for standardisation loading was performed for 48 hours in further experiments and temperature was fixed to 21°C.

Drawing a conclusion between loading and loading per production costs, dsU4T was the cheapest NP, but loaded only a small absolute amount of brimonidine. Beyond the aptamers, U4T-Bra3 and U4T-Bra3.1 showed good results. U4T-Bra3.2 was the NP with the highest costs and the lowest absolute loading abilities and thus was left out of consideration from this point on.

4.2.3 Release of brimonidine from nanoparticle with bound aptamers

Relative analysis of results revealed that both aptamer samples released in about the same speed, with slightly better properties being attributed to the Bra3.1 aptamer. The dsU4T NPs liberated the drug faster. Looking at adjusted amounts of brimonidine in the

release devices, the differences are very small and all DNA samples set the drug free in about the same speed. Only the buffer control liberated the drug faster.

Compared to the release experiment with hydrophobic interaction, dsU4T and buffer set more drug free regarding the absolute and relative values after four hours. dsU4T reached relative release values of around 85% for the aptamer experiment, but only around 45% for the hydrophobic experiment. This is most likely due to the room temperature which varied by a difference of 10°C.

As temperature influenced the release, consequently the ocular temperature needs to be considered. Ocular surface temperature is around 34 °C and thus lower than the normal body core temperature (Konieczka et al., 2018). Compared to the aptamer experiment, the ocular temperature did not differ much from the room temperature. As seen before, a higher temperature led to a higher release in the same time, so an even slightly faster release in-vivo at 34°C may be expected. For a quantitative statement, more experiments would be needed. Most realistic would be in-vivo experiments with the ocular surface temperature of 34°C as they will be conducted as logical following step on the way of establishing the drug carrier for clinical use.

It can be concluded, that there is an advantage of using aptamer functionalized NP compared to hydrophobically loaded ones. Both Bra3 and Bra3.1 NPs showed beneficial behaviour in retaining the drug. Due to the better binding, loading and release properties of Bra3.1 aptamer functionalized NPs, it was decided to use this design for further testing.

4.2.4 Findings in the context of current research results

As seen for the hydrophobic loading, the incorporation of brimonidine via aptameric interactions achieves equal or superior results. In one study, lipid NPs containing docetaxel showed an immediate release of 45% of the loaded drug. Only a single NP released more and achieved up to 85% delivery (Feng et al., 2011). The DNA NPs with aptamers reached up to 85 - 90%. However, as mentioned (chapter 4.1.3), the experimental set up is different. Nevertheless, it can be said that DNA NPs achieved comparable or superior results.

Aptamers are widely used for targeted drug delivery. Aptamers can serve as recognition unit and deliver the drugs or carrier to the targeted structure, e.g. cancer cells (Salata, 2004). One example for that kind of use of aptamers is the delivery of doxorubicin to retinoblastoma cells. To this end two aptamers were linked together, one side for recognition of the retinoblastoma cells, the other expressing a stem-loop structure which is able to load doxorubicin. In this study, it could be shown that the release from aptamers was around half of the release of the free drug in the same time. Release from aptamers was thus slower and the aptamer chimers could be considered as drug depot. The aptamer chimers released 37% of all drug in four hours (Subramanian et al., 2012). Due to different presentations of cumulative release in this study and the relative release to the amount that was set free after 28 hours, direct comparison is difficult. When looking at the retention of the drug in aptamer NPs and buffer, the NP liberated between 70 – 75%, whereas buffer released 95% of the drug. This would indicate that the aptamer chimer exhibited more retaining effects than DNA NPs.

To reach the aim of increased and prolonged drug delivery, other modes than topical administration of eye drops have been investigated, e.g. using in-situ gels. One workgroup established the use of hydrogels loaded with brimonidine and timolol and found that the combination of both drugs loaded into hydrogel was superior to timolol loaded alone into hydrogel. To investigate into the release a similar set up to the here used one was employed. The release from brimonidine as well as timolol loaded hydrogels reached around 70 % after four hours, whereas it is not clarified which value was set as 100% (Dubey and Prabhu, 2014). Presuming that the relative release is represented in a comparable way, the DNA NPs reached slightly lower levels of drug that was set free after four hours and thus showed a more retaining behaviour than the hydrogel. However, the major advantage of using DNA NPs is that they can be administered as eye drops. Hydrogels have a higher viscosity, which may lead to a (longer lasting) blurred vision and foreign body sensation. This is not the case for eye drops containing DNA NPs.

4.3 Evaluation of adherence time of brimonidine nanoparticles

Commercial available eye drops are cleared away from the eye rapidly. Different methods have been tested and are employed to prolong the adherence time of the formulations and drug to the corneal surface (Baranowski et al., 2014).

The in-vitro evaluation on pig eyes showed the superiority of DNA NP to the pure fluorophore. Thereby, the U4T + cU4T-Bra3.1 samples (t = 4 hours: 8%) achieved inferior relative levels than dsU4T (26%). This is most likely due to the larger size and a more complex structure of loaded NP which might influence the binding of the NP to the cornea. However, the increased adherence time was proven up to four hours after application. The in-vivo evaluation revealed an adherence of U4T + cU4T-Bra3.1 NPs to rat cornea, with a decrease of positive eyes over time. Nevertheless, 60 minutes after application there were still NPs detectable. The in-vivo experiment was conducted up to 60 minutes in order to use a smaller number of animals.

Chitosan-dextran sulfate NPs were tested upon their potential of adherence to the cornea. Fluorescent NPs were applied in an ex-vivo experiment to porcine cornea and then washed with a continual stream of buffer to imitate blinking. After 60 minutes, NPs could be detected (Chaiyasan et al., 2013). The finding concerning the adherence time to the cornea are in agreement with the here found results where NPs were still detectable after 60 minutes. Even if the used NPs and the experimental set up are completely different, this gives an idea which period of adherence time other NPs are able to achieve.

U4T was found previously on rat cornea up to four hours. The with aptamers functionalized and with kanamycin and neomycin loaded NPs adhered to rat cornea for at least two hours (de Vries et al., 2018) (Herrmann, A., De Vries, J. W., Spitzer, M. S., & Schnichels, S. O. inventors; 2015, Means and methods for ocular drug delivery, International publication number: WO 2015/041520 Al, 26.3.2015). The here found results are in agreement with the ones of the experiments of de Vries et al.

4.4 Safety evaluation of DNA nanoparticles using different in-vitro and in-vivo assays

For safety evaluation, the effects of administration of different DNA NPs were studied in-vitro using primary cornea epithelium cells and in-vivo in rats.

4.4.1 Safety evaluation of DNA nanoparticles using an in-vitro cell culture assay

Both applied samples, dsU4T and U4T + cU4T-Bra3.1 did not show a significantly different quantity regarding the cell amount (Figure 25). For marketing authorisations (DIN ISO 10993-5) a decrease of viability over 30% is considered as cytotoxic. According to this and the fact that both samples showed even increased levels of viability (Figure 26), dsU4T and U4T + cU4T-Bra3.1 would be considered safe. The increased viability is explainable regarding the simultaneously increased levels of caspase 3/7 activity (apoptosis induction) (Figure 27) when bearing in mind that the level of caspase 3/7 activity was much smaller for the NP samples (dsU4T: 3.11x, U4T + cU4T-Bra3.1: 1.47x) than for the death control (staurosporine: 17,38x). Comparing dsU4T and U4T + cU4T-Bra3.1 with each other, U4T + cU4T-Bra3.1 is the less harmful NP as the cell amount and viability was higher and the apoptosis induction lower than for dsU4T.

Regarding all results it can be stated that dsU4T and U4T + cU4T-Bra3.1 can be considered as not harmful whereas U4T + cU4T-Bra3.1 is the best performing sample.

4.4.2 Safety evaluation of DNA nanoparticle using an in-vivo rat eye assay

None of the tested DNA NP expressed a significant higher apoptosis rate than the brimonidine control (=brimonidine tartrate). dsU4T showed less apoptic cells than U4T + cU4T-Bra3.1.

The in-vitro experiment found that U4T + cU4T-Bra3.1 resulted in better effects than application of dsU4T. When having a closer look on the apoptosis induction, in-vitro and in-vivo findings are not in complete agreement with each other. The concentration of the starting samples is the same. In-vitro cells were incubated for four hours in 500

µM of samples. In-vivo only one drop was applied. As seen in the adherence experiment (chapter 3.3.1), most of the sample is cleared away rapidly from the cornea. So, cells in-vitro were exposed relatively longer to a higher concentration and so these small differences can be explained. Furthermore, in-vivo experiments are more meaningful than in-vitro experiments as they represent a complex living organism and more realistic conditions. For these reasons attention should be turned towards the in-vivo findings.

4.4.3 Findings in the context of current research results

One example of already mentioned NPs for which a safety profile was evaluated, is a lipid NPs loaded with docetaxel (chapter 4.1.3). These NPs were found to achieve superior results as the free drug regarding the release and showed lower toxicity than free docetaxel. Toxicity was evaluated using an in-vitro model of human prostate cancer cells with the help of an MTT assay that assesses the viability. However, here the lipid chain length had an important influence on the toxicity. The longer the lipid chain, the lower the toxicity (Feng et al., 2011). The finding that the free drug is more toxic than the loaded one goes along with this paper. Looking at the results of the biosafety of dsU4T and the NPs with aptamer modification, it is difficult to state that the length of the DNA or of the alkyl chain has any influence on the safety profile. However, as the biocompatibility is also dependant on the length of the lipid chain for the lipid NP, it would be interesting to investigate this for DNA NPs as well.

A paper giving exact numbers on toxic effects and not only a statement about expression of toxic/ nontoxic effects is the study about hydrogels made from polyacrylic or polyitaconic acid NPs. Both NP have been shown to be able to bind to human cornea and achieve sustained release of brimonidine. Viability of cells after incubation with the formulations was tested using tryptan blue and it could be shown that poyacrylic acid did not cause any impact on viability after 30 minutes in-vitro. However, this is in contrast to the results found for polyitaconic acid, for which viability decreased by 90% in the same time period (De et al., 2004). For the here presented NPs, dsU4T revealed an increase of viability which was 97% and U4T + cU4T-Bra3.1 even 265% higher than the one of brimonidine after four hours of incubation which was assessed with the MTS

assay. MTS measures the glycolysis rate, a direct factor of viability. In contrast, trypan blue determines viability indirectly, as the method is based on the integrity of the cell membrane. For this reason comparison is difficult as indirect measurements can be false negative as well as false positive. Additionally, the trypan blue assay is evaluated manually, a further source of possible errors (Strober, 2015). For in-vivo experiments, irritation was most often evaluated by visual examination and parameters like hyperaemia, corneal and conjunctival aspects and slit-lamp examination (Bhagav et al., 2011) (Dubey and Prabhu, 2014) (Natarajan et al., 2012). Hence, comparison and classification of the here presented data is difficult. Nevertheless, the found results do not implement a decreased biosafety implicating that the here presented NPs could be considered as safe for further studies.

DNA NPs for antibiotics, namely kanamycin and neomycin, have been evaluated on their cytotoxic potential. No significant toxic effects regarding cell amount, viability and apoptosis induction were found for the antibiotic NPs (de Vries et al., 2018) (Herrmann, A., De Vries, J. W., Spitzer, M. S., & Schnichels, S. O. inventors; 2015, Means and methods for ocular drug delivery, International publication number: WO 2015/041520 Al, 26.3.2015) . The experiments were conducted with some small differences. First of all, the NP were prepared at 20 µM. Incubation time for the NPs was 24 hours and the tested cells were RGC-5, 661W and ARPE-19 cell lines. These cell lines are derived from retinal cells and of rodent or human origin. Here, primary epithelium cells from pig cornea were used for the reason that the toxic impact on the cornea was examined. The findings are in agreement with the brimonidine experiments.

4.5 Stability evaluation of U4T under different storage conditions over time

Stability is a crucial aspect in establishing a new drug delivery platform. When a carrier undergoes fast degradation under specific conditions, storage becomes difficult. Also, fast degradation results in the accumulation of unknown products, which might impose side effects.

As can be seen in the HPLC results (chapter 3.5, Figure 30), storage at 4 °C with protection from light is favourable for the stability of U4T. Degradation found for samples stored at room temperature with protection from light is also small. Changes that were detected in HPLC are mostly an increase in the second peak, which is most likely due to the accumulating of hydrophobic material. Such material elutes at higher concentrations of organic buffer and can be formed due to minor degradations of DNA nucleotides or to changes in aggregation of U4T. Degradation of DNA would implicate that other degradation products, like free nucleobases, should be observed, which was not the case. Light seems to enhance this process and is not favoured for storage of the NPs. In conclusion, U4T is stable when stored with protection from light, lower temperature can be an advantage too.

In the study of Bhagav et al., brimonidine was loaded into NPs made of copolymers of methacrylacid and methylmethacrylate. The degradation behaviour of these NPs was investigated over time. It could be shown that the NP formed aggregates at room temperature and the physical and chemical characteristics were modified after six month of storage. This was not experienced for storage at 4°C or -20°C. Unfortunately, there are no numbers given on the amount of degradation and it is not specified whether samples were stored with or without protection from light (Bhagav et al., 2011). The aggregation and degradation behaviour found in the paper are in agreement with the observed changes for the slightly increased degradation for higher storage temperature in this study. So, storage at -20°C would also indicate that even lower degradation is possible for the used NPs. Nevertheless, the effect seen for protection from light is much more pronounced than the difference from room temperature to 4°C.

4.6 Conclusion

The here presented NPs represent an elegant way to load and release more brimonidine in a solution than without. Thereby the NP with the aptamer modification U4T + cU4T-Bra3.1 showed the most promising results. The adherence was shown in-vitro up to four hours and in-vivo up to one hour. This is an immense improvement compared to the pure drug and thus the NP can serve as drug depot. The safety towards primary epithelium cells as well as towards rat cornea was evaluated. In-vivo none of the samples expressed significantly higher apoptosis rates than brimonidine tartrate, as it is currently used in humans. The least degradation of U4T + cU4T-Bra3.1 was shown for samples stored with protection from light, lower temperatures can be an additional advantage. Degradations after 12 months of storage were small.

These facts represent the groundwork for further studies to enable the formulation of DNA NPs containing eye drops for human use. For that aim, in a next step, studies regarding the ability of with brimonidine loaded NPs to decrease the intraocular pressure are needed. Additionally, a long-time in-vivo safety evaluation and a stability study of U4T + cU4T-Bra3.1 needs to conducted. Some of the mentioned experiments are already under investigation and further studies are still coming. In total, this is a very promising approach in aiming for an improved glaucoma treatment. Furthermore, these lipid-modified NPs are not limited to one drug and could open up many more possibilities which might improve treatment in various medical fields.

5. Summary

Nanoparticles (NP) are a widely used way to improve treatment in medicine and ophthalmology. Various materials are available. One very elegant is DNA. Lately, a NP made of DNA with lipid modification was presented (de Vries et al., 2018) and patented (Herrmann, A., De Vries, J. W., Spitzer, M. S., & Schnichels, S. O. inventors; Means and methods for ocular drug delivery, International publication number: WO 2015/041520 Al, 26.3.2015). This NP was here evaluated for brimonidine with the aim of an improved glaucoma treatment.

Two different ways of loading DNA NPs were established. Loading of brimonidine using hydrophobic interaction benefits from both higher DNA and brimonidine feed concentration as well as the use of dsU4T. The same applies for the release. Finally, using brimonidine tartrate for co-formulation of the loaded NPs revealed an influence on the release behaviour. The second possibility to load NPs is the use of different aptamers. Here, U4T + cU4T-Bra3.1 performed best regarding binding, loading and release. It is advantageous for retained release of the drug and thus for the use as a depot when applied as eye drops. The in-vitro safety evaluation showed no harmful effects of the tested entities. In-vivo none of the samples expressed higher levels of apoptosis rate than brimonidine tartrate as it is currently used in humans. Regarding the efficacy of the developed carrier, the adhesion of aptamer functionalized NP could be shown in-vitro up to at least four hours and in-vivo up to at least one hour. Finally, the stability of U4T samples was tested. Especially light enhanced degradation and should be avoided in future applications.

It could be shown that the use of loaded DNA NPs is advantageous for binding, loading and release of brimonidine. Two different loading strategies were successfully established and the safety and stability of the carrier was confirmed. The efficacy of the NPs was tested and showed promising results for future applications.

The next steps in evaluating with brimonidine loaded NPs for more effective glaucoma treatment will be the in-vivo testing of those NPs, the evaluation of stability of U4T + cU4T-Bra3.1 as well as a long-term safety study.

5.1 Zusammenfassung

Nanopartikel (NP) stellen eine weitverbreitete Methode dar, um Behandlungen in der Medizin und Augenheilkunde zu verbessern. Dazu stehen verschiedenste Materialien zur Verfügung. Eine sehr elegante Möglichkeit ist die Verwendung von DNA. Vor kurzem wurde ein DNA NP mit Lipidmodifikationen vorgestellt (de Vries et al., 2018) und patentiert (Herrmann, A., De Vries, J. W., Spitzer, M. S., & Schnichels, S. O. Erfinder; Means and methods for ocular drug delivery, Internationale Patent Nummer: WO 2015/041520 Al, 26.3.2015). Diese NP wurden mit dem Ziel einer verbesserten Glaukombehandlung in der vorliegenden Arbeit mit Brimonidin evaluiert.

Zwei verschiedene Wege zur Beladung von DNA NP wurden evaluiert. Die Aufnahme von Brimondin in NP mittels hydrophober Interaktion profitiert von höheren Anfangskonzentrationen von DNA und Brimonidin sowie der Verwendung von dsU4T. Das gleiche konnte für die Freisetzung des Medikaments aus den beladenen NP gezeigt werden. Außerdem zeigte die Nutzung von Brimonidintartrat zur Koformulierung der beladenen NP Auswirkungen auf das Freisetzungsverhalten. Die zweite Möglichkeit NP zu beladen ist die Verwendung von Aptameren. Hier wies U4T + cU4T-Bra3.1 hinsichtlich Bindeverhalten, Beladung und Freisetzung die besten Ergebnisse auf. Es zeigte sich vorteilhaft für eine verzögerte Freisetzung des Medikaments und damit in der Anwendung als Depot in der Verwendung als Augentropfen. Die in-vitro Sicherheitsbeurteilung zeigte für keine der getesteten Proben schädliche Einflüsse. In-vivo wies keine der DNA Proben eine höhere Induktion von Apoptose als Brimonidintartrat auf, wie es aktuell am Menschen eingesetzt wird. Die Effektivität konnte mit Adhäsionen von in-vitro bis zu mindestens vier und in-vivo bis zu einer Stunde bestätigt werden. Abschließend wurden U4T Proben auf ihre Stabilität getestet. Vor allem Licht beschleunigte die Zersetzung und sollte in zukünftigen Anwendungen vermieden werden.

Es konnte gezeigt werden, dass der Gebrauch von beladenen DNA NP vorteilhaft für Bindung, Beladung und Freisetzung von Brimonidin ist. Zwei verschiedene Beladungsstrategien wurden erfolgreich evaluiert, sowie Sicherheit und Stabilität der Carrier bestätigt. Die Effektivität der NP zeigte vielversprechende Ergebnisse für zukünftige Anwendungen. Die nächsten Schritte in der Etablierung von mit Brimonidin beladenen NP für eine effektivere Glaukomtherapie werden die in-vivo Testung dieser NP, Stabilitätsstudien von U4T + cU4T-Bra3.1, sowie Langzeitsicherheitsstudien sein.

6. Literature

ABRISHAMI, M., ABRISHAMI, M., MAHMOUDI, A., MOSALLAEI, N., VAKILI AHRARI ROODI, M. & MALAEKEH-NIKOUEI, B. 2016. Solid Lipid Nanoparticles Improve the Diclofenac Availability in Vitreous after Intraocular Injection. *J Drug Deliv,* 2016**,** 1368481.

AHMED, F. A., HEGAZY, K., CHAUDHARY, P. & SHARMA, S. C. 2001. Neuroprotective effect of alpha(2) agonist (brimonidine) on adult rat retinal ganglion cells after increased intraocular pressure. *Brain Res,* 913**,** 133-9.

AKMAN, A., CETINKAYA, A., AKOVA, Y. A. & ERTAN, A. 2004. Comparison of additional intraocular pressure-lowering effects of latanoprost vs brimonidine in primary open-angle glaucoma patients with intraocular pressure uncontrolled by timolol-dorzolamide combination. *Eye,* 19**,** 145-151.

AL-SHAHWAN, S., AL-TORBAK, A. A., TURKMANI, S., AL-OMRAN, M., AL-JADAAN, I. & EDWARD, D. P. 2005. Side-effect profile of brimonidine tartrate in children. *Ophthalmology,* 112**,** 2143.

ALM, A., GRIERSON, I. & SHIELDS, M. B. 2008. Side effects associated with prostaglandin analog therapy. *Surv Ophthalmol,* 53 Suppl1**,** S93-105.

AMRITE, A. C., EDELHAUSER, H. F. & KOMPELLA, U. B. 2008. Modeling of corneal and retinal pharmacokinetics after periocular drug administration. *Invest Ophthalmol Vis Sci,* 49**,** 320-32.

ANAYA, M., KWAK, M., MUSSER, A. J., MULLEN, K. & HERRMANN, A. 2010. Tunable hydrophobicity in DNA micelles: design, synthesis, and characterization of a new family of DNA amphiphiles. *Chemistry,* 16**,** 12852-9.

AUSTIN, L. A., AHMAD, S., KANG, B., ROMMEL, K. R., MAHMOUD, M., PEEK, M. E. & EL-SAYED, M. A. 2015. Cytotoxic effects of cytoplasmic-targeted and nuclear-targeted gold and silver nanoparticles in HSC-3 cells--a mechanistic study. *Toxicol In Vitro,* 29**,** 694-705.

BAHLER, C. K., HOWELL, K. G., HANN, C. R., FAUTSCH, M. P. & JOHNSON, D. H. 2008. Prostaglandins increase trabecular meshwork outflow facility in cultured human anterior segments. *Am J Ophthalmol,* 145**,** 114-9.

BARANOWSKI, P., KAROLEWICZ, B., GAJDA, M. & PLUTA, J. 2014. Ophthalmic drug dosage forms: characterisation and research methods. *ScientificWorldJournal,* 2014**,** 861904.

BATTISTINI, F. D., TÁRTARA, L. I., BOIERO, C., GUZMÁN, M. L., LUCIANI-GIACCOBBE, L. C., PALMA, S. D., ALLEMANDI, D. A., MANZO, R. H. & OLIVERA, M. E. 2017. The role of hyaluronan as a drug carrier to enhance the bioavailability of extended release ophthalmic formulations. Hyaluronan-timolol ionic complexes as a model case. *European Journal of Pharmaceutical Sciences,* 105**,** 188-194.

BHAGAV, P., UPADHYAY, H. & CHANDRAN, S. 2011. Brimonidine tartrate-eudragit long-acting nanoparticles: formulation, optimization, in vitro and in vivo evaluation. *AAPS PharmSciTech,* 12**,** 1087-101.

BHARGAVA, J. S., PATEL, B., FOSS, A. J., AVERY, A. J. & KING, A. J. 2006. Views of glaucoma patients on aspects of their treatment: an assessment of patient preference by conjoint analysis. *Invest Ophthalmol Vis Sci,* 47**,** 2885-8.

BOLAND, M. V., ERVIN, A. M., FRIEDMAN, D. S., JAMPEL, H. D., HAWKINS, B. S., VOLLENWEIDER, D., CHELLADURAI, Y., WARD, D., SUAREZ-

CUERVO, C. & ROBINSON, K. A. 2013. Comparative effectiveness of treatments for open-angle glaucoma: a systematic review for the U.S. Preventive Services Task Force. *Ann Intern Med,* 158**,** 271-9.

BOWMAN, R. J., COPE, J. & NISCHAL, K. K. 2004. Ocular and systemic side effects of brimonidine 0.2% eye drops (Alphagan) in children. *Eye (Lond),* 18**,** 24-6.

BVA & DOG. 2006. *Leitlinie Nr. 15 a Primäres chronisches Offenwinkelglaukom, Normaldruckglaukom und okuläre Hypertension* [Online]. Available: http://augeninfo.de/leit/leit15a.pdf [Accessed 09 october 2017].

CHAIYASAN, W., SRINIVAS, S. P. & TIYABOONCHAI, W. 2013. Mucoadhesive chitosan-dextran sulfate nanoparticles for sustained drug delivery to the ocular surface. *J Ocul Pharmacol Ther,* 29**,** 200-7.

CRABB, D. P., SMITH, N. D., GLEN, F. C., BURTON, R. & GARWAY-HEATH, D. F. 2013. How does glaucoma look?: patient perception of visual field loss. *Ophthalmology,* 120**,** 1120-6.

CRAWLEY, L., ZAMIR, S. M., CORDEIRO, M. F. & GUO, L. 2012. Clinical options for the reduction of elevated intraocular pressure. *Ophthalmol Eye Dis,* 4**,** 43-64.

DE JONG, C., STOLWIJK, T., KUPPENS, E., DE KEIZER, R. & VAN BEST, J. 1994. Topical timolol with and without benzalkonium chloride: epithelial permeability and autofluorescence of the cornea in glaucoma. *Graefe's Archive for Clinical and Experimental Ophthalmology,* 232**,** 221-224.

DE, T. K., BERGEY, E. J., CHUNG, S. J., RODMAN, D. J., BHARALI, D. J. & PRASAD, P. N. 2004. Polycarboxylic acid nanoparticles for ophthalmic drug delivery: an ex vivo evaluation with human cornea. *J Microencapsul,* 21**,** 841-55.

DE VRIES, J. W. 2015. *DNA nanoparticles as ocular drug delivery platform.* University of Groningen.

DE VRIES, J. W., SCHNICHELS, S., HURST, J., STRUDEL, L., GRUSZKA, A., KWAK, M., BARTZ-SCHMIDT, K.-U., SPITZER, M. S. & HERRMANN, A. 2018. DNA nanoparticles for ophthalmic drug delivery. *Biomaterials,* 157**,** 98-106.

DERICK, R. J., ROBIN, A. L., WALTERS, T. R., BARNEBEY, H. S., CHOPLIN, N., SCHUMAN, J., KELLEY, E. P., CHEN, K. & STOECKER, J. F. 1997. Brimonidine tartrate: a one-month dose response study. *Ophthalmology,* 104**,** 131-6.

DIETLEIN, T. S., ROSENTRETER, A. & LAPPAS, A. 2016. [Complexities of Medical Glaucoma Therapy--the Elderly Patient in Focus]. *Klin Monbl Augenheilkd,* 233**,** 138-42.

DUBEY, A. & PRABHU, P. 2014. Formulation and evaluation of stimuli-sensitive hydrogels of timolol maleate and brimonidine tartrate for the treatment of glaucoma. *Int J Pharm Investig,* 4**,** 112-8.

DUBINER, H. B., MROZ, M., SHAPIRO, A. M., DIRKS, M. S. & BRIMONIDINE VS. LATANOPROST STUDY, G. 2001. A comparison of the efficacy and tolerability of brimonidine and latanoprost in adults with open-angle glaucoma or ocular hypertension: a three-month, multicenter, randomized, double-masked, parallel-group trial. *Clin Ther,* 23**,** 1969-83.

EDMUNDS, B., THOMPSON, J. R., SALMON, J. F. & WORMALD, R. P. 2001. The National Survey of Trabeculectomy. II. Variations in operative technique and outcome. *Eye (Lond),* 15**,** 441-8.

ELLINGTON, A. D. & SZOSTAK, J. W. 1990. In vitro selection of RNA molecules that bind specific ligands. *Nature,* 346**,** 818-22.

ENYEDI, L. B. & FREEDMAN, S. F. 2001. Safety and efficacy of brimonidine in children with glaucoma. *J AAPOS,* 5**,** 281-4.

FENG, L., WU, H., MA, P., MUMPER, R. J. & BENHABBOUR, S. R. 2011. Development and optimization of oil-filled lipid nanoparticles containing docetaxel conjugates designed to control the drug release rate in vitro and in vivo. *Int J Nanomedicine,* 6**,** 2545-56.

FIELD, A., TYTELL, A., LAMPSON, G. & HILLEMAN, M. 1967. Inducers of interferon and host resistance. II. Multistranded synthetic polynucleotide complexes. *Proceedings of the National Academy of Sciences,* 58**,** 1004-1010.

FUNG, A. T., REID, S. E., JONES, M. P., HEALEY, P. R., MCCLUSKEY, P. J. & CRAIG, J. C. 2007. Meta-analysis of randomised controlled trials comparing latanoprost with brimonidine in the treatment of open-angle glaucoma, ocular hypertension or normal-tension glaucoma. *Br J Ophthalmol,* 91**,** 62-8.

GREENFIELD, D. S., LIEBMANN, J. M. & RITCH, R. 1997. Brimonidine: a new alpha2-adrenoreceptor agonist for glaucoma treatment. *J Glaucoma,* 6**,** 250-8.

GROVE, K., DOBISH, J., HARTH, E., INGRAM, M. C., GALLOWAY, R. L. & MAWN, L. A. 2014. Trans-meningeal drug delivery to optic nerve ganglion cell axons using a nanoparticle drug delivery system. *Exp Eye Res,* 118**,** 42-5.

HAYREH, S. S., PODHAJSKY, P. & ZIMMERMAN, M. B. 1999. Beta-blocker eyedrops and nocturnal arterial hypotension. *Am J Ophthalmol,* 128**,** 301-9.

HEIJL, A., LESKE, M. C., BENGTSSON, B., HYMAN, L., BENGTSSON, B., HUSSEIN, M. & EARLY MANIFEST GLAUCOMA TRIAL, G. 2002. Reduction of intraocular pressure and glaucoma progression: results from the Early Manifest Glaucoma Trial. *Arch Ophthalmol,* 120**,** 1268-79.

HERMANN, M. M., BRON, A. M., CREUZOT-GARCHER, C. P. & DIESTELHORST, M. 2011. Measurement of adherence to brimonidine therapy for glaucoma using electronic monitoring. *J Glaucoma,* 20**,** 502-8.

HERNANDEZ, M., URCOLA, J. H. & VECINO, E. 2008. Retinal ganglion cell neuroprotection in a rat model of glaucoma following brimonidine, latanoprost or combined treatments. *Exp Eye Res,* 86**,** 798-806.

HERRMANN, A., DE VRIES, J. W., SPITZER, M. S., SCHNICHELS, S. O. inventors, 2015, Means and methods for ocular drug delivery, International publication number: WO 2015/041520 Al, 26.3.2015

JIANG, F., LIU, B., LU, J., LI, F., LI, D., LIANG, C., DANG, L., LIU, J., HE, B., BADSHAH, S. A., LU, C., HE, X., GUO, B., ZHANG, X. B., TAN, W., LU, A. & ZHANG, G. 2015. Progress and Challenges in Developing Aptamer-Functionalized Targeted Drug Delivery Systems. *Int J Mol Sci,* 16**,** 23784-822.

JOHANNESSON, G., MOYA-ORTEGA, M. D., ASGRIMSDOTTIR, G. M., LUND, S. H., THORSTEINSDOTTIR, M., LOFTSSON, T. & STEFANSSON, E. 2014. Kinetics of gamma-cyclodextrin nanoparticle suspension eye drops in tear fluid. *Acta Ophthalmol,* 92**,** 550-6.

JU-NAM, Y. & LEAD, J. R. 2008. Manufactured nanoparticles: An overview of their chemistry, interactions and potential environmental implications. *Science of The Total Environment,* 400**,** 396-414.

KIRWAN, J. F., NIGHTINGALE, J. A., BUNCE, C. & WORMALD, R. 2002. Beta blockers for glaucoma and excess risk of airways obstruction: population based cohort study. *BMJ,* 325**,** 1396-7.

KONIECZKA, K., SCHOETZAU, A., KOCH, S., HAUENSTEIN, D. & FLAMMER, J. 2018. Cornea Thermography: Optimal Evaluation of the Outcome and the Resulting Reproducibility. *Translational vision science & technology,* 7**,** 14-14.

KRUMAN, I., GUO, Q. & MATTSON, M. P. 1998. Calcium and reactive oxygen species mediate staurosporine-induced mitochondrial dysfunction and apoptosis in PC12 cells. *Journal of neuroscience research,* 51**,** 293-308.

KRUPIN, T., LIEBMANN, J. M., GREENFIELD, D. S., RITCH, R., GARDINER, S. & LOW-PRESSURE GLAUCOMA STUDY, G. 2011. A randomized trial of brimonidine versus timolol in preserving visual function: results from the Low-Pressure Glaucoma Treatment Study. *Am J Ophthalmol,* 151**,** 671-81.

LESKE, M. C., HEIJL, A., HUSSEIN, M., BENGTSSON, B., HYMAN, L., KOMAROFF, E. & EARLY MANIFEST GLAUCOMA TRIAL, G. 2003. Factors for glaucoma progression and the effect of treatment: the early manifest glaucoma trial. *Arch Ophthalmol,* 121**,** 48-56.

MAIER, P. C., FUNK, J., SCHWARZER, G., ANTES, G. & FALCK-YTTER, Y. T. 2005. Treatment of ocular hypertension and open angle glaucoma: meta-analysis of randomised controlled trials. *BMJ,* 331**,** 134.

MATSUMOTO, M. & SEYA, T. 2008. TLR3: Interferon induction by double-stranded RNA including poly(I:C). *Advanced Drug Delivery Reviews,* 60**,** 805-812.

MCKEAGUE, M., VELU, R., HILL, K., BARDOCZY, V., MESZAROS, T. & DEROSA, M. C. 2014. Selection and characterization of a novel DNA aptamer for label-free fluorescence biosensing of ochratoxin A. *Toxins (Basel),* 6**,** 2435-52.

MERODIO, M., IRACHE, J. M., VALAMANESH, F. & MIRSHAHI, M. 2002. Ocular disposition and tolerance of ganciclovir-loaded albumin nanoparticles after intravitreal injection in rats. *Biomaterials,* 23**,** 1587-94.

MINCKLER, D. S., FRANCIS, B. A., HODAPP, E. A., JAMPEL, H. D., LIN, S. C., SAMPLES, J. R., SMITH, S. D. & SINGH, K. 2008. Aqueous shunts in glaucoma: a report by the American Academy of Ophthalmology. *Ophthalmology,* 115**,** 1089-98.

MURTHY, S. K. 2007. Nanoparticles in modern medicine: state of the art and future challenges. *Int J Nanomedicine,* 2**,** 129-41.

NATARAJAN, J. V., ANG, M., DARWITAN, A., CHATTOPADHYAY, S., WONG, T. T. & VENKATRAMAN, S. S. 2012. Nanomedicine for glaucoma: liposomes provide sustained release of latanoprost in the eye. *Int J Nanomedicine,* 7**,** 123-31.

OSBORNE, S. A., MONTGOMERY, D. M., MORRIS, D. & MCKAY, I. C. 2005. Alphagan allergy may increase the propensity for multiple eye-drop allergy. *Eye (Lond),* 19**,** 129-37.

PASCOLINI, D. & MARIOTTI, S. P. 2012. Global estimates of visual impairment: 2010. *Br J Ophthalmol,* 96**,** 614-8.

PETERS, D., BENGTSSON, B. & HEIJL, A. 2013. Lifetime risk of blindness in open-angle glaucoma. *Am J Ophthalmol,* 156**,** 724-30.

PRATT, N. L., RAMSAY, E. N., KALISCH ELLETT, L. M., NGUYEN, T. A. & ROUGHEAD, E. E. 2015. Association between Ophthalmic Timolol and Hospitalisation for Bradycardia. *J Ophthalmol,* 2015**,** 567387.

RÖSLER, A., VANDERMEULEN, G. W. M. & KLOK, H.-A. 2012. Advanced drug delivery devices via self-assembly of amphiphilic block copolymers. *Advanced Drug Delivery Reviews,* 64**,** 270-279.

SALATA, O. V. 2004. Applications of nanoparticles in biology and medicine. *Journal of nanobiotechnology,* 2**,** 3.

SALL, K. 2000. The Efficacy and Safety of Brinzolamide 1% Ophthalmic Suspension (Azopt®) as a Primary Therapy in Patients With Open-Angle Glaucoma or Ocular Hypertension1, 2. *Survey of Ophthalmology,* 44**,** S155-S162.

SALL, K. N., GREFF, L. J., JOHNSON-PRATT, L. R., DELUCCA, P. T., POLIS, A. B., KOLODNY, A. H., FLETCHER, C. A., CASSEL, D. A., BOYLE, D. R. & SKOBIERANDA, F. 2003. Dorzolamide/timolol combination versus concomitant administration of brimonidine and timolol: six-month comparison of efficacy and tolerability. *Ophthalmology,* 110**,** 615-24.

SARPONG, K. & DATTA, B. 2012. Nucleic-Acid-binding chromophores as efficient indicators of aptamer-target interactions. *J Nucleic Acids,* 2012**,** 247280.

SCHLOTE, T., GRÜBE, M., MIELKE, J. & ROHRBACH, M. (eds.) 2004. *Taschenatlas Augenheilkunde,* Stuttgart: Georg Thieme Verlag KG.

SCHUMAN, J. S. 2000. Antiglaucoma medications: A review of safety and tolerability issues related to their use. *Clinical Therapeutics,* 22**,** 167-208.

SHULMAN, S., JOHANNESSON, G., STEFANSSON, E., LOEWENSTEIN, A., ROSENBLATT, A. & HABOT-WILNER, Z. 2015. Topical dexamethasone-cyclodextrin nanoparticle eye drops for non-infectious Uveitic macular oedema and vitritis - a pilot study. *Acta Ophthalmol,* 93**,** 411-5.

SIMMONS, S. T. & EARL, M. L. 2002. Three-month comparison of brimonidine and latanoprost as adjunctive therapy in glaucoma and ocular hypertension patients uncontrolled on β-blockers. *Ophthalmology,* 109**,** 307-314.

SMITH, L. M. 2006. Nanostructures: the manifold faces of DNA. *Nature,* 440**,** 283-4.

STROBER, W. 2015. Trypan Blue Exclusion Test of Cell Viability. *Current Protocols in Immunology,* 111**,** A3.B.1-A3.B.3.

SUBRAMANIAN, N., RAGHUNATHAN, V., KANWAR, J. R., KANWAR, R. K., ELCHURI, S. V., KHETAN, V. & KRISHNAKUMAR, S. 2012. Target-specific delivery of doxorubicin to retinoblastoma using epithelial cell adhesion molecule aptamer. *Mol Vis,* 18**,** 2783-95.

THAM, Y. C., LI, X., WONG, T. Y., QUIGLEY, H. A., AUNG, T. & CHENG, C. Y. 2014. Global prevalence of glaucoma and projections of glaucoma burden through 2040: a systematic review and meta-analysis. *Ophthalmology,* 121**,** 2081-90.

TORIS, C. B., CAMRAS, C. B. & YABLONSKI, M. E. 1999. Acute versus chronic effects of brimonidine on aqueous humor dynamics in ocular hypertensive patients. *Am J Ophthalmol,* 128**,** 8-14.

TORIS, C. B., GLEASON, M. L., CAMRAS, C. B. & YABLONSKI, M. E. 1995. Effects of brimonidine on aqueous humor dynamics in human eyes. *Arch Ophthalmol,* 113**,** 1514-7.

TSAI, J. C. 2006. Medication adherence in glaucoma: approaches for optimizing patient compliance. *Curr Opin Ophthalmol,* 17**,** 190-5.

TSAI, J. C. 2009. A comprehensive perspective on patient adherence to topical glaucoma therapy. *Ophthalmology,* 116**,** S30-6.

TSAI, T., ROBIN, A. L. & SMITH, J. P., 3RD 2007. An evaluation of how glaucoma patients use topical medications: a pilot study. *Trans Am Ophthalmol Soc,* 105**,** 29-33; discussion 33-5.

TUOMELA, A., LIU, P., PURANEN, J., RONKKO, S., LAAKSONEN, T., KALESNYKAS, G., OKSALA, O., ILKKA, J., LARU, J., JARVINEN, K., HIRVONEN, J. & PELTONEN, L. 2014. Brinzolamide nanocrystal formulations for ophthalmic delivery: reduction of elevated intraocular pressure in vivo. *Int J Pharm,* 467**,** 34-41.

VAN DER VALK, R., WEBERS, C. A., LUMLEY, T., HENDRIKSE, F., PRINS, M. H. & SCHOUTEN, J. S. 2009. A network meta-analysis combined direct and indirect comparisons between glaucoma drugs to rank effectiveness in lowering intraocular pressure. *J Clin Epidemiol,* 62**,** 1279-83.

VAN DER VALK, R., WEBERS, C. A., SCHOUTEN, J. S., ZEEGERS, M. P., HENDRIKSE, F. & PRINS, M. H. 2005. Intraocular pressure-lowering effects of all commonly used glaucoma drugs: a meta-analysis of randomized clinical trials. *Ophthalmology,* 112**,** 1177-85.

VOLOTINEN, M., HAKKOLA, J., PELKONEN, O., VAPAATALO, H. & MAENPAA, J. 2011. Metabolism of ophthalmic timolol: new aspects of an old drug. *Basic Clin Pharmacol Toxicol,* 108**,** 297-303.

WEBERS, C. A., BECKERS, H. J., ZEEGERS, M. P., NUIJTS, R. M., HENDRIKSE, F. & SCHOUTEN, J. S. 2010. The intraocular pressure-lowering effect of prostaglandin analogs combined with topical beta-blocker therapy: a systematic review and meta-analysis. *Ophthalmology,* 117**,** 2067-74 e1-6.

WEINREB, R. N., AUNG, T. & MEDEIROS, F. A. 2014. The pathophysiology and treatment of glaucoma: a review. *JAMA,* 311**,** 1901-11.

WEST, S. 2007. Epidemiology of Cataract: Accomplishments over 25 years and Future Directions. *Ophthalmic Epidemiology,* 14**,** 173-178.

WINFIELD, A. J., JESSIMAN, D., WILLIAMS, A. & ESAKOWITZ, L. 1990. A study of the causes of non-compliance by patients prescribed eyedrops. *Br J Ophthalmol,* 74**,** 477-80.

WU, L. L., HUANG, P., GAO, Y. X., WANG, Z. X. & LI, B. 2011. A 12-week, double-masked, parallel-group study of the safety and efficacy of travoprost 0.004% compared with pilocarpine 1% in Chinese patients with primary angle-closure and primary angle-closure glaucoma. *J Glaucoma,* 20**,** 388-91.

XIAO, Z., JI, C., SHI, J., PRIDGEN, E. M., FRIEDER, J., WU, J. & FAROKHZAD, O. C. 2012. DNA self-assembly of targeted near-infrared-responsive gold nanoparticles for cancer thermo-chemotherapy. *Angew Chem Int Ed Engl,* 51**,** 11853-7.

ZAJAC-PYTRUS, H. M., PILECKA, A., TURNO-KRECICKA, A., ADAMIEC-MROCZEK, J. & MISIUK-HOJLO, M. 2015. The Dry Form of Age-Related Macular Degeneration (AMD): The Current Concepts of Pathogenesis and Prospects for Treatment. *Adv Clin Exp Med,* 24**,** 1099-104.

ZHANG, W., PRAUSNITZ, M. R. & EDWARDS, A. 2004. Model of transient drug diffusion across cornea. *J Control Release,* 99**,** 241-58.

ZHANG, X. Q., XU, X., LAM, R., GILJOHANN, D., HO, D. & MIRKIN, C. A. 2011. Strategy for increasing drug solubility and efficacy through covalent attachment to polyvalent DNA-nanoparticle conjugates. *ACS Nano,* 5**,** 6962-70.

ZIPPER, H., BRUNNER, H., BERNHAGEN, J. & VITZTHUM, F. 2004. Investigations on DNA intercalation and surface binding by SYBR Green I, its structure determination and methodological implications. *Nucleic Acids Res,* 32**,** e103.

7. Erklärung zum Eigenanteil

Die Arbeit wurde in der Universitätsaugenklinik Tübingen unter Betreuung von Prof. Dr. Martin Spitzer durchgeführt.

Die Konzeption der Studie erfolgte gemeinsam mit Prof. Dr. Martin Spitzer, Dr. Sven Schnichels, Dr. Jan-Willem de Vries und Dr. José Hurst.

Die Versuche wurden wie folgt durchgeführt. Die Versuche der Kapitel 3.1 und 3.2 wurden von mir nach Einarbeitung durch Dr. Jan-Willem de Vries eigenständig durchgeführt. Bei den Fluorophotometerversuchen, sowie den histologischen Schnitten wurde ich von Felix Frößl und Karin Tiedemann unterstützt. Die Zellkulturversuche wurden in Zusammenarbeit mit Dr. José Hurst durchgeführt. Alle Tierversuche wurden von Dr. José Hurst, Heike Enderle und mir durchgeführt. Die HPLC-Analysen wurde gemeinsam mit Dr. Agnieska Gruska-de Vries ausgeführt.

Die statistische Auswertung erfolgte nach Anleitung durch Dr. Sven Schnichels und Dr. José Hurst durch mich.

Ich versichere, das Manuskript selbstständig verfasst zu haben und keine weiteren als die von mir angegebenen Quellen verwendet zu haben.

Tübingen, den 03.05.2019